



저작자표시-비영리-변경금지 2.0 대한민국

이용자는 아래의 조건을 따르는 경우에 한하여 자유롭게

- 이 저작물을 복제, 배포, 전송, 전시, 공연 및 방송할 수 있습니다.

다음과 같은 조건을 따라야 합니다:



저작자표시. 귀하는 원저작자를 표시하여야 합니다.



비영리. 귀하는 이 저작물을 영리 목적으로 이용할 수 없습니다.



변경금지. 귀하는 이 저작물을 개작, 변형 또는 가공할 수 없습니다.

- 귀하는, 이 저작물의 재이용이나 배포의 경우, 이 저작물에 적용된 이용허락조건을 명확하게 나타내어야 합니다.
- 저작권자로부터 별도의 허가를 받으면 이러한 조건들은 적용되지 않습니다.

저작권법에 따른 이용자의 권리는 위의 내용에 의하여 영향을 받지 않습니다.

이것은 [이용허락규약\(Legal Code\)](#)을 이해하기 쉽게 요약한 것입니다.

[Disclaimer](#)

이학박사학위논문

지방조직 불변성 자연살해 T 세포의
대사 항상성 조절 기전 규명

Study on the mechanisms of adipose tissue
invariant natural killer T cells
in the control of metabolic homeostasis

2025 년 2 월

서울대학교 대학원

생명과학부

한 상 문

**Study on the mechanisms of adipose tissue
invariant natural killer T cells
in the control of metabolic homeostasis**

**A dissertation submitted in partial fulfillment
of the requirement for degree of
DOCTOR OF PHILOSOPHY**

**To the Faculty of the
School of Biological Sciences**

At

SEOUL NATIONAL UNIVERSITY

By

Sang Mun Han

February, 2025

Data Approved

지방조직 불변성 자연살해 T 세포의 대사 항상성 조절 기전 규명

Study on the mechanisms of adipose tissue
invariant natural killer T cells
in the control of metabolic homeostasis

지도교수 김 재 범

이 논문을 이학박사 학위논문으로 제출함
2025 년 2 월

서울대학교 대학원

생명과학부

한 상 문

한상문의 이학박사 학위논문을 인준함
2025 년 2 월

위원장	<u> 황 대 희 </u>	(인)
부위원장	<u> 김 재 범 </u>	(인)
위원	<u> 정 연 석 </u>	(인)
위원	<u> 허 진 영 </u>	(인)
위원	<u> 황 수 석 </u>	(인)

ABSTRACT

Study on the mechanisms of adipose tissue invariant natural killer T cells in the control of metabolic homeostasis

Sang Mun Han

Adipose tissue is a central metabolic organ that regulates whole-body energy homeostasis by storing and supplying energy, secreting various hormones, and communicating with immune cells in obesity. In response to obesity, adipose tissue undergoes significant remodeling, including adipocyte enlargement, heightened inflammation, increased adipocyte turnover, and the development of insulin resistance. Adipose tissue is also composed of numerous immune cells, which play key roles in its pathophysiology, particularly in regulating inflammation. Among various immune cells, invariant natural killer T (iNKT) cells have unique characteristics and are critical for maintaining adipose tissue homeostasis in obesity. iNKT cells directly interact with adipocytes by recognizing lipid antigens presented on CD1d molecules on the surface of adipocytes. This interaction is essential for adipose iNKT cells to inhibit inflammation and promote adipocyte turnover, thereby mitigating pathological remodeling of obese adipose tissue. However, the mechanisms by which adipose iNKT cells orchestrate these diverse

functions remain largely unknown.

An intriguing aspect of adipose iNKT cells is their tissue-specific features, which differ from iNKT cells in other organs. Since peripheral immune cells, such as adipose iNKT cells, begin their maturation in primary lymphoid organs and then migrate to peripheral tissues, it is crucial for them to adapt to the local microenvironment. Despite this, a comprehensive understanding of how these distinct characteristics are generated in adipose iNKT cells is still lacking.

In Chapter I, I investigated the unique characteristics of adipose iNKT cells by comparing them to iNKT cells from other organs. I discovered a distinct subpopulation of adipose iNKT cells that upregulates KLRG1, a feature not observed in iNKT cells from other organs. This subpopulation, termed adipose-specific (As)-iNKT1 cells, appeared to be induced by secretory factors from adipocytes.

In Chapter II, I explored the regulatory mechanisms by which adipose iNKT cells contribute to adipose tissue homeostasis in obesity, with a particular focus on adipocyte turnover. In response to diet-induced obesity, As-iNKT1 cells differentiated into a cytotoxic subpopulation that upregulates Fas ligand and granzyme B, referred to as adipose cytotoxic (Ac)-iNKT1 cells. These Ac-iNKT1 cells were capable of inducing adipocyte death both *in vitro* and *in vivo*. Moreover, Ac-iNKT1 cells expressed high levels of the macrophage chemotactic cytokine CCL5. Additionally, in obesity, adipose iNKT17 cells increased the expression of amphiregulin (AREG), which binds

to EGFR. AREG stimulated the proliferation of adipose stem and progenitor cells, subsequently promoting adipogenesis. These findings suggest that various adipose iNKT cell subpopulations coordinate to regulate the process of adipocyte turnover.

In conclusion, this thesis elucidates the regulatory mechanisms of adipose iNKT cells and their roles in maintaining adipose tissue homeostasis. Adipose iNKT cells acquire tissue-specific characteristics that enhance adipocyte turnover in obesity. This study broadens our understanding of peripheral immune cells, particularly with iNKT cells, in the regulation of adipose tissue physiology.

Keywords: adipose tissue, white adipose tissue, invariant natural killer T (iNKT) cell, adipocyte turnover, adipose tissue remodeling, obesity

Student Number: 2019-28710

1. Abstract.....	63
2. Introduction	64
3. Materials and Methods	66
4. Results	78
5. Discussion.....	103
CONCLUSION	107
1. Adipose Tissue Microenvironment Mediates the Distinct Characteristics of Adipose iNKT Cells	109
2. Various Adipose iNKT Cell Subpopulations Regulate Adipocyte Turnover in Obesity	111
ACKNOWLEDGEMENTS	114
REFERENCES	115
구분 초록	128

LIST OF FIGURES

Figure 1. Diverse functions of adipose tissue.....	2
Figure 2. Overview of adipocyte turnover.....	8
Figure 3. Types of innate and adaptive lymphocytes	13
Figure 4. Development and heterogeneity of iNKT cells in thymus.....	19
Figure 5. scRNA-seq data of adipose and thymic iNKT cells.....	43
Figure 6. DEGs between adipose and thymic iNKT cells.....	44
Figure 7. Adipose iNKT cells comprise three major subpopulations.....	45
Figure 8. KLRG1 and Ly6C distinguish three major adipose iNKT subpopulations.....	46
Figure 9. A2 subpopulation exhibits adipose tissue-specific features.....	47
Figure 10. A2 marker gene, KLRG1-expressing iNKT cells are enriched in adipose tissue.....	48
Figure 11. As-iNKT1 cells accumulate in adipose tissue as age increases ..	53
Figure 12. Adipose iNKT cell precursors are not identified among thymic iNKT cells.....	54
Figure 13. Adipose tissue microenvironment induces As-iNKT1 cell generation	55
Figure 14. Secretory factors from adipocytes mediate As-iNKT1 cell generation	56
Figure 15. As-iNKT1 cells highly express Th1-type cytokines	57
Figure 16. DEGs between Au-iNKT1 and As-iNKT1 cells	58
Figure 17. scRNA-seq data of adipose iNKT cells isolated from variable length of HFD feeding conditions	81
Figure 18. CX3CR1 distinguishes Ac-iNKT1 cells from As-iNKT1 cells ..	82
Figure 19. DEGs between NCD- and 8w HFD-fed conditions of each adipose iNKT cell subpopulation	83

Figure 20. As-iNKT1 cells give rise to Ac-iNKT1 cells in obesity.....	84
Figure 21. Ac-iNKT1 cells exhibit low clonal diversity	85
Figure 22. Ac-iNKT1 cells highly express cytotoxicity-related genes.....	89
Figure 23. FFA treatment induces adipocyte hypertrophy models	90
Figure 24. Characteristics of adipose iNKT cells in α -GC-induced iNKT cell <i>in vivo</i> expansion	91
Figure 25. Ac-iNKT1 cells specifically remove hypertrophic and inflamed adipocytes <i>in vitro</i>	92
Figure 26. Ac-iNKT1 cells remove adipocytes <i>in vivo</i> and exhibit characteristics similar to CD8 ⁺ effector T cells	93
Figure 27. Ac-iNKT1 cells highly express macrophage-recruiting cytokine, CCL5	94
Figure 28. Activation of iNKT cells stimulates ASPC proliferation without inducing adipocyte death	98
Figure 29. Injection of A-iNKT17 cells induces ASPC proliferation	99
Figure 30. A-iNKT17 cells produce amphiregulin (AREG) which stimulates ASPC proliferation	100
Figure 31. AREG-induced ASPC proliferation increases adipogenesis	101
Figure 32. The proportion of iNKT cell subtypes in various organs.....	102
Figure 33. Graphical abstract of Chapters I and II	108

LIST OF TABLES

Table 1. Effects of adipocyte turnover in metabolic phenotypes.....	9
Table 2. Primer sequences in Chapter I	38
Table 3. List of genes used for iNKT cell subtype annotation	39
Table 4. Primer sequences in Chapter II.....	77

BACKGROUNDS

I. Functions of Adipose Tissue

Adipose tissue is a key energy storage organ that regulates whole-body energy homeostasis [1]. Adipose tissue is composed of adipocytes and various other cell types such as adipose stem and progenitor cells (ASPCs), and immune cells (e.g. macrophages, dendritic cells, T cells, B cells) [2, 3]. Adipose tissues store excess energy in the form of triglycerides (TGs) and cholesteryl esters during periods of energy surplus, while supplying energy in the form of free fatty acids (FFAs) and glycerol upon fasting or cold stimuli [4, 5]. For a long time, adipose tissue has been considered merely a part of connective tissues that stores and supplies energy. However, research over the past few decades has revealed various functions of adipose tissue. Adipose tissue plays a crucial role in regulating systemic energy metabolism through secreting hormones known as adipokines, such as leptin and adiponectin [6, 7]. In addition, adipose tissue is involved in the maintenance of body temperature through thermogenic activity. Certain adipose tissues, composed of brown and beige adipocytes, dissipate energy in the form of heat [8, 9]. Furthermore, adipose tissue is involved in the regulation of systemic inflammation [10]. In obesity, inflammation and immune cell infiltration in adipose tissue increase preceding other organs, exacerbating whole-body metabolic homeostasis [11, 12]. These diverse functions of adipose tissue underscore its crucial roles in regulating systemic energy metabolism (Figure 1).

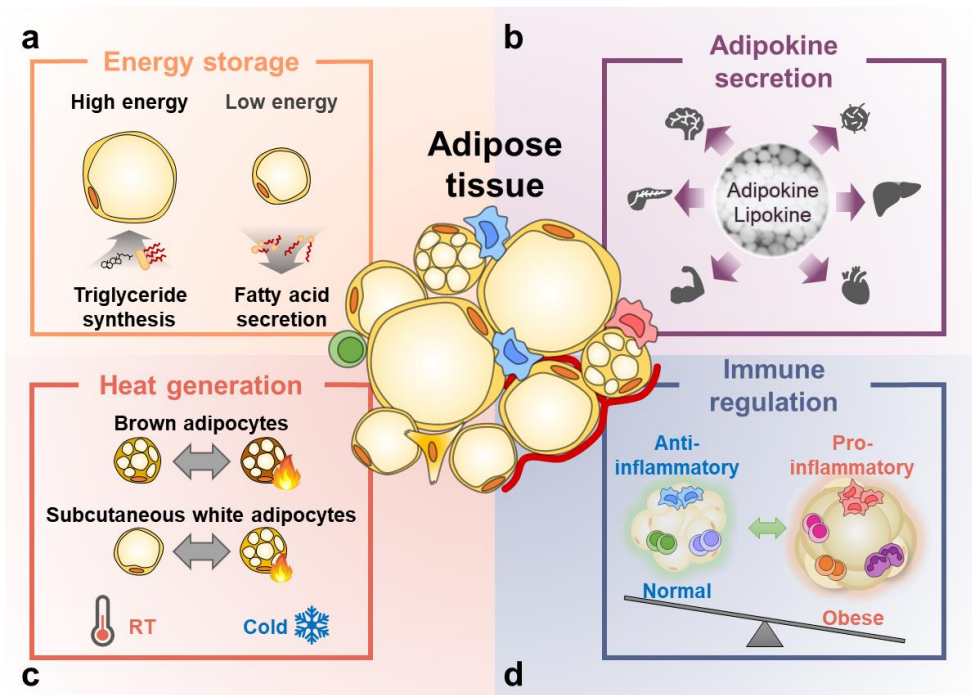


Figure 1. Diverse functions of adipose tissue

Adipose tissue affects whole-body energy metabolism via various functions. Adipose tissues store energy (a), secrete adipokines and lipokines (b), generate heat (c), and regulate inflammatory responses in obesity (d).

1. White Adipose Tissue Remodeling in Obesity

In obesity, adipose tissue, especially visceral white adipose tissue (WAT), is greatly remodeled in the aspect of its morphology and characteristics [1]. During the remodeling process, adipocytes become hypertrophic, and adipose tissue inflammation is induced, resulting in various obesity-related metabolic complications such as type 2 diabetes, atherosclerosis, and metabolic dysfunction-associated fatty liver disease (MAFLD) [11, 13].

Obese adipose tissue expands in two processes, which differ in morphology and metabolic outcomes. Hypertrophic WAT expansion often exhibits pathological phenotypes such as inflammation, hypoxia, and fibrosis, whereas hyperplastic WAT expansion relatively exhibits beneficial phenotypes with a greater ability for energy storage, contributing to improved metabolic parameters [1, 14, 15]. Because both hypertrophic and hyperplastic expansion contribute to increased adipose tissue mass in obesity, metabolic dysfunctions such as inflammation, insulin resistance, adipocyte hypertrophy, hypoxia, and fibrosis are eventually promoted [15].

Pathological phenotypes induced by hypertrophic expansion are associated with metabolic dysfunctions. In obesity, adipose tissue inflammation is induced by several stimuli such as gut microbiota-derived LPS, TLR stimulation by FFAs, and damage-associated molecular patterns (DAMPs) secreted from dead adipocytes [16]. Adipose tissue inflammation is further boosted by the infiltration of pro-inflammatory immune cells such as macrophages and CD8⁺ T cells [17]. In prolonged obesity, chronic

inflammation in adipose tissue impedes insulin signaling by inhibitory phosphorylation of IRS1, leading to insulin resistance [12, 18]. Energy surplus in obesity promotes adipocyte hypertrophy. Adipocyte hypertrophy induces adipocyte death [19, 20] and insulin resistance by inhibiting GLUT4 translocation to the plasma membrane [21]. Hypoxia is induced due to relatively scarce angiogenesis compared to drastic tissue expansion in obesity [22]. In adipose tissue, hypoxia induces adipocyte death, insulin resistance, and fibrosis [23-25]. In addition, an excess amount of extracellular matrix (ECM) components produced by adipocytes and fibroblasts accumulates in obese adipose tissue, leading to fibrosis [26]. Fibrosis promotes ectopic fat accumulation, inflammation, and glucose intolerance [24, 26].

Recent studies imply that a dysfunctional subset of adipocytes would accumulate in obese adipose tissue. The proportion of adipocyte subpopulation upregulating lipid accumulation-, and cellular senescence-related genes and certain genes such as *Lep* (Leptin), *Col4a1* (Collagen 4a 1) is increased in obesity compared to lean subjects [27-29]. Given its pathological characteristics related to adipocyte hypertrophy, senescence, and fibrosis, it would be necessary to remove these dysfunctional adipocytes and replenish them with newly differentiated adipocytes.

2. Cellular Turnover of White Adipocytes

Cellular turnover to remove impaired cells and produce healthy cells is crucial for maintaining tissue homeostasis [30]. In this regard, adipocyte turnover

would be important for adipose tissue homeostasis by removing large and inflamed adipocytes and replacing them with new small adipocytes [14]. Given that the number of adipocytes appears to be constant in adults [31-33], it is likely that adipocyte birth and death are closely associated with each other [34, 35]. Adipocyte turnover involves complex processes wherein multiple cell types should be harmoniously coordinated. Adipocyte turnover is composed of the following steps: induction of adipocyte death, efferocytosis of dead adipocytes by macrophages, ASPC proliferation, and adipocyte differentiation [5, 36].

In humans, adipocyte turnover accounts for the second-highest daily mass turnover (~3.2 g/day) among noncirculating cells [37]. To date, most studies on adipocyte turnover have been conducted using WAT. White adipocytes exhibit unique morphological features such as large unilocular lipid droplet and high lipid contents. Due to their large size, adipocytes exceed the size limit of phagocytes [38]; thus, the clearance of dead adipocytes in adipose tissue is characterized by a crown-like structure (CLS), a structure with multiple phagocytic cells surrounding a dead adipocyte [38, 39]. This unique structure appears to be linked to the slow rate and pro-inflammatory features of adipocyte clearance.

Adipocyte turnover has been primarily investigated in obesity. In obese animals, adipocyte hypertrophy and adverse microenvironments enhance adipocyte death [40]. Subsequently, numerous phagocytes such as macrophages and neutrophils surround and engulf dead adipocytes [41].

Finally, new adipocyte formation is boosted to compensate for adipocyte death [42, 43], implying that adipocyte turnover seems to be facilitated in obesity. An increased rate of adipocyte turnover in this context has been experimentally demonstrated by using several methods such as tracing using isotope (^{14}C and ^2H), bromodeoxyuridine (BrdU), or genetically modified mice (AdipoChaser system and *Pdgfra*-CreERT2) (Figure 2) [31, 43-48].

Adipocyte turnover is crucial for adipose tissue homeostasis, evidenced by systemic metabolic dysfunctions upon defective adipocyte turnover process (Table 1). In obesity, an impairment in proper regeneration from ASPCs exacerbates adipose tissue inflammation, fibrosis, and insulin resistance [49]. When effective clearance of dead adipocytes by macrophages is hindered, insulin resistance and hepatic steatosis are aggravated [28, 50]. In contrast, promoting the elimination of dysfunctional adipocytes and subsequent adipocyte regeneration ameliorates glucose intolerance and adipose tissue inflammation [29, 51]. These findings propose that appropriate adipocyte turnover safeguards adipose tissue homeostasis in rodents, whereas in humans, the beneficial roles of adipogenesis during weight gain or obesity remain a topic of debate. Decreased adipogenesis is associated with insulin resistance and hypertrophic expansion of adipose tissue, a relatively pathological expansion characterized by enlarged adipocytes compared to hyperplastic expansion [52-55]. However, this idea has also been challenged by the findings showing that abundant small adipocytes or increased adipogenic potential could be associated with insulin resistance and ectopic

fat accumulation during weight gain [56-59]. Thus, further investigations are needed to scrutinize the relationship between adipocyte turnover and metabolic homeostasis in humans.

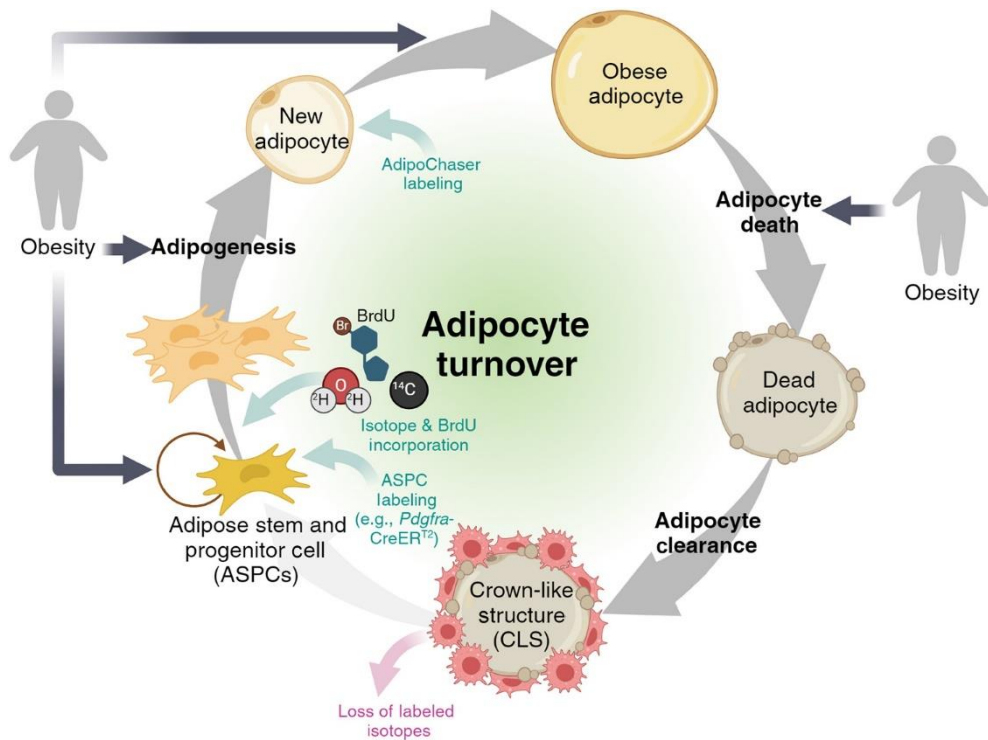


Figure 2. Overview of adipocyte turnover

The steps in adipocyte turnover comprise adipocyte death, clearance, and adipogenesis. When adipocyte death is induced, dead adipocytes are removed by macrophages in CLSs. Consequently, ASPCs proliferate and differentiate into new adipocytes, replacing dead adipocytes. Adipocyte death, clearance, ASPC proliferation, and adipogenesis are promoted in obesity. Image was provided by Han, S. M., *et al.* (2024). “How obesity affects adipocyte turnover”. *Trends Endocrinol Metab.*

Table 1. Phenotypes of mouse models with modulated adipocyte turnover

Steps		Target molecule	Model	Phenotypes	Ref
Adipocyte Death	Excessive adipocyte death	Casp8	<i>Fabp4</i> -FKBPv- <i>Casp8</i> (FAT-ATTAC); <i>ob/ob</i>	Adipocyte apoptosis↑(induced by FK1012-induced Casp8 dimerization, measured by TUNEL), Glucose intolerance↑, Hepatic steatosis↑, Adipokine depletion (Adiponectin, leptin)	[60]
		hCD59	<i>Adipoq</i> -Cre; pCAG-loxP-stop-loxP-hCD59	Adipocyte death↑(induced by Intermedilysin-induced membrane rupture, measured by CLS counting, TUNEL), Adipose tissue inflammation↑, Adipokine (Adiponectin↓, Leptin -), Lipolysis↑, Hepatocyte damage↑	[61]
		IR & IGF1R	<i>Adipoq</i> -CreER ^{T2} ; IR ^{fl/fl} ; IGF1R ^{fl/fl}	Adipocyte death↑(TUNEL, cleaved Casp3), Glucose intolerance↑, Insulin resistance↑, Hepatic steatosis↑, Adipokine depletion (Adiponectin, leptin)	[62]
	Selective removal of dysfunctional adipocytes	-	Senolytic drugs (Dasatinib & Quercetin), DIO	Adipocyte death↑(<i>ex vivo</i>), Glucose intolerance↓, Insulin resistance↓, Adipose tissue inflammation↓, M2-like macrophage gene↑	[29]
		-	iNKT cell ligand (α -GC), DIO	Adipocyte death↑(CLS, TUNEL), Adipocyte regeneration↑(AdipoChaser), Glucose intolerance↓, Insulin resistance↓, M2-like macrophage↑	[51]
Adipocyte Clearance	Dead adipocyte recognition	MBL-A (<i>Mbl1</i>) & MBL-C (<i>Mbl2</i>)	<i>Mbl1</i> ^{-/-} ; <i>Mbl2</i> ^{-/-} , DIO	Macrophage phagocytosis↓(<i>In vitro</i> coculture), Apoptotic cell accumulation↑(CLS, TUNEL), Body weight↑, Adipocyte size↑, Macrophage infiltration↑, Insulin resistance -	[63]
	Degradation	Nox2 (<i>Cybb</i>)	<i>Lyz2</i> -Cre; <i>Nox2</i> ^{fl/fl} , DIO (16 week)	Lysosomal exocytosis↓(LAMP1 in PM), Dead adipocyte accumulation↑(CLS, perilipin-), Body weight↑, Glucose intolerance -, Insulin resistance↑, Hepatic steatosis↑	[50]
		TM4SF19	• <i>Tm4sf19</i> ^{-/-} , DIO • <i>Tm4sf19</i> ^{-/-} → WT (BMT), DIO • <i>Csf1r</i> -CreER ^{T2} ; <i>Tm4sf19</i> ^{fl/fl} , DIO	Lysosomal activity↑(V-ATPase activity), Dead adipocyte clearance↑(<i>In vitro</i> coculture), Body weight↓, Fat mass↓, Glucose intolerance↓, Insulin resistance↓	[28]
Lipid uptake	TREM2	• <i>Trem2</i> ^{-/-} , DIO • <i>Trem2</i> ^{-/-} → WT (BMT), DIO	Lipid contents in macrophages↓(BODIPY), Body weight gain↑, Fat mass↑, Adipocyte size↑, Glucose intolerance↑	[2]	

Steps		Target molecule	Model	Phenotypes	Ref
Generation of new adipocytes	Proliferation	TGFβ3	<i>Tgfb3</i> ^{+/-} , DIO	ASPC proliferation↓(EdU incorporation), Adipocyte size↑, Glucose intolerance↑	[64]
		Akt2	• <i>Akt2</i> ^{-/-} ; <i>ob/ob</i> • <i>Akt2</i> ^{-/-} , DIO • <i>Pdgfra</i> -Cre; <i>Akt2</i> ^{fl/fl} , DIO	ASPC proliferation↓(BrdU incorporation) <i>Akt2</i> ^{-/-} ; <i>ob/ob</i> → Body weight gain↓, Fat mass↓, Adipocyte size↓	[47]
	Adipogenesis	PPARγ	<i>Pdgfrb</i> -rtTA; TRE- <i>Pparg2</i> , DIO	Adipogenesis↑(ASPC labeling), Adipocyte size↓, Adipose tissue inflammation↓, Glucose intolerance↓, Insulin resistance↓	[49]
		PPARγ	<i>Pdgfrb</i> -rtTA; TRE-Cre; <i>Pparg</i> ^{fl/fl} , DIO	Adipogenesis↓(ASPC labeling), Adipocyte size↑, Adipose tissue inflammation↑, Glucose intolerance↑, Insulin resistance↑	[49]
		FGFR1	<i>Pdgfra</i> -CreER ^{T2} ; <i>Fgfr1</i> ^{fl/fl} , DIO	Adipogenesis↓(%BrdU ⁺ adipocytes), Adipocyte number↓, Adipocyte size↑	[65]
		TNF	• <i>Fabp4</i> -dnTNF • <i>Fabp4</i> -RID • <i>Adipoq</i> -rtTA; TRE-RIDα/β, DIO	Adipocyte number↓, Adipocyte size↑, Adiponectin↓, Adipose tissue inflammation↑, Hepatic steatosis↑, Glucose intolerance↑	[66, 67]

↑ increase, ↓ decrease, - no change, methods for determining key parameters of adipocyte turnover are depicted in parentheses. → in the ‘Model’ column indicates bone marrow transplantation.

II. iNKT Cells

In adipose tissue, immune cells are important regulators of adipose tissue metabolism [68]. Adipose immune cells modulate not only adipose tissue inflammation by secreting various cytokines but also adipocyte fate, including adipocyte death, clearance, and adipogenesis [69, 70]. Among numerous adipose immune cells, invariant natural killer T (iNKT) cells have recently garnered significant attentions owing to their ability to directly interact with adipocytes through lipid antigens and their roles in adipose tissue remodeling [70, 71]. Recent studies have suggested that iNKT cells secrete cytokines to regulate adipose tissue inflammation and stimulate adipocyte turnover [51, 72-74].

1. Characteristics of iNKT Cells

iNKT cells (Type I NKT cells) are the most studied cell type among NKT cells that express both NK cell receptors and T cell receptors (TCRs) [75]. iNKT cells were named after their semi-invariant TCRs composed of invariant alpha chains ($V\alpha 14$ - $J\alpha 18$ in mice and $V\alpha 24$ - $J\alpha 18$ in humans) and a limited repertoire of beta chains ($V\beta 2$, 7, 8 in mice and $V\beta 11$ in humans) [76, 77]. The most discernable characteristic of iNKT cells compared to other immune cells is that they recognize CD1d-loaded lipid antigens by their invariant TCR. Due to limited antigen specificity and rapid antigen responses, iNKT cells are regarded as an innate-like T cells bridging adaptive and innate

immunity (Figure 3) [76].

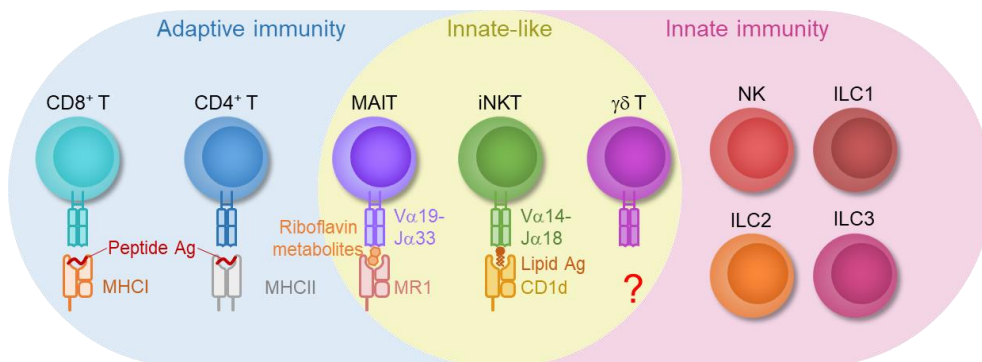


Figure 3. Types of innate and adaptive lymphocytes

T lymphocytes and innate lymphoid cells (ILCs) are categorized into adaptive, innate-like, and innate immune cells. Adaptive T cells are composed of conventional CD8⁺ or CD4⁺ T cells which recognize peptide antigens loaded on MHC I or MHC II, respectively. Innate-like T cells are composed of MAIT, iNKT, and $\gamma\delta$ T cells which possess restricted TCR variance and recognize non-peptide antigens. Ligands for murine $\gamma\delta$ T cells remain unidentified. ILCs do not possess any recombinant antigen-specific receptors. This image was modified from Ruf, B., Greten, T. F., & Korangy, F. (2023). "Innate lymphoid cells and innate-like T cells in cancer—at the crossroads of innate and adaptive immunity." *Nat Rev Cancer* 23(6): 351-371.

iNKT cells show long-term residency in lymphoid or non-lymphoid tissues such as thymus, lymph node, liver, adipose tissue, lung, and colon, where they participate in various pathophysiological processes by secreting cytokines or targeting cells for destruction [78]. The roles of iNKT cells are determined by their localizing tissues and secreting cytokines. In thymus, iNKT cells regulate memory-like phenotypes of CD8⁺ T cells via secreting IL-4 cytokine [79]. In liver or lung, iNKT cells help to combat viral or bacterial infections such as *Borrelia burgdorferi* [80] and Hepatitis C virus infection [81] in liver and pulmonary bacteria [82, 83] or influenza virus infection [84] in lung by secreting various cytokines. On the other hand, iNKT cells exacerbate metabolic-associated steatohepatitis (MASH) [85] or hepatic injury [86] by killing hepatocytes or secreting IFN γ , respectively.

iNKT cells are activated by both TCR and cytokine stimulation [76]. For TCR stimulation of iNKT cells, lipid antigen-loaded CD1d is required. CD1d is a lipid antigen-presenting MHC I homologue. Various lipid antigens have been identified as the ligands for iNKT cells [71, 87]. Every lipid antigen of iNKT cells possesses hydrophobic tails which bind to the hydrophobic cleft of the CD1d molecule and hydrophilic head interacting with iNKT TCRs [71, 88]. Lipid antigens are classified into exogenous and endogenous lipid antigens according to their origins. The most representative exogenous lipid antigen is α -galactosylceramide (α -GC) isolated from a marine sponge [76]. α -GC is a glycolipid in which galactose is linked to a ceramide backbone in α orientation. Several candidate endogenous lipid antigens have been reported

by far. For example, isoglobotrihexosylceramide (iGb3) [89], plasmalogen lysophosphatidyl ethanolamine (pLPE), ether lysophosphatidic acid (eLPA) [87], and a trace amount of α -linked glycosylceramides (e.g. α -glucosylceramide; α -GluCer) [90, 91] have been shown as endogenous lipid antigens. Although iGb3 was initially proposed to play a role in iNKT cell selection and development in the thymus, its role has been challenged by conflicting results from subsequent studies [92, 93]. iNKT cells are also activated by cytokines in the absence or presence of TCR stimulation. These cytokines include IL-12, IL-18, IL-23, and IL-25 [94-98]. IL-12 induces iNKT stimulation and IFN γ secretion, especially during infection [94].

2. Development and Heterogeneity of iNKT Cells

Like other conventional T cells, iNKT cells mature in the thymus, as evidenced by the depletion of iNKT cells in athymic mice [99]. iNKT cell differentiation occurs along the cortical-medulla axis within the thymus [100]. In the cortical region, CD4⁺CD8⁺ double positive (DP) thymocytes express CD1d and present lipid antigens to neighboring DP thymocytes [100, 101]. Thymocytes with proper TCR sequences (V α 14-J α 18 and V β 2, 7, or 8) are selected for positive selection. iNKT cells also undergo negative selection by CD1d⁺ dendritic cells (DCs) [102]. Mouse models with strong TCR stimulation, such as through neonatal injection of α -GC or transgenic expression of a TCR that binds too strongly to the CD1d-lipid antigen

complexes, show a reduction in iNKT cells due to negative selection [103, 104].

Signaling lymphocytic activation molecules (SLAMs) are crucial for the development of iNKT cells. SLAM signal is transduced through SLAM-associated protein (SAP) and the SRC family tyrosine kinase FYN axis and modulates the strength of TCR signaling after positive selection [103]. In turn, mice deficient for *Slamf6* (LY108), *Sh2d1a* (SAP), or *Fyn* exhibit fewer mature iNKT cells [105]. TCR signaling further induces the upregulation of crucial transcription factors for iNKT cell development such as EGR2, RUNX1, and PLZF (*Zbtb16*) [106, 107]. Especially, PLZF is the master transcription factor of innate-like T cells which mediates their effector functions [108].

iNKT cell development is categorized into various stages. There are two different models explaining iNKT cell development: “Linear model” and “Lineage diversification model” (Figure 4) [109]. In “Linear model”, DP thymocytes committed to iNKT cell lineage become CD24⁺CD44^{lo}NK1.1⁻ stage 0 iNKT cells. These cells then sequentially differentiate into CD24⁻CD44^{lo}NK1.1⁻ stage 1 iNKT cells, CD24⁻CD44^{hi}NK1.1⁻ stage 2 iNKT cells, and CD24⁻CD44^{hi}NK1.1⁺ fully mature stage 3 iNKT cells [110]. Intrathymic adoptive transfer studies have demonstrated that NK1.1⁻ iNKT cells could be differentiated into NK1.1⁺ iNKT cells [110, 111]. However, because some mouse strains do not express NK1.1 and certain NK1.1⁻ iNKT cells are functionally mature [79], “Linear model” is no longer actively explored these

days. In “Lineage diversification model”, CD24⁺CD44^{lo}NK1.1⁻ stage 0 iNKT cells are termed iNKT0 cells. These cells become CD24⁻NK1.1⁻CCR7⁺ iNKTp (iNKT precursor) cells which give rise to PLZF^{hi}RORγt⁻Tbet⁻ iNKT2 cells, PLZF^{int}RORγt⁺Tbet⁻ iNKT17 cells, and PLZF^{lo}RORγt⁻Tbet⁺ iNKT1 cells [79, 112, 113]. These nomenclatures are similar to Th2, Th17, and Th1 type cells, respectively, in their cytokine profiles. For example, iNKT2 cells produce IL-4 and IL-13, iNKT17 cells produce IL-17A, and iNKT1 cells secrete IFNγ [79, 114]. It is somewhat controversial whether iNKT2 cells are mature iNKT cell subpopulation. Adoptive transfer of hCD2⁺ iNKT cells isolated from BALB/c KN2 mice in which the first two exons of IL-4 gene have been replaced with human CD2 gene did not give rise to Tbet⁺ iNKT1 cells [79], suggesting that iNKT2 cells are mature subpopulation. However, recent single-cell RNA-sequencing (scRNA-seq) studies of thymic iNKT cells revealed that most iNKT2 cells are located in between immature iNKT cells (iNKT0 and iNKTp) and other mature iNKT cells (iNKT1 and iNKT17) in pseudotime analysis [115-117], and some iNKT2 cells could differentiate into iNKT1 or iNKT17 cells [117]. In addition, iNKT2 cells diminish with age [117, 118]. Thus, further investigation is required to clarify the heterogeneity within iNKT2 cells.

Peripheral iNKT cells exit the thymus during the iNKTp stage, migrate into peripheral tissue, differentiate, and reside in the periphery as long-term residents [112, 118]. Interestingly, even the majority of iNKT cells in the thymus are thymus-resident mature iNKT cells [112]. Tissue residency

of iNKT cells was validated by a parabiosis experiment between 6 to 8 weeks of age [99]. This suggests that peripheral iNKT cells are established before adolescence, and they maintain their number and unique characteristics within the residing tissue. However, compared to thymic iNKT cells, the functions, differentiation processes, and heterogeneity of peripheral iNKT cells are less understood.

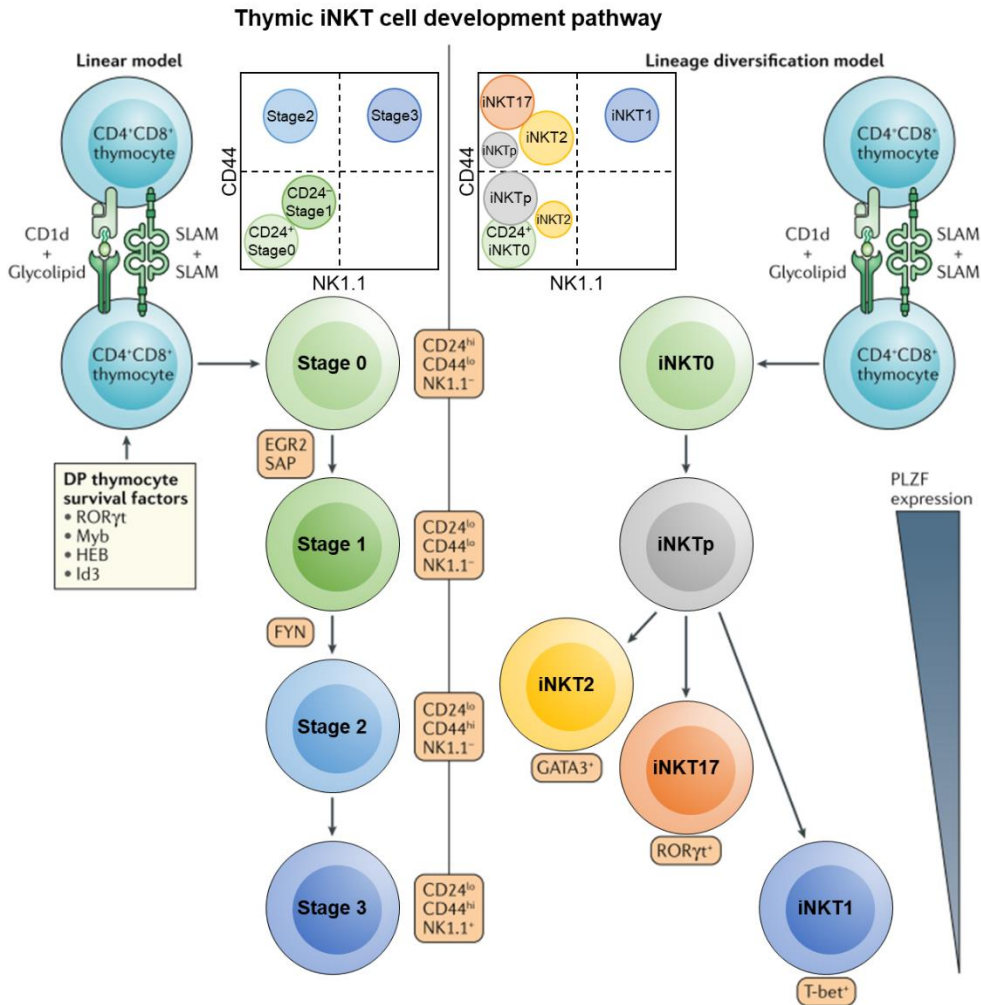


Figure 4. Development and heterogeneity of iNKT cells in thymus
 Two different models for iNKT cell development: “Linear model” and “Lineage diversification model”. This image was modified from Pellicci, D. G., *et al.* (2020). "Thymic development of unconventional T cells: how NKT cells, MAIT cells and $\gamma\delta$ T cells emerge." *Nat Rev Immunol* 20(12): 756-770.

3. iNKT Cells in WAT

iNKT cells make up approximately 5–10% of $\alpha\beta$ T cells in epididymal WAT [72, 119]. iNKT cells recognize lipid antigens loaded on CD1d [76] that is highly expressed in adipocytes [74]. Considering that adipocytes are one of the most crucial cell types in lipid metabolism and they highly express lipid antigen-presenting molecules, it is likely that iNKT cells play essential roles in adipose tissue. Previously, we and other groups have suggested that iNKT cells exert protective roles in adipose tissue [72, 74, 119, 120]. Mechanistically, adipose iNKT cells regulate inflammatory tone via secreting anti-inflammatory cytokines such as IL-4 and IL-10 [72, 74]. In addition, in response to obesity, iNKT cells induces the death of hypertrophic and inflamed adipocytes via upregulating Fas ligand (FasL) [51]. Activation of iNKT cells further stimulates the generation of new small adipocytes which are potent in insulin-stimulated glucose uptake [51].

Interestingly, it has been suggested that adipose iNKT cells display tissue-specific characteristics such as specific upregulation of E4BP4 (*Nfil3*) and its target gene, IL-10 [99, 121, 122]. Several studies have indicated that adipose iNKT cells might possess distinct developmental origins even in the thymus. Adipose iNKT cell development is partially independent of PLZF on their development, evidenced by incomplete depletion of adipose iNKT cells in PLZF KO whereas other iNKT cells are perfectly depleted [99]. Another study suggested the possibility that adipose iNKT cell precursors upregulating E4BP4 and PD-1 are induced in the thymus [123]. On the other

hand, a recent study revealed that adipose tissue microenvironment composed of high concentrations of FFAs could upregulate E4BP4 expression in iNKT cells via ER stress response [121]. The lineage of adipose iNKT cells, whether determined in the thymus or induced after infiltrating adipose tissue, remains to be comprehensively understood.

The heterogeneity of adipose iNKT cells in lean mice has been reported recently. Adipose iNKT cells are composed of two iNKT1 subpopulations and one iNKT17 subpopulation [121]. However, it remains still elusive what the functions of each subpopulation are and how they change in response to obesity.

III. Purpose of This Study

A recent study has proposed the protective roles of adipose iNKT cells in promoting adipocyte turnover [51]. However, the underlying mechanisms by which iNKT cells regulate the adipocyte turnover process, which comprises diverse steps such as adipocyte death and regeneration, remain unclear. Additionally, the influence of tissue-specific characteristics of adipose iNKT cells in orchestrating adipocyte turnover has yet to be investigated. Furthermore, how these protective functions of adipose iNKT cells are established during development and obesity is largely unknown.

In this thesis, I aimed to identify the heterogeneity of adipose iNKT cells, explore their development, and examine the functions of each adipose iNKT cell subpopulation. In Chapter I, I conducted a comparative analysis of iNKT cells in adipose tissue and thymus, where iNKT cell maturation begins. This analysis revealed the heterogeneity of adipose iNKT cells and their developmental process within adipose tissue. In Chapter II, I investigated the changes in adipose iNKT cells in obesity and explored the roles of each adipose iNKT cell subpopulation in adipocyte turnover process. Taken together, this study provides a comprehensive understanding of adipose iNKT cells in their development, functions, and changes in obesity, proposing the underlying mechanisms by which adipose iNKT cells participate in adipose tissue homeostasis.

CHAPTER ONE:

Adipose Tissue Microenvironment Regulates the Generation of Distinct iNKT Cell Subpopulation

1. Abstract

iNKT cell is one of the crucial cell types for adipose tissue homeostasis. Although recent studies have reported that adipose iNKT cells exhibit distinct molecular features compared to iNKT cells from other organs, the underlying mechanisms behind this transcriptional pattern have not been fully elucidated. Here, by comparing adipose iNKT cells with those from other organs, I demonstrated that adipose iNKT cells are composed of distinct subpopulations induced by adipose tissue microenvironment. I conducted scRNA-seq of adipose and thymic iNKT cells from lean mice and found that adipose iNKT cells are composed of three major subpopulations: two iNKT1 subpopulations and one iNKT17 subpopulation. Adipose and thymic iNKT cells showed distinct transcriptomes, with an adipose tissue gene signature being more pronounced in a specific adipose iNKT1 subpopulation, which I named adipose-specific iNKT1 (As-iNKT1) cells. Adoptive transfer experiments revealed that these KLRG1⁺ As-iNKT1 cells are induced among adipose tissue-infiltrated iNKT cells, but are significantly less induced in liver-infiltrated ones. Since CD1d ablation did not abolish As-iNKT1 cell generation in adipose tissue, it seems that secretory factors might induce the generation of As-iNKT1 cells. Taken together, these data propose that adipose tissue microenvironment promotes the distinct characteristics of iNKT cells within adipose tissue.

2. Introduction

Immune cells in adipose tissue are important regulators of adipose tissue metabolism. They play key roles in various pathophysiological processes in adipose tissue such as inflammation control, lipolysis, lipogenesis, adipocyte death, and regeneration [69, 70]. Among numerous adipose immune cells, iNKT cells have garnered attentions due to their ability to directly communicate with adipocytes via lipid antigens presented by adipocytes [74, 119]. iNKT cells are a type of innate-like T cells that recognize CD1d-loaded lipid antigens. In the early stage of development, iNKT cells are recruited into adipose tissue from the thymus, and they maintain their number and unique characteristics in adipose tissue after adolescence [99, 121, 124]. Adipose iNKT cells exhibit tissue-specific molecular features, such as upregulation of E4BP4 (*Nfil3*) and its target gene, IL-10 [99, 121, 122]. However, research on adipose iNKT cells has primarily focused on the E4BP4-IL-10 axis, while other significantly differing genes, such as *Klrg1* and *Stk32c* [99], have not been thoroughly examined. This limited understanding of adipose iNKT cells might hinder a comprehensive characterization of their functions in adipose tissue.

Peripheral immune cells play crucial roles in peripheral tissues, such as maintaining tissue homeostasis or exacerbating pathological conditions. These immune cells begin their maturation in bone marrow or thymus, then migrate to peripheral tissues where they undergo further maturation and

perform their functions [125]. Peripheral tissues often present distinct microenvironments, characterized by different metabolite availability and varying concentrations of certain molecules or cytokines compared to primary lymphoid organs [125]. For immune cells to function properly and survive in these environments, they should adapt by altering their characteristics. Given the highly resident nature of iNKT cells in adipose tissue [99] and the distinct microenvironment of adipose tissue, which is rich in lipid metabolites [121, 126], it is likely that adipose tissue microenvironment would significantly influence the characteristics of iNKT cells.

Recent study has suggested that the FFA-rich environment of adipose tissue could activate the ER stress-E4BP4 axis in certain subpopulations of adipose iNKT cells, explaining the expression of IL-10 [121]. However, the mechanisms underlying the expression of other adipose iNKT gene signatures have not been investigated. Additionally, adipose iNKT cells have yet to be comprehensively compared to other iNKT cells at single-cell resolution, despite their distinct characteristics. Furthermore, although previous reports suggested that the characteristics of adipose iNKT cells might be pre-determined in thymus [99, 123], this has not been fully elucidated.

In this study, I utilized scRNA-seq analysis to examine adipose iNKT cells at single-cell resolution and compared them with iNKT cells from other tissues, including thymus. I demonstrated that adipose iNKT cells are

enriched with KLRG1⁺ iNKT cells, which exhibit higher expression of adipose-specific gene signatures. Furthermore, I explored how adipose tissue microenvironment could induce KLRG1⁺ iNKT cells. Together, this study provides a comprehensive understanding of adipose iNKT cells in terms of their generation, functional heterogeneity, and the changes they undergo in adipose tissue.

3. Materials and Methods

Animals and treatments

2 ~ 24-week-old C57BL/6N male mice, 10-week-old C57BL/6N female mice, and 10-week-old BALB/c (000651, The Jackson Laboratory) male mice were purchased from JA BIO Incorporation (Suwon-si, Gyeonggi-do, Republic of Korea). *Cd1d* KO [127] and *Ja18* KO [128] mice were gifted by Doo Hyun Chung (Seoul National University College of Medicine, Seoul, Republic of Korea). CD45.1 (002014, The Jackson Laboratory) and 4Get mice (004190, The Jackson Laboratory) were gifted by Ro Hyun Seong (Seoul National University, Seoul, Republic of Korea). Adipocyte-specific *Cd1d1* knockout mice were generated by breeding *Cd1d1*-floxed mice (016929, The Jackson Laboratory) with *Adipoq*-Cre mice. The mice were housed in a specific pathogen-free, temperature- (22°C) and humidity- (50%) controlled animal facility under a 12-h/12-h light/dark cycle. High-fat diet (HFD) feeding experiments were performed using mice older than 8 weeks of age and fed a diet consisting of 60% calories from fat (D12492, Research Diets). To expand adipose iNKT cells *in vivo*, mice were intraperitoneally injected with α -galactosylceramide (α -GC) (1 μ g/mouse, AG-CN2-0013, AdipoGen) and sacrificed after 1 week. The animal studies were approved by the Institutional Animal Care and Use Committee of the Seoul National University.

Human participants

Human omental adipose tissue samples were obtained during weight reduction laparoscopic bypass surgery at the Metabolic Surgery Center in Seoul National University Bundang Hospital (SNUBH). This study was conducted in accordance with the Declaration of Helsinki and was approved by the Ethics Committee of the SNUBH (IRB No. B-1801445301 & B-1812513302). All participants provided their written informed consent. All participants were female, aged 30-50 years, and BMI between 35-50 kg/m². Tissue samples consisted of 25-mg tissue blocks. The processing of the tissues was initiated within 3 hours after removal from the patients without snap-frozen or cryo-preservation.

scRNA-seq library preparation

iNKT cells (TCR β^{int} CD1d.PBS57 tetramer⁺) were sorted from stromal vascular fraction (SVF) of epididymal WAT and cell suspension from thymus by flow cytometry (Fig. 5a). Tissue processing procedures are described below in adipose tissue fractionation and lymphocyte preparation sections. The sequencing library was generated using Chromium Single Cell 5' Library & Gel Bead Kit (PN-1000014, 10X Genomics), Chromium Single Cell A Chip kit (PN-1000009, 10X Genomics), and Chromium i7 Multiplex Kit (PN-120262, 10X Genomics). Single-cell suspension was loaded on the Single Cell A Chip (10X Genomics) and run in the Chromium Controller to generate gel bead-in-emulsions (GEMs) aiming to capture 4000 cells per channel. Following reverse transcription was performed using C1000 thermocycler

(Bio-Rad). Subsequent cDNA purification and library generation were performed according to the manufacturer's instructions provided.

scRNA-seq data analysis

Raw reads of sorted iNKT cells were mapped to a mouse reference genome (GRCm38) using the Cell Ranger software (v3.1.0) and the GRCm38.99 GTF file. A gene-by-cell count matrix for each sample was generated with default parameters, except for expected cells = 4000 (Adipose iNKT cells). Empty droplets were excluded using the emptyDrops function of the DropletUtils (v1.6.1) R package [129] with a false discovery rate (FDR) < 0.05. To filter out poor quality cells, cells with less than 1000 unique molecular identifiers (UMIs) and higher than 10% of UMIs mapped to mitochondrial genes were excluded using the calculateQCMetrics function of the scater (v1.14.0) R package [130]. To remove cell-specific biases, cell-specific size factors were calculated using the computeSumFactors function of the scran (v1.14.6) R package [131]. The aggregated UMI count matrix were divided by cell-specific size factors and log₂ transformed by adding a pseudocount of highly variable genes (HVGs) which were defined as genes with FDR < 0.05 for biological variability using the modelGeneVar function of the scran package. All cells across the samples were clustered into 21 clusters using the FindClusters function of the Seurat (v3.1.5) R package [132] on the first 15 principal components (PCs) of HVGs with resolution = 0.8. Clusters annotated as non-T and CD8⁺ T cell clusters were removed. After removing

non-iNKT cell clusters, cells were grouped into 15 clusters using the same method described above with the first 20 PCs. Cells annotated as non-T, gamma delta T, innate lymphoid cell, and CD8⁺ T cell clusters were excluded. Cells were regrouped into 13 clusters using the same method as described above with the first 15 PCs. Cells in the normal chow diet (NCD) and only adipose iNKT cells of NCD were grouped into 10 and 8 clusters, respectively, and visualized in the UMAP plot using the same method, with the first 15 PCs of 1000 HVGs.

To identify cell type-specific marker genes, the FindAllMarkers function of the Seurat package was used. Cell type signature score was calculated by the AddModuleScore function of the Seurat package. For gene ontology analysis, a database for annotation, visualization and integrated discovery (DAVID) [133, 134] was used. To project thymic, splenic, hepatic, and lymph node iNKT cells onto NCD adipose iNKT cells, for every non-adipose iNKT cell, k-Nearest Neighbors (k-NNs, k = 5) were inferred from NCD adipose iNKT cells with respect to the Pearson correlation coefficients of normalized expression data of HVGs for NCD adipose iNKT cells by using the knn.index.dist function of the KernelKnn (v1.0.8) R package [135]. To obtain the projection coordinate of non-adipose iNKT cells in UMAP plot, two-dimensional coordinates of 5-NNs in the UMAP plot of NCD adipose iNKT cells were averaged.

Adipose tissue fractionation

Adipose tissues were fractionated as described previously [136], with minor modifications. Briefly, epididymal WAT was minced and digested with collagenase buffer [0.1 M HEPES (Sigma-Aldrich), 0.125 M NaCl, 5 mM KCl, 1.3 mM CaCl₂, 5 mM glucose, 1.5% (w/v) bovine serum albumin (BSA) (A0100-010, GenDEPOT), and 0.1% (w/v) collagenase I (49A18993, Worthington)] in a shaking incubator at 37°C for 30 min. After centrifugation at 450 × g, 4°C for 3 min, the pelleted SVF was collected. The SVF was incubated in red blood cell (RBC) lysis buffer (17 mM Tris, pH 7.65, and 0.16 M NH₄Cl) for 3 min. Then, the SVFs were washed with phosphate-buffered saline (PBS) several times, passed through a 100-μm filter (93100, SPL), and collected by centrifugation at 450 × g for 3 min.

Isolation of SVFs from human adipose tissue

Human adipose tissues were rinsed in PBS twice, manually minced, and digested with collagenase buffer [0.1 M HEPES, 0.125 M NaCl, 5 mM KCl, 1.3 mM CaCl₂, 5 mM glucose, 1.5% (w/v) BSA, and 0.1% (w/v) collagenase I] in a shaking water bath at 37°C for 30–60 min. The subsequent steps were the same as those for preparing mouse adipose tissue fractionation.

Lymphocyte preparation from liver, spleen, thymus, and blood

Liver mononuclear cells (MNCs) were isolated using Percoll gradient as previously described [137]. Briefly, liver was gently passed through a nylon mesh and suspended in PBS. The cell suspension was centrifuged at 450 × g,

4°C for 3 min. The obtained cell pellet was resuspended in 40% Percoll (17-0891-01, Cytiva). Resuspended cell solution was carefully layered onto 70% Percoll and centrifuged at $800 \times g$, room temperature (RT) for 20 min with no break. MNCs were isolated from the middle layer. Then, the MNCs were washed with PBS several times, passed through a 100- μm filter (93100, SPL), and collected by centrifugation at $450 \times g$ for 3 min.

To isolate thymic or splenic lymphocytes, the thymus or spleen was mechanically disrupted in between two glass slides. Obtained cell suspension was centrifuged at $450 \times g$, 4°C for 3 min. The cell pellet was incubated in RBC lysis buffer for 3 min, washed with PBS several times, passed through a 100- μm filter, and collected by centrifugation at $450 \times g$ for 3 min.

To isolate blood MNCs, blood samples were collected in a Greiner Leucosep tube (GN163290, Sigma Aldrich) pre-equilibrated with 3 mL of Nycoprep 1.077 (1114550, Axis-Shield PoC AS). After centrifugation at $450 \times g$, RT for 10 min, the middle layer was carefully isolated, washed with PBS several times, passed through a 100- μm filter, and collected by centrifugation at $450 \times g$ for 3 min.

Fluorescence-activated cell sorting (FACS)

FACS was carried out as previously described [136], with minor modifications. Single-cell suspensions were incubated in Fc-receptor blocking antibody (1:300, 101302, BioLegend) at RT for 15 min prior to surface antigen staining. Then, the cells were stained with anti-TCR β chain

(1:300, 109220, BioLegend), CD1d.PBS57 tetramer (1:300, NIH Tetramer Core Facility), anti-KLRG1 (1:300, 138412 or 138418, BioLegend), anti-Ly6C (1:300, 128006 or 128012, BioLegend), anti-CD45.1 (1:300, 110722, BioLegend), anti-human CD3 (1:300, 300317, BioLegend), or anti-human TCR V α 24-J α 18 (1:300, 342903, BioLegend) at 4°C for 30 min. To detect intracellular proteins, the SVFs were fixed, permeabilized with Foxp3 / Transcription Factor Staining Buffer Set (00-5523-00, Thermo Fisher), and stained with anti-T-bet (1:100, 644810, BioLegend), anti-PLZF (1:100, 53-9320-80, Thermo Fisher), anti-ROR γ t (1:100, 25-6981-82, Thermo Fisher), or anti-Ki-67 (1:300, 151212, BioLegend) for 30 min. To detect cytokines, fixed and permeabilized cells were stained with anti-IFN γ (1:100, 557649, BD), anti-TNF α (1:100, 506324, BioLegend), or anti-IL-17A (1:100, 506922, BioLegend) for 30 min. The cells were analyzed or sorted using a FACS Canto II instrument (BD Biosciences) or FACS Aria II instrument (BD Biosciences), respectively. Analysis of the flow cytometry data was done by FlowJo software (FlowJo v10).

Intracellular cytokine staining

To investigate cytokine production of adipose iNKT cells, WAT was digested as described above, and SVF was activated as described previously [74], with minor modifications. Briefly, SVF was cultured for 4–6 hours in the presence of phorbol 12-myristate 13-acetate (50 ng/ml, P8139, Thermo Fisher), Ionomycin (1 μ g/ml, I0634, Thermo Fisher), and Brefeldin A (5 μ g/ml,

420601, BioLegend). Cultures were in complete RPMI media [10% fetal bovine serum (FBS) (Young In Frontier), 1% penicillin/streptomycin (Welgene), 10 mM HEPES, 1% non-essential amino acid (Welgene), 1 mM sodium pyruvate, 50 μ M β -mercaptoethanol, and 2 mM L-glutamine]. The cells were washed with PBS, stained, and analyzed by FACS Canto II instrument as described above.

Generation of primary iNKT cells

Primary iNKT cells were prepared as reported previously [138]. Briefly, the sorted TCR β^{int} CD1d.PBS57 tetramer⁺ iNKT cells from spleen were stimulated with anti-CD3e (3 μ g/mL, 14-0031-82, Thermo Fisher) and anti-CD28 antibodies (1 μ g/mL, 10312-20, Biogems) for three days and then expanded with mouse recombinant IL-2 (10 ng/mL, 212-12, Peprotech) and IL-7 (10 ng/mL, 217-17, Peprotech) for 10 days in complete RPMI media described above or adipocyte-conditioned media described below. The culture media of primary iNKT cells was changed every two days.

iNKT cell adoptive transfer

Primary iNKT cells ($\sim 5 \times 10^5$ cells/mouse), prepared as indicated above, were intravenously injected into 3- or 8-week-old male mice and analyzed after 8 weeks. *In vivo*-expanded Adipose iNKT cell subpopulations (donor cells) were purified by FACS from WAT of WT or CD45.1 male mice 1 week after α -GC injection. Each adipose iNKT cell subpopulation was concentrated to

~1000 cells/ μ l by centrifugation. Donor cells (20 μ l) were injected into the fat pads of WT C57BL/6 adult male mice. Donor CD45.1⁺ cells were harvested from the recipient animals 3 weeks after transplantation and subjected to FACS analysis.

Primary cell conditioned media (CM) preparation

Primary adipocytes were obtained from the floating fraction of fractionated epididymal WAT as described above and primary hepatocytes were isolated by collagenase perfusion method as described previously [139] from 12-to-16-week-old male mice. Primary cells were cultured in complete RPMI media for 2 days. CM was collected and frozen at -80°C until use.

DN32.D3 cell culture

DN32.D3 iNKT hybridoma cell line was cultured in complete RPMI media. Adipocyte conditioned media (AD CM) and primary hepatocyte conditioned media (Hep CM), made as described above, were mixed in a 1:1 ratio with fresh complete RPMI media and treated to 2×10^4 DN32.D3 cells in a 12-well plate. DN32.D3 cells were incubated for 2 days in CM and harvested.

RNA isolation and RT-qPCR

For primary adipocytes or DN32.D3 iNKT hybridoma, total RNA was isolated as previously described [51]. For sorted iNKT cells and *in vivo*-expanded adipose iNKT cell subpopulations, total RNA was isolated by using

Direct-zol™ RNA MiniPrep (R2062, Zymo Research) following the manufacturer's protocol. The isolated RNA was reverse-transcribed using the ReverTra Ace qPCR RT Kit (Toyobo). RT-qPCRs were run using SYBR Green master mix (DQ384-40h, BioFact). Target gene expression levels were normalized to *Rplp0* (36B4) expression. Primer sequences are listed in Table 2.

Statistical analysis

Data are presented as the mean \pm standard deviation (SD). n-Values indicated in the figures refer to biological replicates. The means of the two groups were compared using a two-tailed Student's t-test. Means of multiple groups were compared using one-way ANOVA followed by Tukey's post-hoc test. Two independent variables were compared using two-way ANOVA followed by Sidak's multiple comparisons test. Statistical analyses were performed using GraphPad Prism (GraphPad Software v10).

Table 2. Primer sequences in Chapter I

Primers for qRT-PCR			
Species	Gene	Forward (5' to 3')	Reverse (5' to 3')
Mouse	<i>Actg1</i>	CCCTATCGAACACGGCATTG	CCTGAATGGCCACGTACATG
	<i>Adipoq</i>	GGCAGGAAAGGAGAGCCTGG	GGCCTTGTCTTCTTGAAGA
	<i>AW112010</i>	GATGCAACAATACCTGGCGT	TGACGACCTGGGTCTGGTAT
	<i>Bhlhe40</i>	TGGTGATTTGTCGGGAAGAAA	ACGGGCACAAGTCTGGA AAC
	<i>Ccl4</i>	TTCTGTCTGTTTCTTTACACCT	CTGTCTGCCTTTTTGGTCAG
	<i>Cd1d1</i>	ACGTCCTGGCAGACAGTCCCAGG	TTAATGTTGAAAAGAGCGTACTGGC
	<i>Cd226</i>	CTGTCTGCAGAACCTGGACA	CATGGCATTGGAATGATGA
	<i>Dusp5</i>	ACCACCCACCTACACTACAA	CCTTCTCCCTGACACAGTCAATA
	<i>Gem</i>	ACAGCGACTGTGAGGTCTTG	GCCATTCGTTCTCCCCCTTA
	<i>Hspa1a</i>	TGGTGACGTCCGACATGAAG	GCTGAGAGTCTGTAAGTAGGC
	<i>Irfng</i>	TACTGCCACGGCAGTCAAGTGA	GCAGCGACTCCTTTTCCGCTTCTT
	<i>Irfngr1</i>	AGGTGTATTCGGTTCCTGG	AATACGAGGACGGAGAGCTG
	<i>Ifrd1</i>	AGAGTGCGAAGACAAGACAGG	TTCAGACAGCGCTCAATGCT
	<i>Il7r</i>	GGAAGTGGATGGAAGTCAAC	TGCGATAAACGACTTTCAGGT
	<i>Itga4</i>	CTCCCTCAAGATGATAAGTTGTTCAA	TGTGCAAATGTACTCTCTTCCA
	<i>Junb</i>	GACCTGCACAAGATGAACCACG	ACTGCTGAGGTTGGTGTAGACG
	<i>Klf2</i>	TGTGAGAAATGCCTTTGAGTTACTG	CCCTTATAGAAATACAATCGGTCATAGTC
	<i>Klrg1</i>	CCTCTGGACGAGGAATGGTA	ACCTCCAGCCATCAATGTTT
	<i>Maf</i>	AGCAGTTGGTGACCATGTCTG	TGGAGATCTCTGCTTGAGG
	<i>Nfil3</i>	CAGTCAGGTGACGAACATT	TTCCACCACCTGTTTTGA
	<i>Nr4a1</i>	TGTGAGGGCTGCAAGGGCTTC	AAGCGGCAGAACTGGCAGCGG
	<i>Pnpla2</i>	ACCATCACAGTGTCCCCATT	CTCCAGCGGCAGAGTATAGG
	<i>Rgs1</i>	TTGGAATGGACGTGAAAACA	CCTCACAAGCCAACCAGAAT
	<i>Rplp0</i> (Normalization gene)	GAGGAATCAGATGAGGATATGGGA	AAGCAGGCTGACTTGGTTGC
	<i>Satb1</i>	TGATAGAGATGGCGTTGCTG	TTTTGAGGGTGACCACATGA
	<i>Socs2</i>	CTGCGCGAGCTCAGTCAA	CAATCCGAGGTTAGTCGGT
	<i>Stk32c</i>	CCTTTGAGCTGGAGGAGATG	TCACGAAGTCTTGCTGGATG
	<i>Tbx21</i>	AGCAAGGACGGCGAATGTT	GGGTGGACATATAAGCGTTTC
	<i>Txnip</i>	ATCCCAGATACCCAGAAGC	TGAGAGTCGTCCACATCGTC
	<i>Val4-Ja18</i>	CTAAGCACAGCAGCTGCAC	CAGGTATGACAATCAGCTGACTCC
<i>Vim</i>	CCTGGCCGAGGACATCAT	TTCAAGGTCAAGACGTGCCA	
<i>Vps37b</i>	AGGACACTGAGAACATGGCAG	TCCGCTTGTCTGGTAGAC	

Table 3. List of genes used in iNKT cell subtype annotation

Gene List		
iNKT1 score	iNKT2 score	iNKT17 score
<i>Nkg7</i>	<i>Plac8</i>	<i>Tmem176a</i>
<i>Tbx21</i>	<i>Tesc</i>	<i>Serpina1a</i>
<i>Klrd1</i>	<i>9530036M11Rik</i>	<i>Blk</i>
<i>Ifitm10</i>	<i>Il4</i>	<i>Tmem176b</i>
<i>Ly6c2</i>	<i>Psmg2</i>	<i>Pxdc1</i>
<i>Klrb1c</i>	<i>Zbtb16</i>	<i>S100a4</i>
<i>Klrk1</i>	<i>Izumo1r</i>	<i>Actn2</i>
<i>Xcl1</i>	<i>Drosha</i>	<i>Il1r1</i>
<i>Fasl</i>	<i>Slamf6</i>	<i>Il23r</i>
<i>Gzmb</i>		<i>Ccr6</i>
<i>Cxcr3</i>		<i>Rorc</i>
<i>Gimap3</i>		<i>Aqp3</i>
<i>Klra3</i>		<i>Lrrc17</i>
<i>Ms4a4b</i>		<i>Tuba8</i>
<i>Klra9</i>		<i>Il17re</i>
<i>AW112010</i>		<i>Cabin1</i>
<i>Slamf7</i>		<i>Cd7</i>
<i>Klrc2</i>		<i>Chad</i>
<i>Lrrk1</i>		<i>Apol7b</i>
<i>H2-Q7</i>		<i>Tnfrsf25</i>
<i>Il2rb</i>		<i>Stab2</i>
<i>Rgs1</i>		<i>Emb</i>
<i>Fcer1g</i>		<i>Sdc1</i>
<i>Hsd11b1</i>		<i>Itgae</i>
<i>H2-Q6</i>		<i>Kcnk1</i>
<i>Stat4</i>		<i>Cxcr6</i>
<i>Fgl2</i>		<i>Aypl</i>
<i>Klre1</i>		<i>Preld2</i>
<i>Ctla2a</i>		<i>Ramp3</i>
<i>Klra5</i>		<i>5830411N06Rik</i>
<i>Klrc1</i>		<i>Plekhf1</i>
<i>Dapk2</i>		<i>Abhd15</i>
<i>Ppm1j</i>		<i>Abi3bp</i>
<i>Styk1</i>		<i>Jag1</i>
<i>Il12rb2</i>		<i>Mycn</i>
<i>Itga1</i>		<i>Vax2</i>
<i>H2-K1</i>		<i>Npl</i>
<i>Pik3ap1</i>		<i>1700113H08Rik</i>
<i>Klra8</i>		<i>Gm16271</i>
<i>Klra</i>		<i>Mmp25</i>
<i>Klra10</i>		<i>Rnf208</i>

4. Results

scRNA-seq analysis reveals distinct subpopulations of adipose iNKT cells

Although it has been reported that adipose iNKT cells upregulate E4BP4-IL-10 axis compared to iNKT cells from other organs [99, 121], it is largely unknown about other tissue-specific features of adipose iNKT cells and their functions. To address this, scRNA-seq of iNKT cells sorted from epididymal WAT was performed and these cells were compared with iNKT cells sorted from thymus (Fig. 5a), where iNKT cell development takes place. As shown in Fig. 5b, c, adipose iNKT cells and thymic iNKT cells were separately clustered, indicating that there would be distinct molecular features with tissue-specific gene expressions: *Nfil3* (E4BP4), *Klrg1*, and *Nr4a1* in WAT and *Zbtb16* (PLZF) and *Il7r* in thymus. These tissue-specific gene expression profiles were similar to those from a previous report comparing splenic and adipose iNKT cells [99], implying that there would be distinct transcriptome profiles in adipose iNKT cells (Fig. 6).

To examine heterogeneity, adipose iNKT cells were selected and re-clustered (Fig. 7a). Among the six subpopulations of adipose iNKT cells (A1–A6), most were either *Tbx21* (Tbet)-expressing iNKT1 cells (A1, A2, and A4–A6) or *Rorc* (ROR γ t)-expressing iNKT17 cells (A3) (Fig. 7b–d) [79, 140, 141]. Most adipose iNKT cell subpopulations except A4 and A6 were transcriptionally similar to previously reported subpopulations (Fig. 7e) [121]. As three minor subpopulations (A4–A6) composed less than 2.5% of the total

adipose iNKT cells (Fig. 7c), I primarily focused on three major subpopulations (A1–A3) in further analyses. KLRG1 and Ly6C were selected as surface antigens to distinguish the three subpopulations (Fig. 8a–e). KLRG1⁻Ly6C⁺, KLRG1⁺, and KLRG1⁻Ly6C⁻ adipose iNKT cells matched with A1, A2, and A3 subpopulations, respectively. Distinguishing adipose iNKT cells using these surface antigens successfully reflected both subtype ratio and expression of key transcription factors (Fig. 8f, g).

Even though thymic and adipose iNKT cells have distinct transcriptome profiles, the origin of their tissue-specific adaptations is largely unknown. To characterize shared and tissue-specific features of adipose iNKT cell subpopulations, Projection analysis was performed using thymic, splenic, hepatic, and lymph node iNKT cells [141]. iNKT cells from other organs were mostly projected on A1 subpopulation, but not on A2 subpopulation or the lower portion of A3 subpopulation (Fig. 9a–e). These data imply that A2 subpopulation and a subset of A3 subpopulation might have adipose-specific characteristics, whereas A1 subpopulation shows shared gene expression profiles across organs. In addition, tissue-specific genes of adipose iNKT cells were highly expressed in A2 subpopulation (Fig. 7b and 9f–h), indicating that the A2 subpopulation might determine tissue-specific characteristics of adipose iNKT cells.

To verify whether A2 would indeed be an adipose-specific subpopulation, various iNKT cell-bearing organs were tested to determine whether they express the A2 subpopulation-specific surface marker KLRG1.

KLRG1⁺ iNKT cells were barely detected in other organs, whereas approximately 30% of iNKT cells from WAT were KLRG1⁺ (Fig. 10a). To test whether this pattern would be sex- or strain-specific, female C57BL/6 and male BALB/c mice were examined. As they exhibited similar patterns to male C57BL/6 mice (Fig. 10b, c), A2 subpopulation was named as ‘adipose-specific (As)-iNKT1’. Also, there were KLRG1⁺ iNKT cells in human omental adipose tissue (Fig. 10d), suggesting that humans might contain an analogous iNKT subpopulation. On the other hand, as KLRG1⁻Ly6C⁺ iNKT cells were abundant in other organs (Fig. 10e), I named A1 subpopulation as ‘adipose universal (Au)-iNKT1’. A3–A6 subpopulations were named as ‘A-iNKT17’, ‘adipose cytotoxic (Ac)-iNKT1’, ‘A-Cycling iNKT1’, and ‘A-interferon stimulated gene (ISG) iNKT1’, respectively (Fig. 10f), following their signature gene expression profiles (Fig. 7b). Together, these data suggest that adipose tissue-selective KLRG1⁺ As-iNKT1 cells might mediate distinct features of adipose iNKT cells.

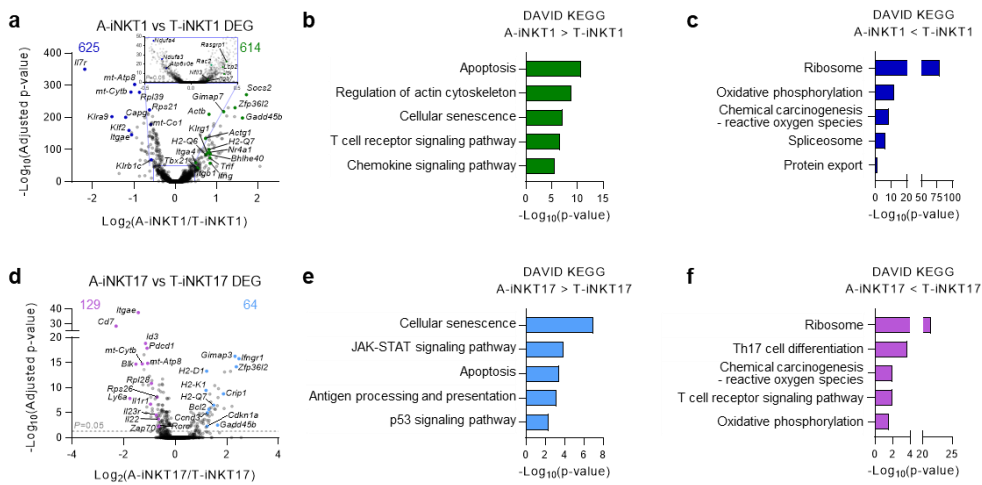


Figure 6. DEGs between adipose and thymic iNKT cells

a, Differentially expressed genes (DEGs) between A-iNKT1 and T-iNKT1 cells (Adjusted $P < 0.05$). **b,c**, KEGG pathway analysis of A-iNKT1 high-DEGs (**b**) and T-iNKT1 high-DEGs (**c**). **d**, DEGs between A-iNKT17 and T-iNKT17 cells (Adjusted $P < 0.05$). **e,f**, KEGG pathway analysis of A-iNKT17 high-DEGs (**e**) and T-iNKT17 high-DEGs (**f**).

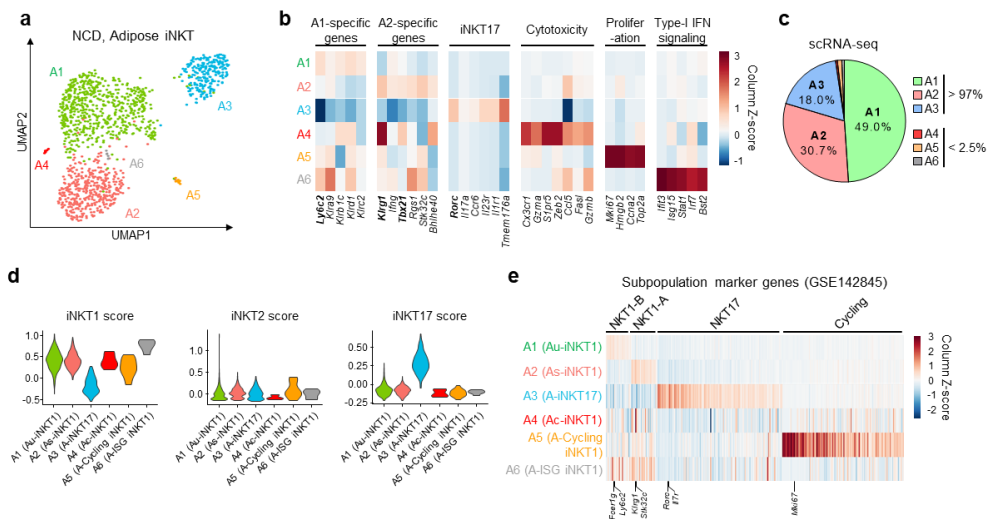
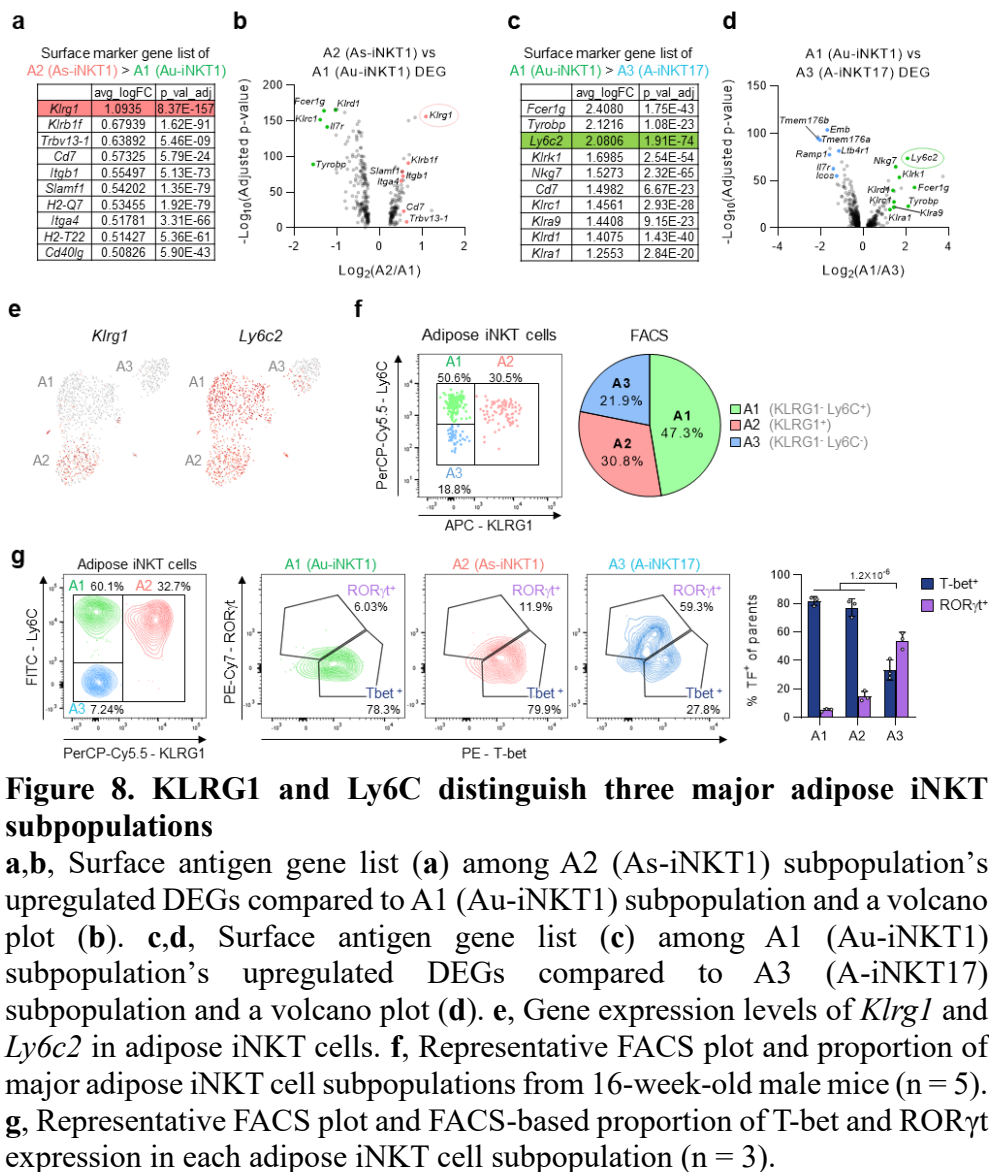


Figure 7. Adipose iNKT cells comprise three major subpopulations

a, Unsupervised clustering of adipose iNKT cells from 16-week-old male mice on a UMAP plot. **b**, Heatmap showing the expression levels of subpopulation marker genes. **c**, The ratio of each adipose iNKT cell subpopulation in scRNA-seq data. **d**, Gene signature score of iNKT1, iNKT2, and iNKT17 in adipose iNKT cells. Used genes are listed in Table 3. **e**, Heatmap showing the expression levels of subpopulation marker genes from previously reported adipose iNKT cell scRNA-seq data (GSE142845).



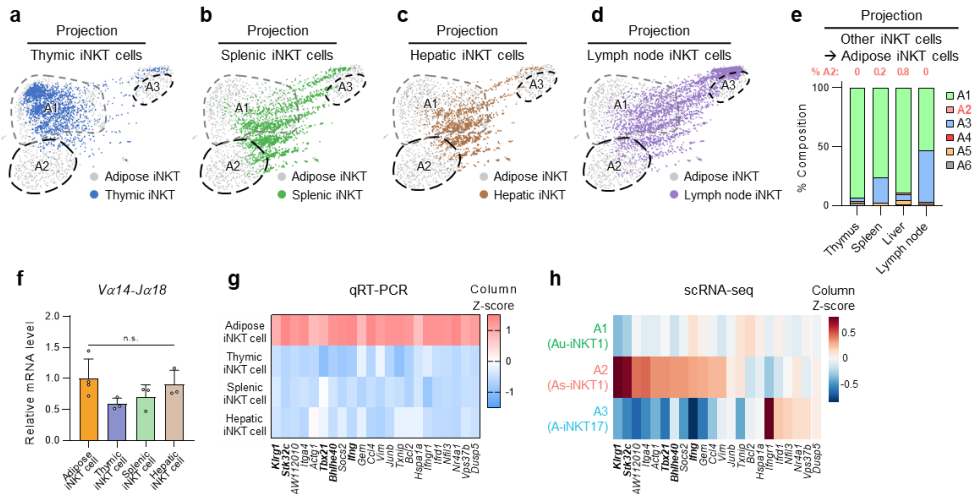


Figure 9. A2 subpopulation exhibits adipose tissue-specific features
a–d, Projection plots of iNKT cells from other organs to adipose iNKT cells. iNKT cells from other organs are projected to average of similar adipose iNKT cells' coordinates. Adipose iNKT cells are shown in gray, and iNKT cells from other organs are shown in color. Thymic, splenic, hepatic, and lymph node iNKT cells were used. scRNA-seq data of splenic, hepatic, and lymph node iNKT cells were obtained from GSE161495. **e**, Result of reference mapping of iNKT cells from other organs on adipose iNKT cells. The ratio of other iNKT cells mapped to specific adipose iNKT cell subpopulations was depicted as bar graphs and the percentage of cells mapped to A2 subpopulation was indicated on each bar graph. **f**, mRNA level of iNKT TCR alpha chain gene (*Va14-Ja18*) in iNKT cells from WAT (n = 4), thymus, spleen, and liver (n = 3). **g**, Heatmap showing the mRNA levels of adipose iNKT cell-specific genes in iNKT cells from WAT (n = 4), thymus, spleen, and liver (n = 3). qRT-PCR data was converted to heatmap. **h**, Heatmap showing the expression levels of adipose iNKT cell-specific genes in A1 (Au-iNKT1), A2 (As-iNKT1), and A3 (A-iNKT17) subpopulations.

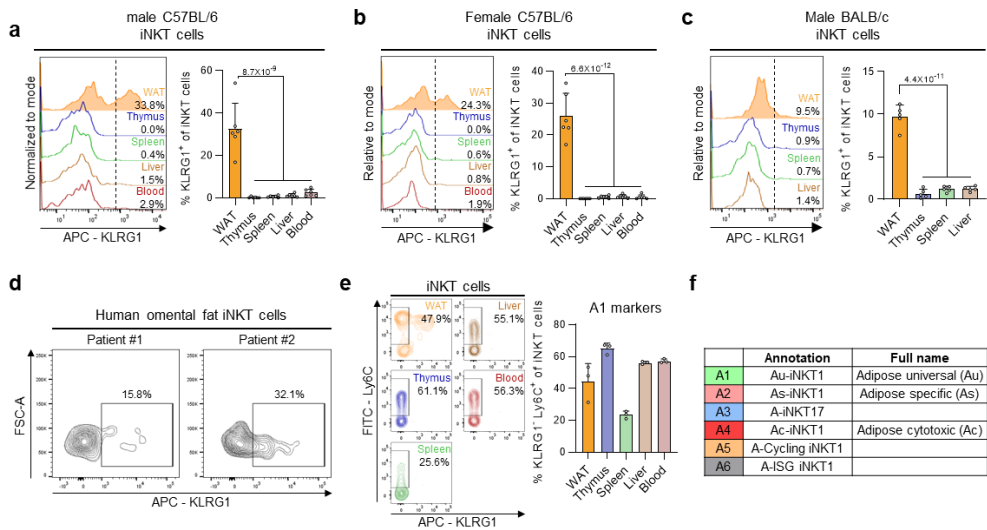


Figure 10. A2 marker gene, KLRG1-expressing iNKT cells are enriched in adipose tissue

a–c, Representative FACS plots and proportion of KLRG1⁺ iNKT cells from 10-week-old male mice (n = 6) (**a**), 10-week-old female C57BL/6 mice (n = 6) (**b**), and 10-week-old male BALB/c mice (n = 5) (**c**). **d**, Representative FACS plots of iNKT cells from human omental adipose tissue (n = 2). **e**, Representative FACS plots and proportion of KLRG1⁻Ly6C⁺ cells from 10-week-old male mice (n = 3). **f**, Annotation table of each adipose iNKT cell subpopulation.

Adipose tissue microenvironment generates As-iNKT1 cells

Peripheral iNKT cells start their maturation in the thymus, migrate into peripheral tissues via circulation, and remain in peripheral organs as long-term residents [78, 112, 124]. Consistent with a previous report [99], I observed that the number of iNKT cells increased with age in WAT (Fig. 11a). To investigate the underlying mechanisms by which KLRG1⁺ As-iNKT1 cells would be enriched in WAT, when As-iNKT1 cells could emerge in adipose tissue was carefully examined. Only a very few As-iNKT1 cells were found in WAT until 4 weeks, whereas their proportion increased after 8 weeks (Fig. 11b). To examine the generation of As-iNKT1 cells after 4 weeks of age, I tested when iNKT cells would infiltrate into adipose tissue during developmental process by adoptive transfer experiments using recipient mice of different ages (Fig. 11c). As shown in Fig. 11d, CD45.1⁺ iNKT cells injected at 3 weeks of age accounted for approximately 8% of the total adipose iNKT cells, and this ratio greatly decreased when they were injected at 8 weeks of age. More importantly, these data propose that the majority of adipose iNKT cells would infiltrate into adipose tissue in the early stage of life even before mice turned 3 weeks old. Thus, I speculated that the increase in As-iNKT1 cells after 4 weeks of age might be mediated by fat tissue microenvironment wherein iNKT cells reside. In addition, contrary to previous reports regarding the thymic determination of adipose iNKT cell lineage [123, 142], I could not identify any iNKT precursor cells co-expressing both *Nfil3* (E4BP4) and *Pdcd1* (PD-1) or expressing *Klrg1* in the

thymus (Fig. 12). These results further support the possibility that As-iNKT1 cells might be induced within adipose tissue, rather than being derived from pre-determined precursors of As-iNKT1 cells in the thymus. To test this idea, primary iNKT cells established from splenic iNKT cells were injected and subjected to examine the degree of KLRG1 expression according to infiltrated organs (Fig. 13a–c). The proportion of KLRG1⁺ iNKT cells was significantly higher in WAT, indicating that adipose tissue-specific microenvironment would be prone to mediate the transition of KLRG1⁻ iNKT cells into KLRG1⁺ iNKT cells (Fig. 13d). Also, a small subset of injected Au-iNKT1 cells converted into KLRG1⁺ As-iNKT1 cells after three weeks (Fig. 13e–g). In WAT, As-iNKT1 cells were more proliferative than other iNKT cells, which could facilitate their increase after adolescence (Fig. 13h).

Next, I attempted to identify the adipose tissue-specific factor(s) involved in As-iNKT1 cell generation. To figure out adipose tissue-specific microenvironmental factor(s) upregulated after 4 weeks of age, adipocytes from 4-, 8-, and 16-week-old mice were tested for their mRNA expression profiles. Adipocytes upregulated microenvironment-associated genes, such as *Cd1d1*, *Adipoq*, and *Pnpla2* (ATGL), which correspond to a lipid antigen-presenting molecule, adipokine, and lipolytic gene, respectively, as age increased (Fig. 14a). To examine whether As-iNKT1 cell generation might be mediated by chronic activation via CD1d-loaded lipid antigen(s), two mouse models were examined; adoptive transfer of CD45.1⁺ iNKT cells into young WT mice or *Cd1d* KO littermates and adipocyte-specific *Cd1d1* deficient

mouse model. As indicated in Fig. 14b–d, no differences were observed between the two genotypes in the ratio of As-iNKT1 cells. Thus, I tested whether adipocyte-derived secretory factor(s) could affect As-iNKT1 generation. Intriguingly, adipocyte-conditioned media (AD CM) upregulated several marker genes of As-iNKT1 cells, such as *Klrg1*, *Bhlhe40*, and *Rgs1* while downregulating Au-iNKT1 marker genes (Fig. 14e–i). These patterns were less prominent in hepatocyte-conditioned media (Hep CM)-treated group than in AD CM-treated group (Fig. 14e, g). Thus, these data suggest that factor(s) secreted from adipocytes would mediate the generation of As-iNKT1 cells in adipose tissue microenvironment.

In adipose tissue, iNKT cells actively secrete pro-inflammatory and anti-inflammatory cytokines to modulate adipose tissue immunity [70, 72, 74, 121]. To investigate the immunomodulatory characteristics of major iNKT cell subpopulations, including As-iNKT1, Au-iNKT1, and A-iNKT17 cells, cytokine profiles were examined. These subpopulations were distinguished by the expression pattern of KLRG1 and Ly6C after activation (Fig. 15a). Among three major subpopulations, As-iNKT1 cells showed the highest IFN γ and TNF α production after activation (Fig. 15b–d). A-iNKT17 cells produced high levels of IL-17A and IL-4, whereas Au-iNKT1 cells showed an intermediate level of Th1- and Th2-type cytokine production (Fig. 15b–d). Thus, it seems that inflammatory tone of adipose iNKT cells might be partly determined by relative ratio of each adipose iNKT cell subpopulation upon various metabolic stimuli, such as 1-week HFD feeding (Fig. 15e).

To further characterize As-iNKT1 cells, I compared two major iNKT1 cell subpopulations: Au-iNKT1 and As-iNKT1 cells. KEGG pathway analysis revealed that Th1/Th2 differentiation and TCR signaling pathway were enriched in As-iNKT1 cells while NK cell-mediated cytotoxicity-related genes were enriched in Au-iNKT1 cells (Fig. 16a). Accordingly, As-iNKT1 cells highly expressed TCR signaling components and their downstream genes, such as *Lat*, *Lcp2*, and *Nr4a1*, whereas Au-iNKT1 cells abundantly expressed activating or inhibitory NK receptors, such as *Ncr1*, *Klrk1*, *Klrc1*, and *Klrkl* (Fig. 16b) [143, 144]. Taken together, these data propose that adipose tissue microenvironment would mediate the generation of As-iNKT1 cells.

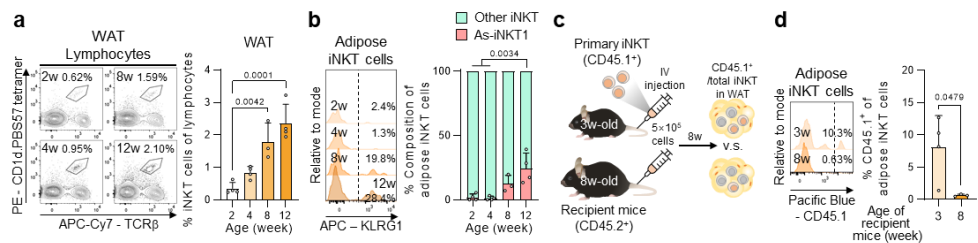


Figure 11. As-iNKT1 cells accumulate in adipose tissue as age increases
a,b, Representative FACS plots and proportion of iNKT cells (**a**) and As-iNKT1 cells (**b**) from male mice WAT (2w, 4w, 12w ($n=4$), and 8w ($n=3$)). **c** Experimental scheme for adoptive transfer of primary iNKT cells established from spleen. **d** Representative FACS plot and proportion of CD45.1⁺ iNKT cells among adipose iNKT cells (3w ($n=4$) and 8w ($n=3$)).

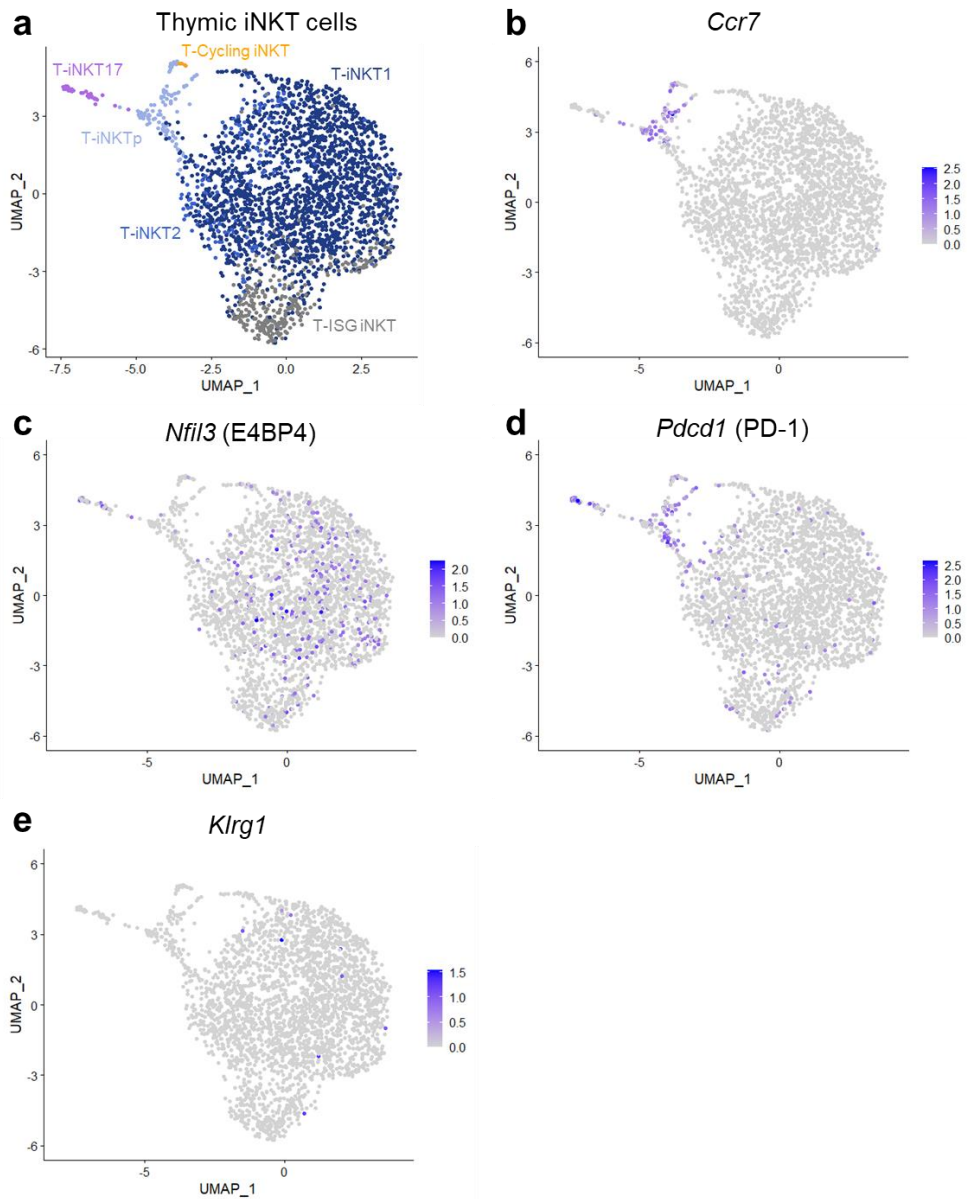


Figure 12. Adipose iNKT cell precursors are not identified among thymic iNKT cells

a, UMAP of thymic iNKT cells clustered as Fig. 5b. **b–e**, Gene expression levels of *Ccr7*, *Nfil3*, *Pcdcl1*, and *Klrg1* in thymic iNKT cells

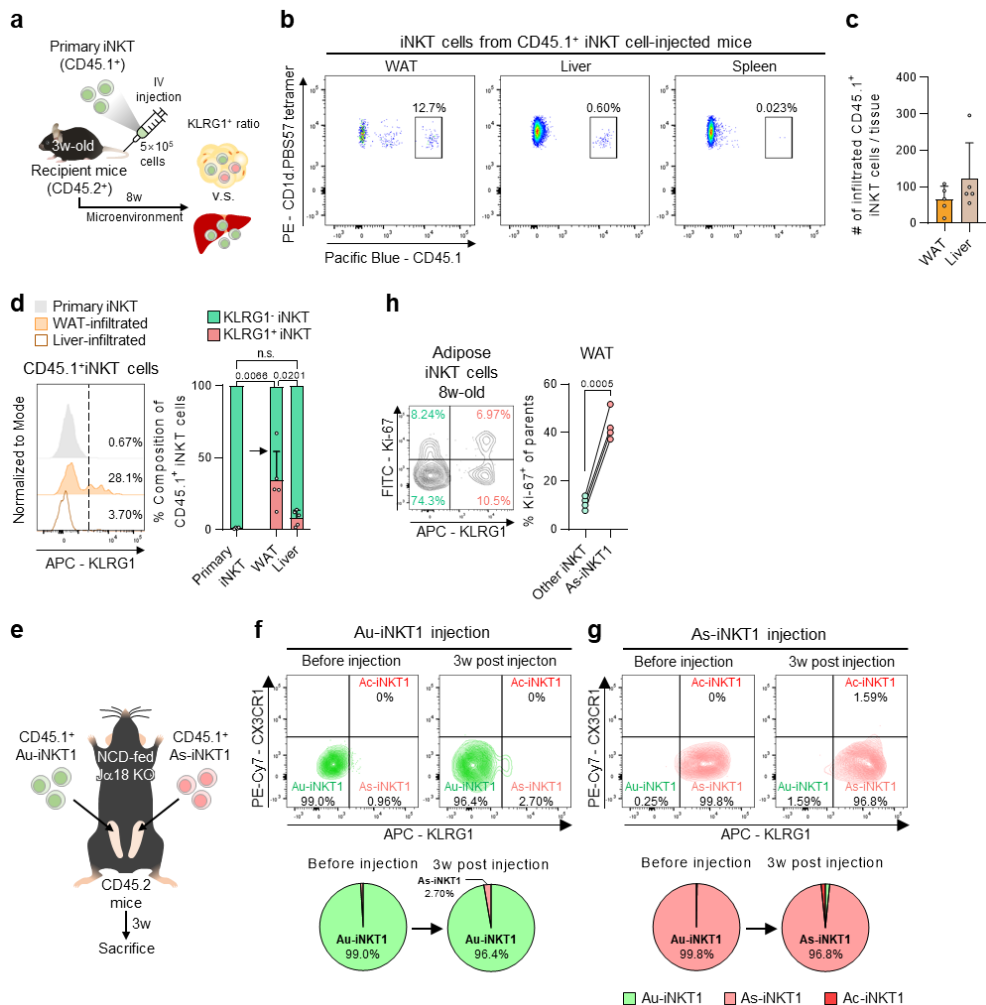


Figure 13. Adipose tissue microenvironment induces As-iNKT1 cell generation

a, Experimental scheme for adoptive transfer of primary iNKT cells. **b**, Representative FACS plots of CD45.1⁺ iNKT cells infiltrated into WAT, liver, and spleen in (a). **c**, Absolute number of infiltrated CD45.1⁺ iNKT cells in WAT and liver per mouse in (a) (n = 5). **d**, Representative FACS plot and proportion of KLRG1⁺ cells among primary iNKT cells (n = 4) and infiltrated CD45.1⁺ iNKT cells (n = 5). **e**, Experimental scheme for adoptive transfer of CD45.1⁺ Au-iNKT1 and As-iNKT1 cells. Sorted *in vivo*-expanded CD45.1⁺ iNKT cells were injected into each WAT fat pad of 16-week-old CD45.2 α 18 KO mice. **f,g**, FACS plots and composition of injected CD45.1⁺ donor iNKT cells in recipient mice after 3 weeks (n = 1). **h**, Representative FACS plot and proportion of Ki-67⁺ cells from 8-week-old male mice (n = 4).

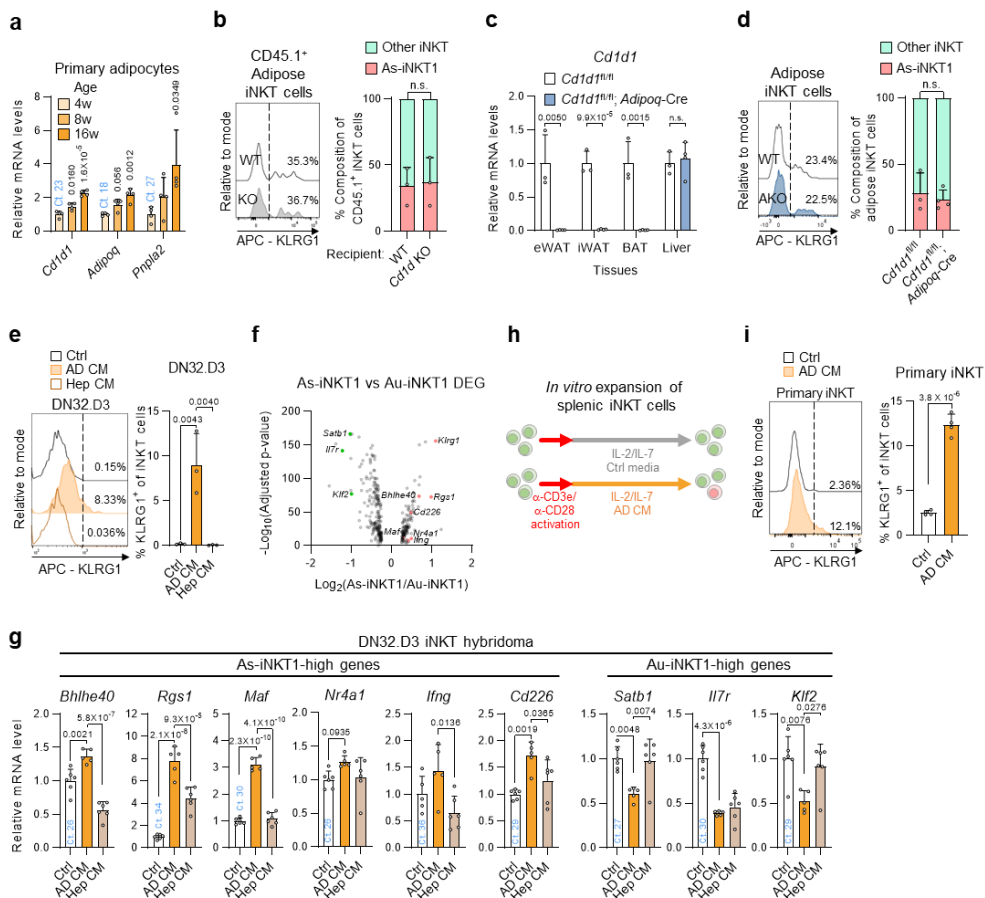


Figure 14. Secretory factors from adipocytes mediate As-iNKT1 cell generation

a, mRNA levels in adipocyte fraction of WAT from male mice (n = 4). p-values: versus 4-week-old. **b**, Representative FACS plot and proportion of KLRG1⁺ cells among CD45.1⁺ iNKT cells infiltrated into WAT of WT or *Cd1d* KO mice (n = 3). **c**, mRNA levels of *Cd1d1* in *Cd1d1*-floxed (n = 3) and adipocyte-specific *Cd1d1* KO mice (n = 4). **d,e**, Representative FACS plots and proportion of KLRG1⁺ cells among adipose iNKT cells (**d**) and among DN32.D3 iNKT hybridoma cells after culture with Control media (Ctrl), primary adipocyte-conditioned media (AD CM), or primary hepatocyte-conditioned media (Hep CM) (n = 3) (**e**). **f**, Volcano plot of DEGs between As-iNKT1 and Au-iNKT1 cells. **g**, mRNA levels in DN32.D3 cells after culture with Ctrl (n = 6), AD CM (n = 5), or Hep CM (n = 6). **h**, Experimental scheme of AD CM treatment to primary iNKT cells. **i**, Representative FACS plot and proportion of KLRG1⁺ cells among primary iNKT cells (n = 4).

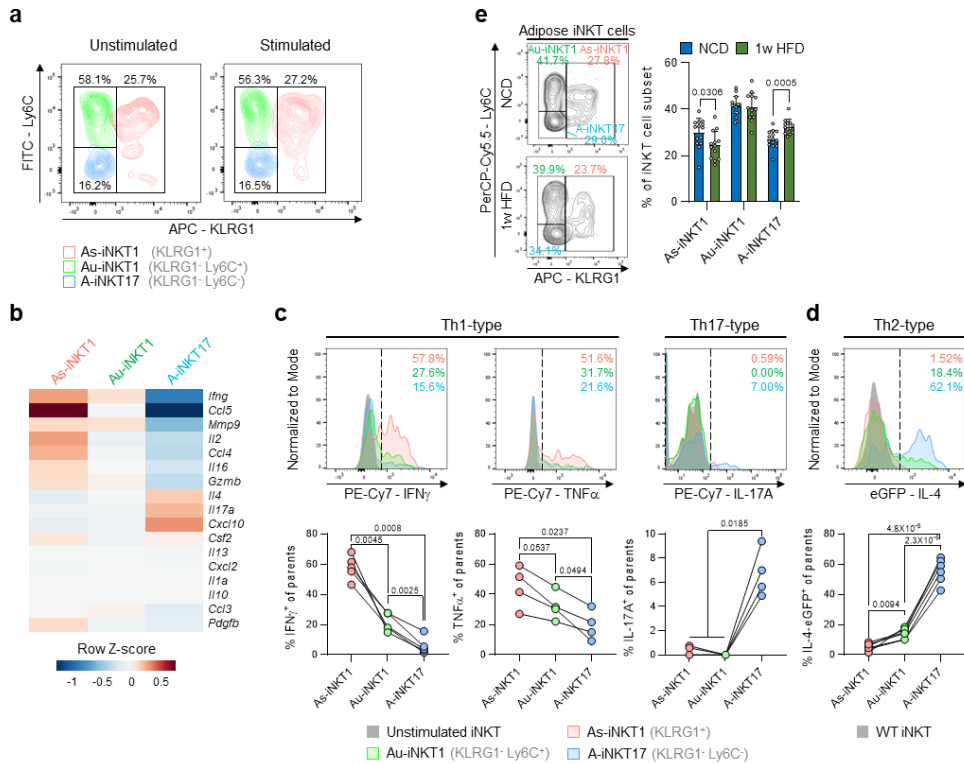


Figure 15. As-iNKT1 cells highly express Th1-type cytokines

a, Representative FACS plots of adipose iNKT cell subpopulations with or without activation using PMA/Ionomycin for 4 hours. **b**, Heatmap showing the expression levels of cytokine genes. **c**, Intracellular cytokine staining of As-iNKT1, Au-iNKT1, and A-iNKT17 cells from WT mice stimulated with PMA/Ionomycin. Representative FACS plots and proportion of cytokine-positive cells among each adipose iNKT cell subpopulation (TNF α , IL-17A (n=4), and IFN γ (n=5)). **d**, Representative FACS plot and proportion of eGFP⁺ cells among As-iNKT1, Au-iNKT1, and A-iNKT17 cells from IL-4/GFP enhanced transcript (4Get) mice (n=6). Connected dots represent paired cell populations in a single SVF (**c** and **d**). **e**, Representative FACS plots and FACS-based proportion of each subpopulation among total adipose iNKT cells in NCD- (n = 14) or 1-week HFD-fed mice (n = 13).

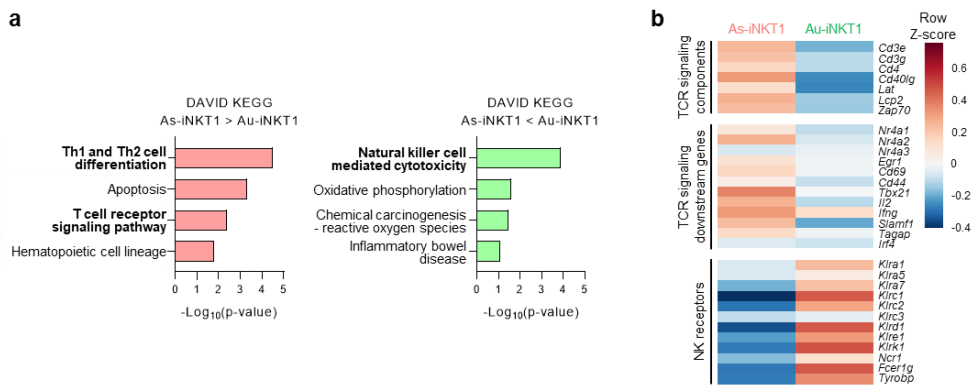


Figure 16. DEGs between Au-iNKT1 and As-iNKT1 cells
a, KEGG pathway analysis of As-iNKT1 high-DEGs and Au-iNKT1 high-DEGs ($P < 0.05$). **b**, Heatmap showing the expression levels of TCR signaling pathway-related genes, TCR signaling downstream genes, and NK receptors.

5. Discussion

It has been reported that adipose iNKT cells exhibit tissue-specific gene expression signatures, such as the upregulation of E4BP4 (*Nfil3*) [99, 121]. However, a comprehensive characterization of these adipose-specific genes, as well as how their expression is induced, has not been adequately explored.

In this study, I compared iNKT cells from multiple organs at single-cell resolution. Several lines of evidence suggest the existence of an adipose tissue-specific iNKT cell subpopulation, whose differentiation is likely determined by adipose tissue microenvironment. First, adipose and thymic iNKT cells exhibited distinct transcriptomes. Second, projection analysis of thymic, splenic, hepatic, and lymph node iNKT cells revealed that KLRG1⁺ As-iNKT1 cells barely overlapped with iNKT cells in other organs. In addition, As-iNKT1 cells upregulated several genes that are specifically expressed in adipose iNKT cells. Furthermore, adoptive transfer experiments demonstrated that adipose tissue microenvironment promotes the generation of As-iNKT1 cells in a CD1d-independent manner. Collectively, these data reveal distinct characteristics of adipose iNKT cells that have not been previously identified.

As-iNKT1 cells upregulated several genes compared to Au-iNKT1 cells. These include exhaustion-related genes such as *Klrg1* and *Rgs1* [145, 146], a transcription factor related to IFN γ production, *Bhlhe40* [147], surface receptor stimulating immune response, *Cd226* (DNAM-1) [148], TCR

downstream genes such as *Nr4a1* and *Nr4a2* [149], and genes with unknown functions in T cells such as *Gimap7* and *Stk32c*. The functions of As-iNKT1 cells in adipose tissue require further investigation. One hypothesis is that As-iNKT1 cells, which highly expressed Th1-type cytokines such as IFN γ and TNF α , would exacerbate adipose tissue inflammation in obesity. On the other hand, considering that adipose tissue inflammation could lead to adipogenesis [66, 67], As-iNKT1 cells might be involved in physiological adipose tissue expansion. Additionally, since the Th1 response is associated with cytotoxic functions, As-iNKT1 cells might contribute to adipocyte death in obesity.

Previously, KLRG1⁺ iNKT cells have been reported in peripheral organs such as liver, lung, and spleen after injection of α -GC [150-152]. These α -GC-induced KLRG1⁺ iNKT cells also exhibit Th1-polarized phenotypes in their cytokine profiles, cytotoxicity, and transcription factor expression, similar to those of As-iNKT1 cells [150]. Although these findings imply that KLRG1⁺ iNKT cells would be generated by α -GC, a strong iNKT cell stimulator, in various organs, I found that in lean adipose tissue, KLRG1⁺ iNKT1 cells were produced in adipose tissue microenvironment, independent from CD1d-mediated activation processes. In addition, adipocyte-derived secretory factors could upregulate some As-iNKT1 characteristic gene expressions. Recently, it has been suggested that distinct characteristics of adipose tissue-resident immune cells would be determined by adipose tissue microenvironment with high contents of lipid metabolites, adipokines, and sex hormones [121, 125, 153]. Future studies are needed to investigate which

factor(s) from the adipose tissue microenvironment could induce adipose-specific iNKT cell generation.

In conclusion, I examined and scrutinized heterogenous adipose iNKT cell subpopulations and compared their characteristics with iNKT cells from other organs. I found that adipose tissue microenvironment would induce a distinct adipose iNKT cell subpopulation producing Th1-type cytokines.

CHAPTER TWO:

Unique Subpopulations of Adipose iNKT Cells

Regulate Adipocyte Turnover

1. Abstract

Obese adipose tissue undergoes pathological remodeling characterized by adipocyte hypertrophy, inflammation, and insulin resistance. Adipocyte turnover, which includes the clearance of old adipocytes and the generation of new ones, could ameliorate this pathological remodeling in obesity. Although recent studies have suggested that the activation of adipose iNKT cells stimulates adipocyte turnover by inducing both adipocyte death and adipogenesis, the underlying mechanisms by which adipose iNKT cells mediate these diverse functions remain largely unknown. In this study, I identified obesity-induced changes in adipose iNKT cell subpopulations and investigated their roles in adipocyte turnover. Specifically, KLRG1⁺ As-iNKT1 cells differentiated into a CX3CR1⁺ cytotoxic subpopulation in obese mice. Moreover, CX3CR1⁺ iNKT cells specifically targeted and killed enlarged and inflamed adipocytes while also recruiting macrophages through CCL5. Additionally, adipose iNKT17 cells had the potential to secrete amphiregulin (AREG), which was involved in stimulating adipose stem and progenitor cell (ASPC) proliferation. Collectively, these data suggest that each adipose iNKT cell subpopulation plays a crucial role in regulating adipocyte turnover through interactions with adipocytes, ASPCs, and macrophages in adipose tissue.

2. Introduction

WAT is the major energy storage organ that undergoes dynamic remodeling in response to fluctuations in energy states [1, 5, 154]. In obesity, unhealthy WAT remodeling occurs with expanded adiposity and immune cell infiltration, resulting in obesity-related metabolic complications [16, 155]. Obese adipose tissue likely expands through two different processes that differ in morphology and metabolic outcomes. Hypertrophic WAT expansion often exhibits pathological phenotypes such as inflammation, hypoxia, and fibrosis, whereas hyperplastic WAT expansion tends to exhibit relatively beneficial phenotypes with a greater ability for energy storage, contributing to improved metabolic parameters [1, 14, 15].

Cellular turnover, which removes impaired cells and produces healthy ones, is crucial for maintaining tissue homeostasis [30, 156]. Indeed, it has been suggested that adipocyte turnover is important for adipose tissue homeostasis. Impaired adipocyte clearance or adipogenesis in obesity exacerbates metabolic dysfunctions [28, 49, 50]. Moreover, since the number of adipocytes appears to remain constant in adults [31-33], it is likely that adipocyte birth and death are closely associated with each other [34, 35, 42]. Adipocyte turnover involves complex processes that require the harmonious coordination of multiple cell types, including adipocytes, macrophages, and ASCs [5]. However, the precise regulatory mechanisms of adipocyte turnover process remain elusive.

Immune cells in adipose tissue are important regulators of adipose tissue metabolism [69]. Among various immune cells in adipose tissue, our group recently demonstrated that adipose iNKT cells could stimulate adipocyte turnover [51, 70]. In obesity, adipose iNKT cells facilitate the death of hypertrophic and inflammatory adipocytes while promoting ASPC proliferation, ultimately mitigating obesity-related metabolic dysfunctions [51]. However, the heterogeneity of adipose iNKT cells and their roles in orchestrating adipocyte turnover have not been fully elucidated.

In this study, by adopting scRNA-seq analysis and TCR repertoire analysis, I investigated adipose iNKT cell subpopulations involved in regulating each step of adipocyte turnover process. In response to obesity, A-iNKT1 cells differentiated into Ac-iNKT1 cells via clonal expansion. Ac-iNKT1 cells selectively removed hypertrophic and inflamed adipocytes and produced CCL5, which has macrophage-recruiting activity. Meanwhile, A-iNKT17 cells stimulated ASPC proliferation through the secretion of AREG. Collectively, these data suggest that adipose iNKT cell subpopulations coordinate adipocyte fate and adipose immune responses, thereby contributing to adipose tissue homeostasis.

3. Materials and Methods

Animals and treatments

8 ~ 24-week-old C57BL/6N male mice were purchased from JA BIO Incorporation (Suwon-si, Gyeonggi-do, Republic of Korea). α 18 KO mice [128] were gifted by Doo Hyun Chung (Seoul National University College of Medicine, Seoul, Republic of Korea). CD45.1 (002014, The Jackson Laboratory) mice were gifted by Ro Hyun Seong (Seoul National University, Seoul, Republic of Korea). 8 ~ 14-week-old adipocyte lineage-tracing mice (*Adipoq*-rtTA (033448, The Jackson Laboratory); TRE-Cre (006234, The Jackson Laboratory); *rosa26-loxp-stop-loxp*-YFP (006148, The Jackson Laboratory)) (CL57BL/6J) were obtained from the UNIST. The mice were housed in a specific pathogen-free, temperature- (22°C) and humidity- (50%) controlled animal facility under a 12-h/12-h light/dark cycle. High-fat diet (HFD) feeding experiments were performed using mice older than 8 weeks of age and fed a diet consisting of 60% calories from fat (D12492, Research Diets). Adipocyte lineage tracing mice were fed a doxycycline (600 mg/kg)-containing NCD for 2 weeks from 8 weeks of age. To expand adipose iNKT cells *in vivo*, mice were intraperitoneally injected with α -GC (1 μ g/mouse, AG-CN2-0013, AdipoGen) and sacrificed after 1 week. Amphiregulin (1 μ g/mouse, 989-AR, R&D Systems) or Gefitinib (20 mg/kg, S1025, Selleckchem) was intraperitoneally injected once a day for three consecutive days and mice were sacrificed on the next day. The animal studies were

approved by the Institutional Animal Care and Use Committee of the Seoul National University.

scRNA-seq library preparation

iNKT cells (TCR β^{int} CD1d.PBS57 tetramer⁺) were sorted from SVF of epididymal WAT by flow cytometry (Fig. 17a). Tissue processing procedures are described below in adipose tissue fractionation sections. The sequencing library was generated using Chromium Single Cell 5' Library & Gel Bead Kit (PN-1000014, 10X Genomics), Chromium Single Cell A Chip kit (PN-1000009, 10X Genomics), and Chromium i7 Multiplex Kit (PN-120262, 10X Genomics). Single-cell suspension was loaded on the Single Cell A Chip (10X Genomics) and run in the Chromium Controller to generate gel bead-in-emulsions (GEMs) aiming to capture 4000 cells per channel. Following reverse transcription was performed using C1000 thermocycler (Bio-Rad). Subsequent cDNA purification and library generation were performed according to the manufacturer's instructions provided. To generate a single-cell TCR sequencing library, 1/22.5 of total cDNA was used for V(D)J target enrichment PCR with mouse T cell-specific primer set (PN-1000071, 10X Genomics). The quality of libraries was confirmed using a Bioanalyzer High Sensitivity DNA kit (5067-4626, Agilent). Libraries were sequenced on an Illumina HiSeqX10 (paired-end 100 bp reads) aiming at an average of 50,000 read pairs (transcriptome libraries) or 5000 read pairs (TCR libraries) per cell.

scRNA-seq data analysis

Raw reads of sorted iNKT cells were mapped to a mouse reference genome (GRCm38) using the Cell Ranger software (v3.1.0) and the GRCm38.99 GTF file. A gene-by-cell count matrix for each sample was generated with default parameters, except for expected cells = 4000 (Adipose NCD), 3000 (Adipose 1wHFD), or 2500 (Adipose 8wHFD). Empty droplets were excluded using the emptyDrops function of the DropletUtils (v1.6.1) R package [129] with a false discovery rate (FDR) < 0.05. To filter out poor quality cells, cells with less than 1000 unique molecular identifiers (UMIs) and higher than 10% of UMIs mapped to mitochondrial genes were excluded using the calculateQCMetrics function of the scater (v1.14.0) R package [130]. To remove cell-specific biases, cell-specific size factors were calculated using the computeSumFactors function of the scran (v1.14.6) R package [131]. The aggregated UMI count matrix was divided by cell-specific size factors and log₂ transformed by adding a pseudocount of highly variable genes (HVGs) which were defined as genes with FDR < 0.05 for biological variability using the modelGeneVar function of the scran package. All cells across the samples were clustered into 21 clusters using the FindClusters function of the Seurat (v3.1.5) R package [132] on the first 15 principal components (PCs) of HVGs with resolution = 0.8. Clusters annotated as non-T and CD8⁺ T cell clusters were removed. After removing non-iNKT cell clusters, cells were grouped into 15 clusters using the same method described above with the first 20 PCs. Cells annotated as non-T, gamma delta T, innate lymphoid cell, and CD8⁺ T

cell clusters were excluded. Cells were regrouped into 13 clusters using the same method as described above with the first 15 PCs. Cells in the normal chow diet (NCD) and only adipose iNKT cells of NCD were grouped into 10 and 8 clusters, respectively, and visualized in the UMAP plot using the same method, with the first 15 PCs of 1000 HVGs. Cells in adipose iNKT cells across diet conditions were clustered into 9 clusters and visualized in the UMAP plot using same method except for the first 15 PCs of HVGs with $FDR < 0.05$ for biological variability.

To identify cell type-specific marker genes, the FindAllMarkers function of the Seurat package was used. Cell type signature score was calculated by the AddModuleScore function of the Seurat package. For gene ontology analysis, a database for annotation, visualization and integrated discovery (DAVID) [133, 134] was used. Pseudotime analysis was performed for adipose iNKT cells using the slingshot (v1.4.0) R package [157] based on the UMAP coordinates. To obtain a differentiation trajectory, the getLineages function of the slingshot R package was used with setting a start cluster as Au-iNKT1, and an ending cluster as Ac-iNKT1.

TCR repertoire analysis

Raw reads from paired V(D)J sequencing were processed using the cellranger vdj function of the Cell Ranger software (v3.1.0). To construct V(D)J segment-based reference, cellranger mkvdjref function of the Cell Ranger was used with mouse V(D)J segment sequences from international

ImMunoGeneTics information system (IMGT). For further analysis, contigs assigned as productive and high-confidence were used. Cells sharing the same V/J composition and identical CDR3 sequences both in heavy and light chains are regarded as the same clonotype. To calculate normalized diversity index, the ComputeShannonIndex function of the Stcr R package [158] was processed. CDR3 logo sequences were visualized by using WebLogo (v3.7.4).

Adipose tissue fractionation

Epididymal WAT was obtained from age-matched NCD-fed and 1- or 8-week HFD-fed mice. Adipose tissues were fractionated as described previously [136], with minor modifications. Briefly, adipose tissues were minced and digested with collagenase buffer [0.1 M HEPES (Sigma-Aldrich), 0.125 M NaCl, 5 mM KCl, 1.3 mM CaCl₂, 5 mM glucose, 1.5% (w/v) bovine serum albumin (BSA) (A0100-010, GenDEPOT), and 0.1% (w/v) collagenase I (49A18993, Worthington)] in a shaking incubator at 37°C for 30 min. After centrifugation at 450 × g, 4°C for 3 min, the pelleted SVF was collected. The SVF was incubated in red blood cell (RBC) lysis buffer (17 mM Tris, pH 7.65, and 0.16 M NH₄Cl) for 3 min. Then, the SVFs were washed with phosphate-buffered saline (PBS) several times, passed through a 100-μm filter (93100, SPL), and collected by centrifugation at 450 × g for 3 min.

Fluorescence-activated cell sorting (FACS)

FACS was carried out as previously described [136], with minor

modifications. Single-cell suspensions were incubated in Fc-receptor blocking antibody (1:300, 101302, BioLegend) at RT for 15 min prior to surface antigen staining. Then, the cells were stained with anti-TCR β chain (1:300, 109220, BioLegend), CD1d.PBS57 tetramer (1:300, NIH Tetramer Core Facility), anti-KLRG1 (1:300, 138412 or 138418, BioLegend), anti-Ly6C (1:300, 128006 or 128012, BioLegend), anti-CX3CR1 (1:300, 149020 or 149016, BioLegend), or anti-CD45.1 (1:300, 110722, BioLegend) at 4°C for 30 min. To detect cytokines, fixed and permeabilized cells were stained with anti-IFN γ (1:100, 557649, BD), anti-TNF α (1:100, 506324, BioLegend), or anti-IL-17A (1:100, 506922, BioLegend) for 30 min. Adipose stem cells were identified by anti-CD45 (1:300, 103132, BioLegend), anti-CD31 (1:300, 102410, BioLegend), and anti-PDGFR α (1:300, 562776, BD) among SVFs and their proliferation was assessed by anti-Ki-67 (1:200, 151212, BioLegend). The cells were analyzed or sorted using a FACS Canto II instrument (BD Biosciences) or FACS Aria II instrument (BD Biosciences), respectively. Analysis of the flow cytometry data was done by FlowJo software (FlowJo v10).

Intracellular cytokine staining

To investigate cytokine production of adipose iNKT cells, WAT was digested as described above, and SVF was activated as described previously [74], with minor modifications. Briefly, SVF was cultured for 4–6 hours in the presence of phorbol 12-myristate 13-acetate (50 ng/ml, P8139, Thermo Fisher),

Ionomycin (1 $\mu\text{g/ml}$, I0634, Thermo Fisher), and Brefeldin A (5 $\mu\text{g/ml}$, 420601, BioLegend). Cultures were in complete RPMI media [10% fetal bovine serum (FBS) (Young In Frontier), 1% penicillin/streptomycin (Welgene), 10 mM HEPES, 1% non-essential amino acid (Welgene), 1 mM sodium pyruvate, 50 μM β -mercaptoethanol, and 2 mM L-glutamine]. The cells were washed with PBS, stained, and analyzed by FACS Canto II instrument as described above.

iNKT cell adoptive transfer

In vivo-expanded Adipose iNKT cell subpopulations (donor cells) were purified by FACS from WAT of WT or CD45.1 male mice 1 week after α -GC injection. Each adipose iNKT cell subpopulation was concentrated to \sim 1000 cells/ μl by centrifugation. Donor cells (20 μl) were injected into the fat pads of WT C57BL/6 adult male mice. Donor CD45.1⁺ cells were harvested from the recipient animals 3 weeks after transplantation and subjected to FACS analysis.

Coculture

3T3-L1 pre-adipocytes were grown to confluence and then differentiated in 96- or 48-well culture plates. During differentiation, the cells were incubated in adipogenic medium [Dulbecco's modified Eagle's medium (DMEM) containing 10% FBS, 1 μM dexamethasone, 520 μM Isobutylmethylxanthine, and 850 nM insulin]. Two days after adipogenic induction, the cells were

treated with FI medium [DMEM containing 10% FBS and 850 nM insulin] for two days. Differentiated 3T3-L1 adipocytes were treated with FFA (500 μ M) as previously described [21]. Briefly, FFAs (palmitic acid or oleic acid) were dissolved in ethanol and diluted in DMEM low glucose media containing 1% FBS and 2% BSA at 55°C for 10 min. BSA-conjugated FFA-containing media were used for challenging differentiated 3T3-L1 adipocytes for 2 weeks and media were changed every two days.

For 3T3-L1 adipocyte and iNKT cell coculture experiment, iNKT cell subpopulations were sorted after *in vivo* iNKT cell expansion as indicated above and stained with CellTracker™ Green CMFDA Dye (C2925, Thermo Fisher) at 37°C for 30 min. 10^4 stained iNKT cells were cocultured with FFA-challenged 3T3-L1 adipocytes with or without anti-CD1d antibody (20 μ g/ml, BE0000, Bio X Cell) in 48 well plates. After 3 days of coculture, the cells were incubated with Hoechst 33342 (1:1000, H3570, Thermo Fisher) and propidium iodide (PI) (1:200, 51-66211E, Thermo Fisher) at 37°C for 20 min in the dark. The cells were imaged and quantified using a CQ1 microscope (Yokogawa). Diameters of lipid droplets were calculated by Image J software.

***In Vitro* Adipocyte Clearance by Macrophages**

3T3-L1 adipocytes were differentiated and treated with palmitic acid for 2 weeks in a 12-well plate or confocal dishes as described above. α -GC (100 ng/ml, AG-CN2-0013, AdipoGen) was added to 3T3-L1 adipocytes for 4 hours. After washing, neutral lipids in adipocytes were stained with

BODIPY 493/503 (200 ng/ml, D3922, Thermo Fisher). The adipocytes were then washed and cocultured with 3×10^4 of DN32.D3 cells. After 24 hours, 5×10^4 of Raw 264.7 cells were stained with CellTracker™ Deep Red Dye (C34565, Thermo Fisher) at 37°C for 30 minutes, then added to 3T3-L1 adipocyte-DN32.D3 cell mixture. Raw 264.7 cells were analyzed 24 hours after coculture using the FACS Canto II instrument or the CQ1 microscope (Yokogawa).

Immunohistochemistry

Whole-mount imaging was carried out as previously described with minor modifications [51]. Whole epididymal WAT was fixed in 4% paraformaldehyde overnight and blocked with PBS containing 5% horse serum and 0.3% Triton X-100 for 1 hour. The fixed tissues were incubated with primary antibodies against GFP (1:1000, NB100-62622, Novus Biologicals) and perilipin (1:1000, 20R-PP004, Fitzgerald) at 4°C overnight. The tissues were then washed three times for 10 min each, incubated with secondary antibodies (1:1000, A-21099, Thermo Fisher and 1:1000, ab6904, Abcam) and Hoechst 33342 at RT for 4 hours, washed three times for 10 min each, and mounted on slides in 8-well plates (155409, Nunc Lab-Tek II). Tissues were observed and imaged using a CQ1 microscope. Diameters of lipid droplets were calculated by Image J software.

For immunohistochemistry, small fractions of fat tissues were isolated from mice, fixed in 4% paraformaldehyde, and embedded in paraffin.

The paraffin blocks were cut into 5- μ m sections and stained with hematoxylin and eosin. Tissues were imaged using a digital slide scanner (Axio Scan Z1, Carl Zeiss).

THP-1 monocyte migration assay

Synthetic CCL5 peptides (500 ng/ml, 250-07, Peprotech) were dissolved in serum-free RPMI1640 media and placed in a 24-well culture plate. THP-1 cells were pre-stained with CellTracker™ Deep Red Dye (C34565, Thermo Fisher) for 30 min, and 5×10^4 (per well) THP-1 cells were loaded on the surface of the upper layer of Trans-well insert (8 μ m pore, 3422, Corning). 6 hours after incubation, the upper layer and Trans-well insert were carefully removed. Migrated THP-1 cells were imaged and quantified using the CQ1 confocal microscope and cell counter (NanoEntek), respectively.

RNA isolation and RT-qPCR

For adipose tissue or 3T3-L1 adipocytes, total RNA was isolated as previously described [51]. For *in vivo*-expanded adipose iNKT cell subpopulations, total RNA was isolated by using Direct-zol™ RNA MiniPrep (R2062, Zymo Research) following the manufacturer's protocol. The isolated RNA was reverse-transcribed using the ReverTra Ace qPCR RT Kit (Toyobo). RT-qPCRs were run using SYBR Green master mix (DQ384-40h, BioFact). Target gene expression levels were normalized to *Rplp0* (36B4) expression. Primer sequences are listed in Table 4.

Statistical analysis

Data are presented as the mean \pm standard deviation (SD). N-values indicated in the figures refer to biological replicates. The means of the two groups were compared using a two-tailed Student's t-test. Means of multiple groups were compared using one-way ANOVA followed by Tukey's post-hoc test. Two independent variables were compared using two-way ANOVA followed by Sidak's multiple comparisons test. Statistical analyses were performed using GraphPad Prism (GraphPad Software v10).

Table 4. Primer sequences in Chapter II

Primers for qRT-PCR			
Species	Gene	Forward (5' to 3')	Reverse (5' to 3')
Mouse	<i>Areg</i>	GCAGATACATCGAGAACCTGGAG	CCTTGTCATCCTCGCTGTGAGT
	<i>Bad</i>	GGGATGGAGGAGGAGCTTAG	CCCACCAGGACTGGATAATG
	<i>Bax</i>	TGGAGATGAACTGGACAGCA	GATCAGCTCGGGCACTTTAG
	<i>Casp8</i>	ATCCTATCCCACGGTGACAA	TGTGGTTCTGTTGCTCGAAG
	<i>Ccl2</i>	AGGTCCTGTCTGCTTCTG	TCTGGACCCATTCTTCTTG
	<i>Ccl5</i>	GCTGCTTTGCTACCTCTCC	TCGAGTGACAAACACGACTGC
	<i>Cx3er1</i>	CAGCATCGACCGGTACCTT	GCTGCACTGTCCGGTTGTT
	<i>Fasl</i>	CCCCAGTACACCCTCTGAAA	CAAGACTGACCCCGGAAGTA
	<i>Gzma</i>	TGTGAAACCAGGAACCAGATG	GGTGATGCCTCGCAAATA
	<i>Gzmb</i>	TCGACCCTACATGGCCTTAC	TGGGGAATGCATTTTACCAT
	<i>Il17a</i>	TCCAGAAGGCCCTCAGACTA	AGCATCTTCTCGACCCTGAA
	<i>Il6</i>	AGTTGCCTTCTTGGGACTGA	TCCACGATTTCCAGAGAAC
	<i>Klrg1</i>	CCTCTGGACGAGGAATGGTA	ACCTCCAGCCATCAATGTTC
	<i>Rgs1</i>	TTGGAATGGACGTGAAAACA	CCTCACAGCCAACCAGAAT
	<i>Rorc</i>	TGCAAGACTCATCGACAAGG	AGGGGATTCAACATCAGTGC
	<i>Rplp0</i> (Normalization gene)	GAGGAATCAGATGAGGATATGGGA	AAGCAGGCTGACTTGTTGTC
	<i>Slpr5</i>	GATCCCTTCTGGGTCTAGC	TAGAGCTGCGATCCAAGGTT
	<i>Stk32c</i>	CCTTTGAGCTGGAGGAGATG	TCACGAAGTCTTGCTGGATG
<i>Zeb2</i>	CATGAACCCATTTAGTGCCA	AGCAAGTCTCCCTGAAATCC	

4. Results

In obesity, As-iNKT1 cells give rise to Ac-iNKT1 cells

In obesity, adipose iNKT cells play a protective role in the maintenance of adipose tissue homeostasis through the clearance of detrimental adipocytes [51]. Nonetheless, it remains elusive how adipose iNKT cells would acquire or boost the roles of promoting adipocyte clearance in obesity. To investigate obesity-induced changes in adipose iNKT cells, I performed scRNA-seq paired with TCR repertoire analysis on adipose iNKT cells from NCD-, 1-week, or 8-week HFD-fed age-matched mice (Fig. 17a, b). Adipose iNKT cells were clustered into the six subpopulations (A1–A6) as in NCD condition with similar marker gene expression patterns (Fig. 17c). However, the proportions of iNKT cell subpopulations and their gene expression patterns were altered upon HFD. The proportions of As-iNKT1, Ac-iNKT1, and A-Cycling iNKT1 cells were increased after 8-week HFD feeding, whereas the proportion of Au-iNKT1 cells was relatively decreased, and those of A-iNKT17 and A-ISG iNKT1 cells were not altered (Fig. 17d, e). A-Cycling iNKT1 and A-ISG iNKT1 cells were minor subpopulations accounting for less than 5% of the total adipose iNKT cells under all conditions (Fig. 17d, e). Thus, I decided to exclude A-Cycling iNKT1 and A-ISG iNKT1 cells from further analyses and mainly focused on four subpopulations: Au-iNKT1 (A1), As-iNKT1 (A2), A-iNKT17 (A3), and Ac-iNKT1 cells (A4). To distinguish *Klrg1*-expressing Ac-iNKT1 cells from As-iNKT1 cells, CX3CR1 was

selected as the surface antigen of Ac-iNKT1 cells (Fig. 18a–d). FACS analysis confirmed that As-iNKT1 and Ac-iNKT1 cells were increased upon 8 weeks of HFD feeding, whereas Au-iNKT1 cells were decreased (Fig. 18d, e).

In the previous chapter, As-iNKT1 cells were adipose tissue-selective subpopulation. To understand how obesity could modulate gene expression profiles in As-iNKT1 cells, differentially expressed genes (DEGs) between NCD and 8-week HFD-fed conditions were analyzed. Most adipose iNKT cell subpopulations showed activation-associated phenotypes such as upregulation of *Nur77 (Nr4a1)* (Fig. 19a) [159]. As-iNKT1 cells upregulated proliferation-associated genes (*Hmgb2* and *Plk3*) [117, 160], their characteristic gene associated with IFN γ expression (*Bhlhe40*) [147], and specific TCR V β chain gene (*Trbv13-1*, V β 8.3) upon 8-week-HFD feeding (Fig. 19a, b). On the other hand, several NK receptor genes such as *Cd160* and *Klrk1* (NKG2D) were downregulated in As-iNKT1 cells (Fig. 19a, b). These data suggest that in obesity, As-iNKT1 cells would become more proliferative and certain As-iNKT1 cells with specific V β might be selected. Other adipose iNKT cell subpopulations also changed upon HFD. Au-iNKT1 cells upregulated NK receptors such as *Klrk1* and *Klrk2* (NKG2C) while downregulating *Ifng* (Fig. 19c). A-iNKT17 cells upregulated *Zbtb16* and *Rora* while downregulating some GTPase of immunity-associated protein (GIMAP) family genes and MHC I molecules (Fig. 19d).

It is well known that immune cells could differentiate into subsets

upon pathological stimuli [161]. To test whether As-iNKT1 cells could differentiate into other subpopulations in obesity, I performed pseudotime analysis on three iNKT1 cell subpopulations: Au-iNKT1, As-iNKT1, and Ac-iNKT1 cells. As shown in Fig. 20a, As-iNKT1 cells appeared to be derived from Au-iNKT1 cells and could differentiate into Ac-iNKT1 cells. Clonotype overlap analysis further verified that Ac-iNKT1 cells would share an origin with As-iNKT1 cells (Fig. 20b, c). Further, A-Cycling iNKT1 cells were the proliferating subset of As-iNKT1 and Ac-iNKT1 cells, which might explain their numerical increase in obesity (Fig. 20b). To investigate the hierarchy between Au-iNKT1, As-iNKT1, and Ac-iNKT1 cells *in vivo*, Au-iNKT1 and As-iNKT1 cells were injected into the left and right fat pads of HFD-fed iNKT cell-deficient $J\alpha 18$ KO mice [128], respectively (Fig. 20d). It is interesting to note that Au-iNKT1 cells differentiated into both As-iNKT1 and Ac-iNKT1 cells, whereas As-iNKT1 cells only differentiated into Ac-iNKT1 cells in obesity (Fig. 20e–g). Moreover, the differentiation of As-iNKT1 cells was accompanied by a decrease in the CDR3 β diversity of Ac-iNKT1 cells (Fig. 21a, b), indicating that certain As-iNKT1 cells would differentiate into Ac-iNKT1 cells via clonal expansion. Taken together, these data propose that As-iNKT1 cells could differentiate into Ac-iNKT1 cells upon exposure to obesogenic stimuli.

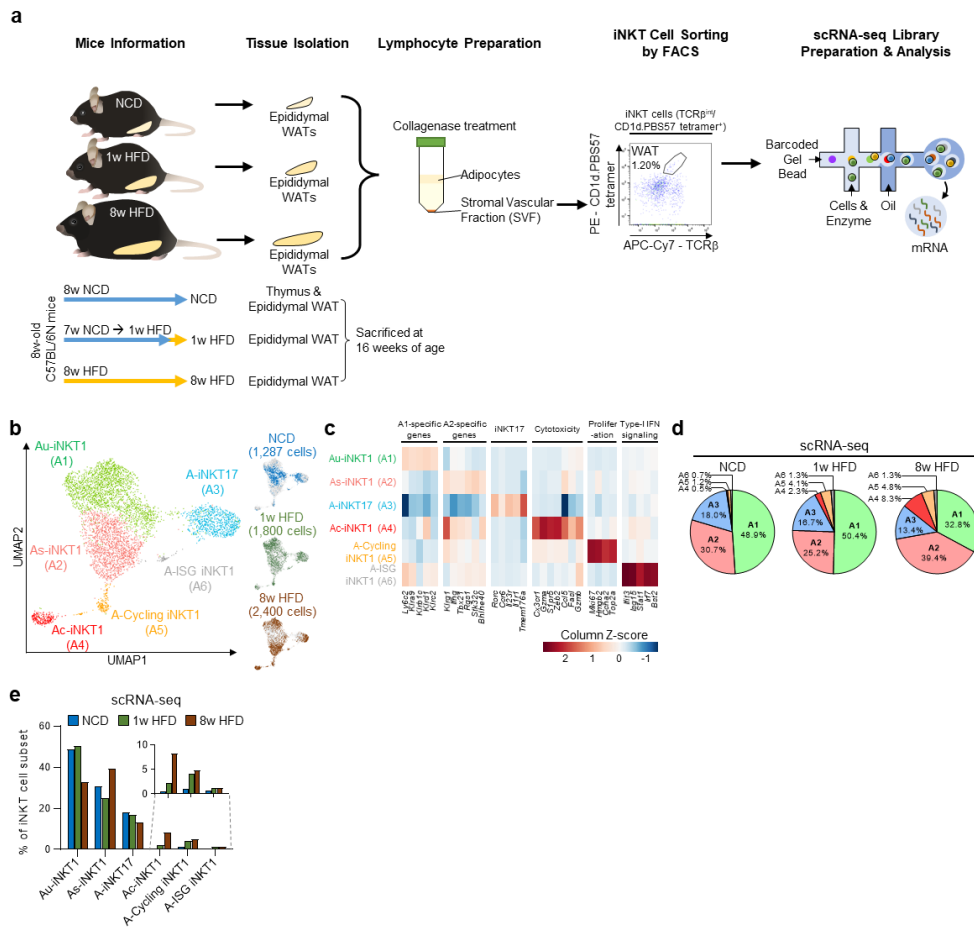


Figure 17. scRNA-seq data of adipose iNKT cells isolated from variable length of HFD feeding conditions

a, Experimental scheme for scRNA-seq. Thymus and epididymal WAT were extracted from 16-week-old male C57BL/6N mice. SVF was obtained through collagenase treatment. iNKT cells ($\text{TCR}\beta^{\text{int}}\text{CD1d.PBS57 tetramer}^{\text{+}}$) were obtained via flow cytometry. A scRNA-seq library was prepared using a 10X genomics platform. **b**, Unsupervised clustering of iNKT cells from WAT of NCD-, 1-week, or 8-week HFD-fed mice. 1,287 cells from NCD-, 1,800 cells from 1-week, and 2,400 cells from 8-week HFD-fed mice on a UMAP plot. **c**, Heatmap showing the expression levels of subpopulation marker genes. **d,e**, Proportion of each adipose iNKT cell subpopulation in scRNA-seq data as pie charts (**d**) or bar graphs (**e**).

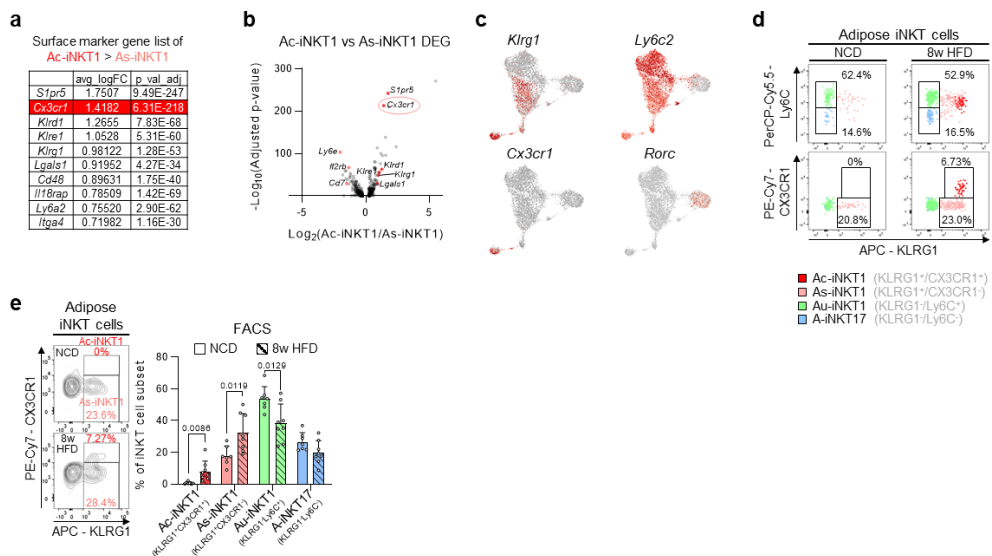


Figure 18. CX3CR1 distinguishes Ac-iNKT1 cells from As-iNKT1 cells
a, Surface antigen gene list among Ac-iNKT1 cells' upregulated DEGs compared to As-iNKT1 cells. **b**, Volcano plot of DEGs between Ac-iNKT1 cells and As-iNKT1 cells. **c**, Gene expression levels of *Klrg1*, *Ly6c2*, *Cx3cr1*, and *Rorc* in adipose iNKT cells. **d**, Representative FACS plot of adipose iNKT cell subpopulations in NCD- or 8-week HFD-fed mice. **e**, Representative FACS plots and proportion of each subpopulation among total adipose iNKT cells in NCD- (n = 7) or 8-week HFD-fed mice (n = 8).

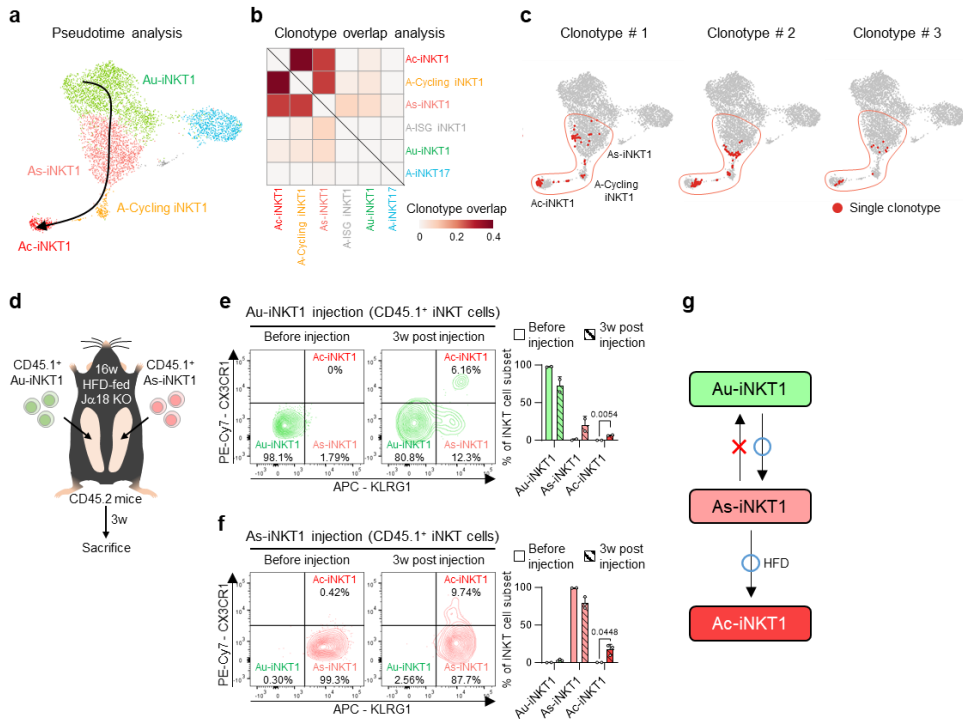


Figure 20. As-iNKT1 cells give rise to Ac-iNKT1 cells in obesity

a, *In silico* pseudotime analysis of adipose iNKT1 cells. **b**, Clonotype overlap analysis of adipose iNKT cell subpopulations. **c**, Representative clones showing clonotype overlapping between As-iNKT1, Ac-iNKT1, and A-Cycling iNKT1 cells. **d**, Experimental scheme for adoptive transfer of CD45.1⁺ Au-iNKT1 and As-iNKT1 cells. iNKT cells were sorted from CD45.1 mice 1-week after α -GC injection and injected into each WAT fat pad of 16-week HFD-fed CD45.2 $J\alpha 18$ KO mice. **e,f**, Representative FACS plots and composition of injected CD45.1⁺ donor iNKT cells in recipient mice after 3 weeks (Before injection (n = 2), Au-iNKT1 post injection (n = 2), and As-iNKT1 post injection (n = 3)). **g**, Schematic diagram of iNKT1 differentiation process in adipose tissue.

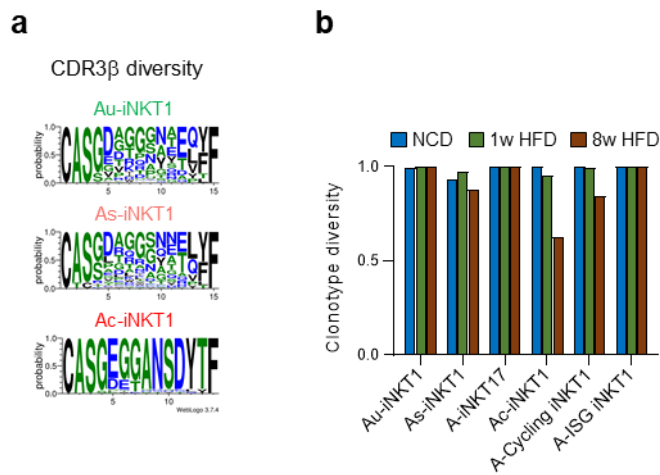


Figure 21. Ac-iNKT1 cells exhibit low clonal diversity

a, CDR3 β amino acid sequences of most prevalent CDR3 β length of each adipose iNKT1 cell subpopulation. Data were collected from 8-week-HFD condition. **b**, Clonotype diversity of each adipose iNKT cell subpopulation in NCD-, 1-week, or 8-week HFD-fed conditions.

Ac-iNKT1 cells kill hypertrophic and inflammatory adipocytes and recruit macrophages by secreting CCL5

Recently, our group have shown that adipose iNKT cells upregulate FasL upon HFD and remove hypertrophic and pro-inflammatory adipocytes [51]. The elevated number and cytotoxic gene expression of Ac-iNKT1 cells in obesity (Fig. 17d, e, 18e, 22a, b) prompted us to examine whether Ac-iNKT1 cells would be a major iNKT cell subpopulation that could remove enlarged and inflamed adipocytes. To address this, the same number of adipose iNKT cell subpopulations was cocultured with palmitic acid (PA)- or oleic acid (OA)-overloaded 3T3-L1 adipocytes (ADs), which have been considered as hypertrophic with pro-inflammatory characteristics or hypertrophic with no inflammatory characteristics, respectively (Fig. 23a–d) [21, 51]. To overcome the technical issue of small number of adipose iNKT cells, I adopted *in vivo* expansion of adipose iNKT cells by using alpha-galactosylceramide (α -GC), a potent lipid antigen for iNKT cells. Gene expression profiles and cytokine production of each adipose iNKT cell subpopulation were largely unaltered by *in vivo* expansion (Fig. 24a–h). I firstly examined the correlation between AD size and death with each iNKT cell subpopulation. PA- or OA-treated 3T3-L1 ADs were categorized into two groups based on their lipid droplet (LD) size. Large ADs were defined as a diameter of LD > 14 μ m, the proportion of which was increased by FFA overloading (Fig. 23a–c). Interestingly, large ADs were selectively killed by Ac-iNKT1 cells, whereas small ADs were less prone to be removed by iNKT cells (Fig. 25a–c). Next,

to test whether cytotoxic activity of Ac-iNKT1 cells would depend on inflammatory characteristics of ADs, PA-treated and OA-treated ADs, which differ in their inflammatory characteristics, were cocultured with each iNKT cell subpopulation. As indicated in Fig. 25d, e, Ac-iNKT1 cells exhibited the greatest cytotoxicity against PA-treated 3T3-L1 ADs, hypertrophic and pro-inflammatory ADs, whereas they did not show significant cytotoxicity toward OA-treated 3T3-L1 ADs, hypertrophic but not inflammatory ADs. Also, Ac-iNKT1 cell-induced PA-treated AD death was largely decreased by CD1d neutralization (Fig. 25f). These data suggest that Ac-iNKT1 cells would selectively remove adipocytes with both hypertrophic and pro-inflammatory characteristics via a TCR/CD1d-dependent manner. To scrutinize the cytotoxicity of Ac-iNKT1 cells *in vivo*, I injected the same number of adipose iNKT cell subpopulations into the right fat pad of HFD-fed iNKT cell-deficient $\alpha 18$ KO mice (Fig. 26a). A higher number of CLSs, a marker of dead adipocytes [19], were detected in Ac-iNKT1 cell-injected fat pads (Fig. 26b, c). Moreover, Ac-iNKT1 cells showed similar gene expression profiles to terminally differentiated CD8⁺ effector T cells (TE) (Fig. 26d, e) [162], indicating that Ac-iNKT1 cells would play key roles to kill enlarged and inflamed adipocytes in obesity.

Macrophages are recruited around dead adipocytes to engulf them and form CLS [19, 39, 163]. To test the possibility that Ac-iNKT1 cells could mediate macrophage recruitment around dead adipocytes after killing them, cytokines involved in macrophage recruitment were examined [164]. As

shown in Fig. 27a, b, *Ccl5*, the most highly expressed cytokine among macrophage-recruiting cytokines, was exclusively expressed in Ac-iNKT1 cells. *Ccr5*, a receptor for *Ccl5* [165], is exclusively expressed in macrophages, monocytes, and NK cells (Fig. 27c) [166], suggesting that CCL5 could play a role in the clearance of dead adipocytes by recruiting macrophages. I aimed to determine whether iNKT cell-derived CCL5 could stimulate adipocyte clearance by macrophages. Since DN32.D3 cells (an iNKT hybridoma cell line) upregulated *Ccl5* upon activation (Figure 27d), 3T3-L1 adipocytes, DN32.D3 cells, and Raw 264.7 cells (a macrophage cell line) were sequentially cocultured (Figure 27e). Activation of iNKT cells stimulated the uptake of adipocyte-derived lipid contents by macrophages (Figure 27f, g). Consistently, I observed that CCL5 could mediate the recruitment of THP1 monocytes (Fig. 27h). Taken together, these data clearly suggest that Ac-iNKT1 cells could selectively remove hypertrophic and pro-inflammatory adipocytes and would recruit macrophages via CCL5 to clean up dead adipocytes in obesity.

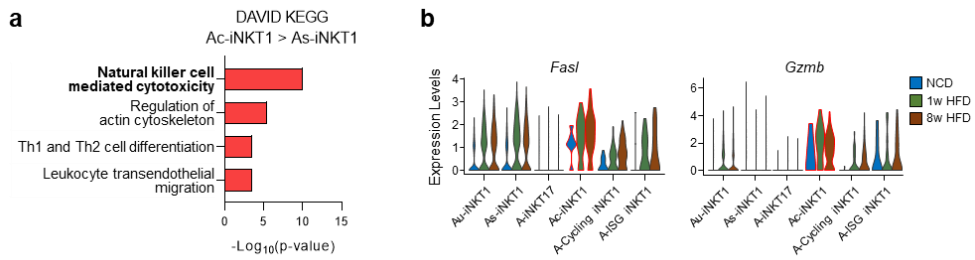


Figure 22. Ac-iNKT1 cells highly express cytotoxicity-related genes
a, KEGG pathway analysis of Ac-iNKT1 high-differentially expressed genes (DEGs) compared to As-iNKT1 cells ($P < 0.05$). **b**, Expression levels of cytotoxic marker genes in adipose iNKT cell subpopulations.

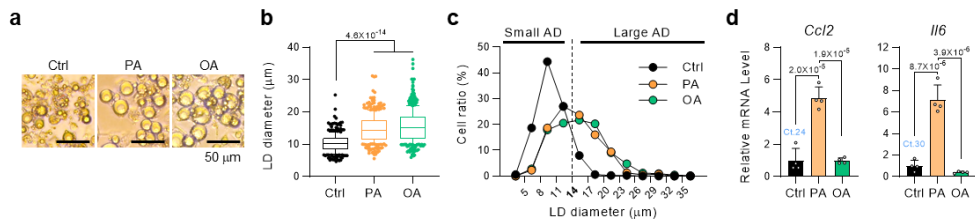


Figure 23. FFA treatment induces adipocyte hypertrophy models

a, Representative images of 3T3-L1 adipocytes treated with Ctrl, palmitic acid (PA), or oleic acid (OA) media for 2 weeks. Scale bars, 50 μm . **b,c**, Lipid droplet (LD) diameters of Ctrl (n = 300), PA (n = 380), or OA media-treated 3T3-L1 adipocytes (n = 419) (**b**) and their distribution (**c**). **d**, mRNA expressions in Ctrl, PA, or OA media-treated 3T3-L1 adipocytes (n = 4).

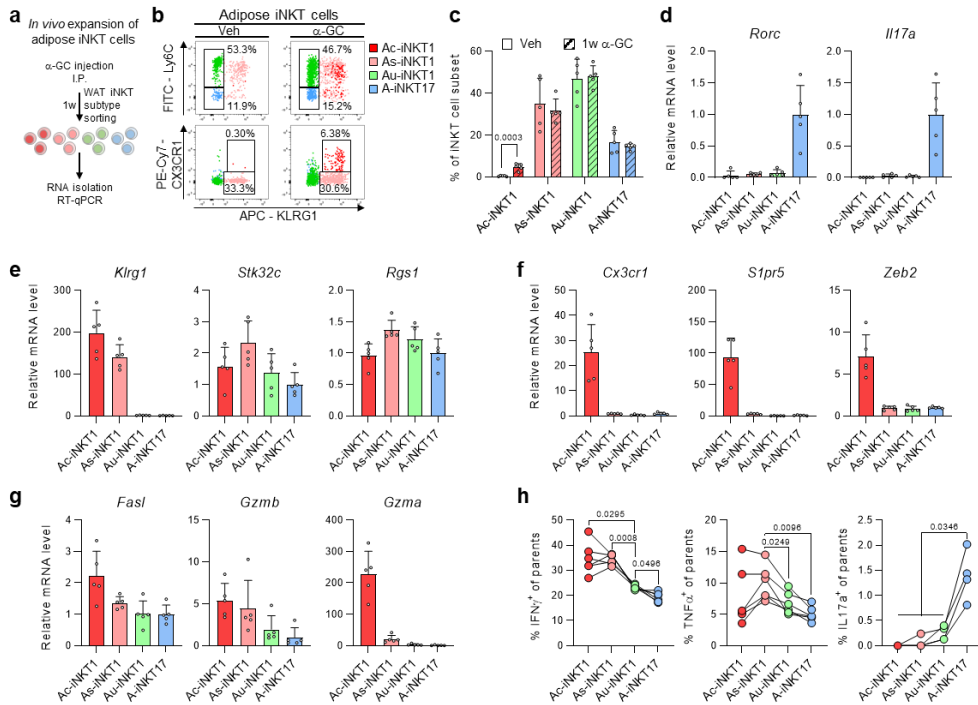


Figure 24. Characteristics of adipose iNKT cells in α -GC-induced iNKT cell *in vivo* expansion

a, Experimental scheme for α -GC-induced *in vivo* adipose iNKT cell expansion. **b,c**, Representative FACS plots (**b**) and proportion (**c**) of adipose iNKT cell subpopulations in vehicle or α -GC injected mice (n = 5) in (**a**). **d–g**, mRNA expressions of A-iNKT17 cell marker genes (**d**), As-iNKT1 cell marker genes (**e**), Ac-iNKT1 marker genes (**f**), and cytotoxic marker genes (**g**) in adipose iNKT cell subpopulations after *in vivo* expansion (n = 5). **h**, Intracellular cytokine staining of *in vivo*-expanded Ac-iNKT1, As-iNKT1, Au-iNKT1, and A-iNKT17 cells. Connected dots represent paired cell populations in a single SVF sample (IFN γ , TNF α (n = 5), and IL-17A (n = 4)).

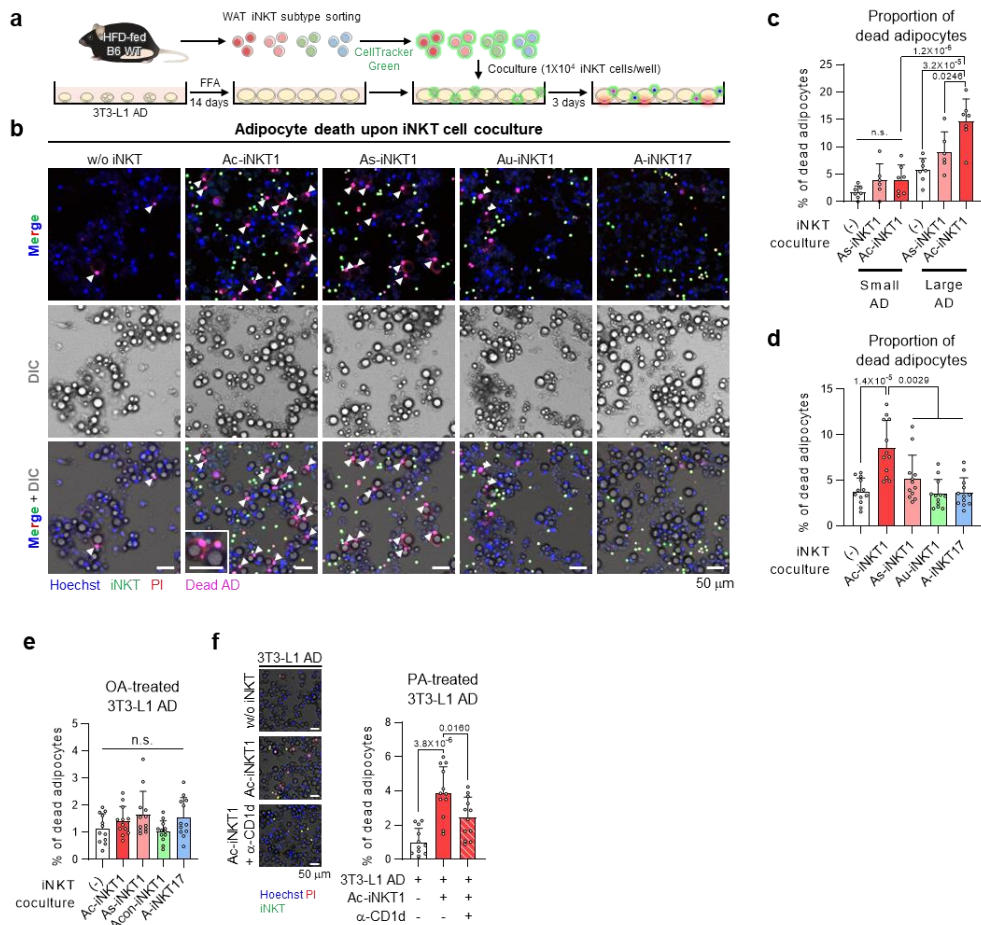


Figure 25. Ac-iNKT1 cells specifically remove hypertrophic and inflamed adipocytes *in vitro*

a, Experimental design for coculture of each iNKT cell subpopulation with hypertrophic adipocytes. **b**, Representative images of coculture between PA-treated 3T3-L1 adipocytes and iNKT cell subpopulations. Arrows; PI⁺ dead adipocytes. Scale bars, 50 μ m. **c,d**, Proportion of PI⁺ adipocytes among large or small adipocytes ((-) (n = 7), As-iNKT1 (n = 6), and Ac-iNKT1 (n = 7)) (**c**) and among total adipocytes (n = 12) (**d**). Cells in (**b**) were counted by using a microscope (**c** and **d**). **e**, Proportion of PI⁺ adipocytes among OA-treated 3T3-L1 adipocytes with or without adipose iNKT cell subpopulations (n = 12). **f**, Representative images and proportion of PI⁺ adipocytes among PA-treated 3T3-L1 adipocytes with or without Ac-iNKT1 cells or CD1d neutralizing antibody (n = 12). Scale bars, 50 μ m.

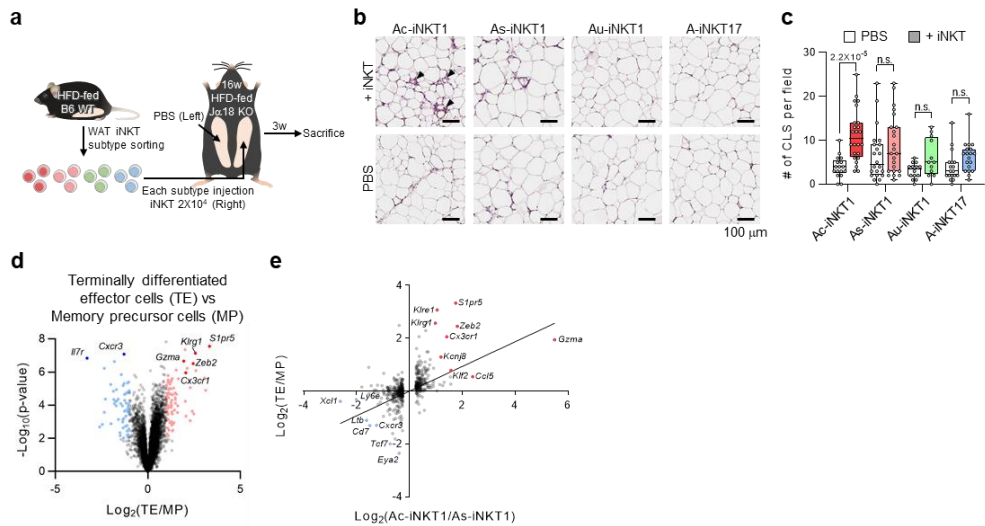


Figure 26. Ac-iNKT1 cells remove adipocytes *in vivo* and exhibit characteristics similar to CD8⁺ effector T cells

a, Experimental scheme for injection of each iNKT cell subpopulation. iNKT cells were sorted from 8-week HFD-fed WT male mice 1-week after α -GC injection and injected into HFD-fed $J\alpha 18$ KO mice. **b**, Representative histological images of PBS or iNKT cell subpopulation-injected WAT fat pads. Arrows; CLS. Scale bars, 100 μ m. **c**, Quantification of the number of CLS (Ac-iNKT1/PBS (n = 17), Ac-iNKT1/+iNKT (n = 24), As-iNKT1/PBS (n = 22), As-iNKT1/+iNKT (n = 23), Au-iNKT1/PBS (n = 14), Au-iNKT1/+iNKT (n = 12), A-iNKT17/PBS (n = 18), and A-iNKT17/+iNKT (n = 19)). **d**, Volcano plot of DEGs between TE and MP cells (GSE148681). **e**, Gene expression correlation between TE/MP signature and Ac-iNKT1/As-iNKT1 cell signature by using dataset in (d). TE/MP fold differences were calculated in DEGs between As-iNKT1 and Ac-iNKT1 cells.

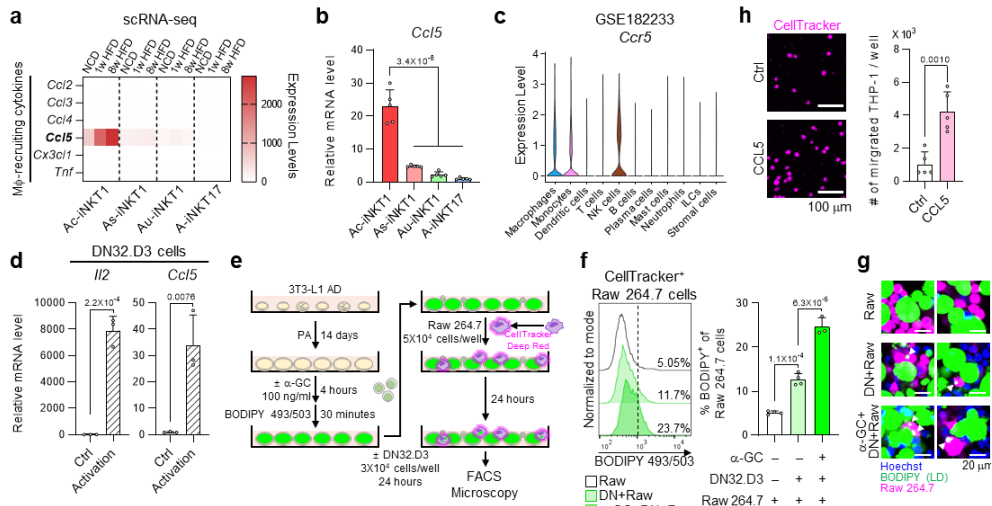


Figure 27. Ac-iNKT1 cells highly express macrophage-recruiting cytokine, CCL5

a, Heatmap showing the expression levels of macrophage-recruiting cytokines in adipose iNKT cell subpopulations. **b**, *Ccl5* mRNA level in *in vivo*-expanded iNKT cell subpopulations sorted from 10-week-old male mice ($n = 5$). **c**, *Ccr5* expression level in immune cells from WAT (GSE182233). **d**, mRNA levels of *Il2* and *Ccl5* in DN32.D3 cells upon activation by α -CD3e/ α -CD28 ($n = 3$). **e**, Experimental design for coculture of hypertrophic adipocytes, iNKT cells, and macrophages. **f,g**, Representative FACS plots, proportion of BODIPY⁺ macrophages (Raw, DN+Raw ($n = 4$), and α -GC+DN+Raw ($n = 3$)), and representative images of coculture. Scale bars, 20 μ m. **h**, Left: representative images of monocyte infiltration with or without CCL5 peptides. Right: quantification of the number of infiltrated THP1 cells ($n = 5$). Scale bars, 100 μ m.

A-iNKT17 cells stimulate adipose stem cell proliferation by secreting amphiregulin

Adipocyte turnover involves not only adipocyte death but also the generation of new adipocytes [5]. In this regard, activation of adipose iNKT cells could stimulate the proliferation of ASPCs in obese mice [51]. Despite these, it is unknown whether ASPC proliferation after adipose iNKT cell activation would be attributable to factor(s) from dead adipocytes or the direct interaction between adipose iNKT cells and ASPCs. To test the hypothesis that iNKT cell activation could directly stimulate ASPC proliferation without stimulating adipocyte death, α -GC was injected into lean mice. α -GC increased the proportion of proliferating ASPCs without stimulating apoptosis in adipose tissue (Fig. 28a, b). Also, increased ASPC proliferation by α -GC further increased the total number of ASPCs in WAT (Fig. 28c). α -GC-induced ASPC proliferation was abolished in iNKT cell-depleted $J\alpha 18$ KO mice (Fig. 28d). These data suggest that adipose iNKT cells could directly stimulate ASPC proliferation upon activation.

To understand which adipose iNKT cell subpopulations would be involved in ASPC proliferation, *in vivo* approaches were used. As the ratio of A-iNKT17 cells was significantly increased by α -GC injection (Fig. 29a), I attempted to verify the role of A-iNKT17 cells in ASPC proliferation. When A-iNKT17 cells were injected into the fat pads of HFD-fed $J\alpha 18$ KO mice, the ratio of proliferating ASPCs was increased by the injection of A-iNKT17 cells, whereas those of other adipose iNKT cell subpopulations were not (Fig.

29b, c). Then, to identify which factor(s) from A-iNKT17 cells could stimulate ASPC proliferation, I examined gene expression profiles in adipose iNKT cell subpopulations. It has been reported that immune cells actively crosstalk with epithelial or mesenchymal cells during tissue regeneration via growth factors or cytokines [167-170]. Interestingly, among previously reported immune cell-derived growth factors [168], amphiregulin (*Areg*), reported to stimulate satellite cell differentiation during muscle repair [171], was exclusively expressed in A-iNKT17 cells, and its expression level was gradually increased upon HFD (Fig. 30a). Also, mRNA level of *Areg* appeared to be abundant in A-iNKT17 cells and was downregulated in iNKT cell-depleted mice upon HFD feeding (Fig. 30b, c). To examine whether AREG could stimulate ASPC proliferation, lean mice were injected with AREG. As indicated in Fig. 30d, AREG potentiated the proportion of proliferating ASPCs in a dose-dependent manner. Also, α -GC-induced ASPC proliferation was decreased by the inhibition of epidermal growth factor receptor (EGFR), a receptor for AREG (Fig. 30e). Next, to investigate whether ASPC proliferation stimulated by AREG would indeed lead to adipogenesis, I adopted adipocyte lineage-tracing mice (*Adipoq*-rtTA; TRE-Cre; *rosa26-loxp-stop-loxp-YFP*). Pre-existing adipocytes were marked with YFP by doxycycline, whereas newly formed adipocytes after vehicle or AREG injection were not labeled by YFP (Fig. 31a). The proportion of perilipin-positive and YFP-negative new adipocytes was increased by AREG injection (Fig. 31b, c), implying that AREG-driven ASPC proliferation would

increase adipogenic potential. In addition, it seemed that AREG-injected WAT showed a smaller adipocyte size (Fig. 31d), which was observed in adipose tissue with activated adipogenesis [172]. Given that the proportion of iNKT17 cells was higher in WAT compared to thymus, spleen, and liver, it seems that A-iNKT17-AREG axis appeared to play a substantial role in the regulation of ASPC proliferation (Fig. 32). Collectively, these data suggest that A-iNKT17 cell-derived AREG could be one of the key mediators to stimulate ASPC proliferation and adipogenesis in adipose tissue homeostasis.

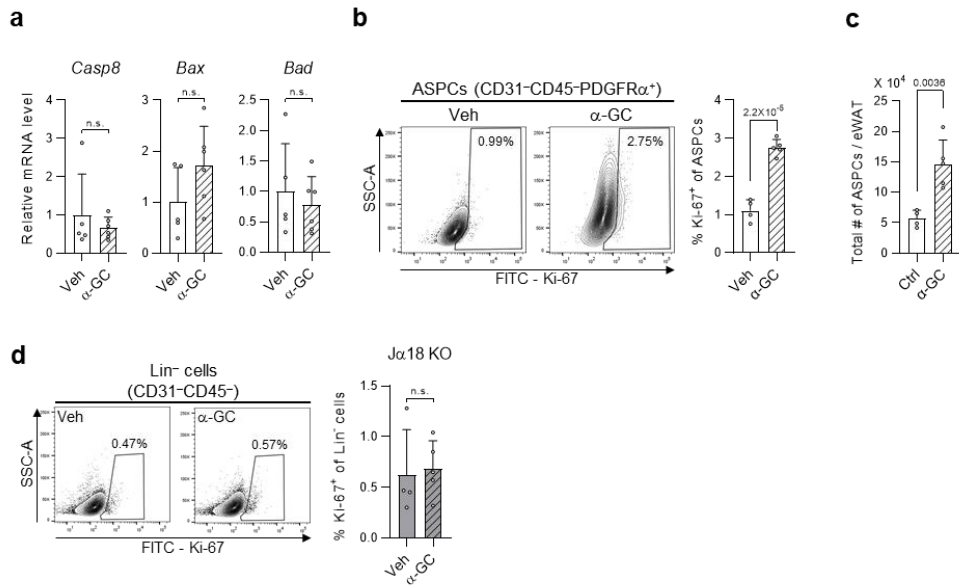


Figure 28. Activation of iNKT cells stimulates ASPC proliferation without inducing adipocyte death

a, mRNA expressions of *Casp8*, *Bax*, and *Bad* in WAT from vehicle or α -GC injected mice. Mice were sacrificed 1 day after vehicle (n = 5) or α -GC injection (n = 6). **b**, Representative FACS plots and proportion of Ki-67⁺ among ASPCs (CD31⁻CD45⁻PDGFR α ⁺) from WT WAT 4-days after vehicle (n=4) or α -GC injection (n = 5). **c**, The total number of ASPCs from WT WAT 1-week after vehicle (n = 4) or α -GC injection (n = 5). **d**, Representative FACS plots and proportion of Ki-67⁺ among lineage (Lin)-negative cells (CD31⁻CD45⁻) from *Ja18* KO WAT. Mice were sacrificed 4 days after vehicle (n = 4) or α -GC injection (n = 5).

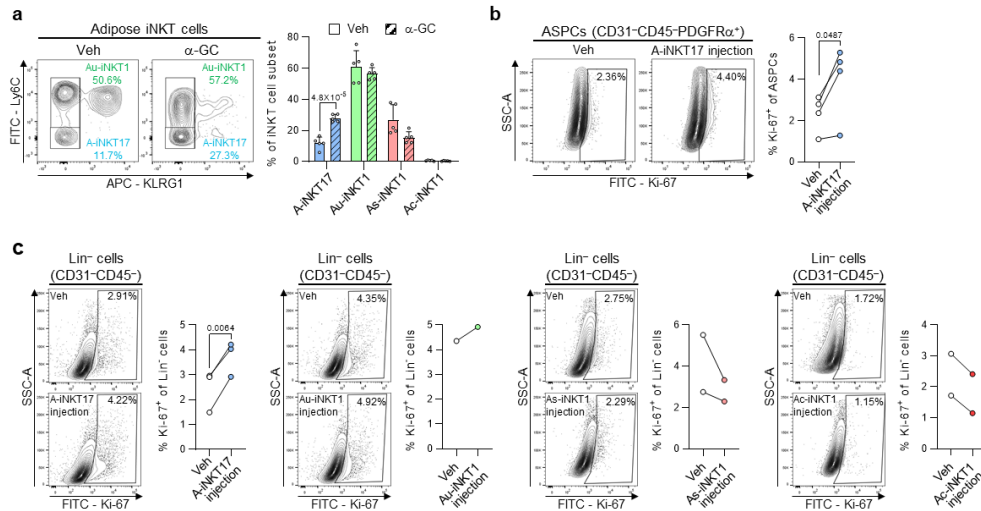


Figure 29. Injection of A-iNKT17 cells induces ASPC proliferation

a, Representative FACS plots and proportion of each adipose iNKT cell subpopulation among total adipose iNKT cells 4 days after vehicle or α -GC injection (n = 5 biologically independent mice). **b**, Representative FACS plots and proportion of Ki-67⁺ among ASPCs from WAT of 12-week HFD-fed *Ja18* KO mice with or without A-iNKT17 cell injection (n = 4 biologically independent mice). Mice were sacrificed 4 days after injection. **c**, Representative FACS plots and proportion of Ki-67⁺ among WAT Lin-negative cells from 16-week HFD-fed *Ja18* KO mice with or without A-iNKT17 (n = 3), Au-iNKT1 (n = 1), As-iNKT1 (n = 2), or Ac-iNKT1 cell injection (n = 2). Mice were sacrificed 3 weeks after injection.

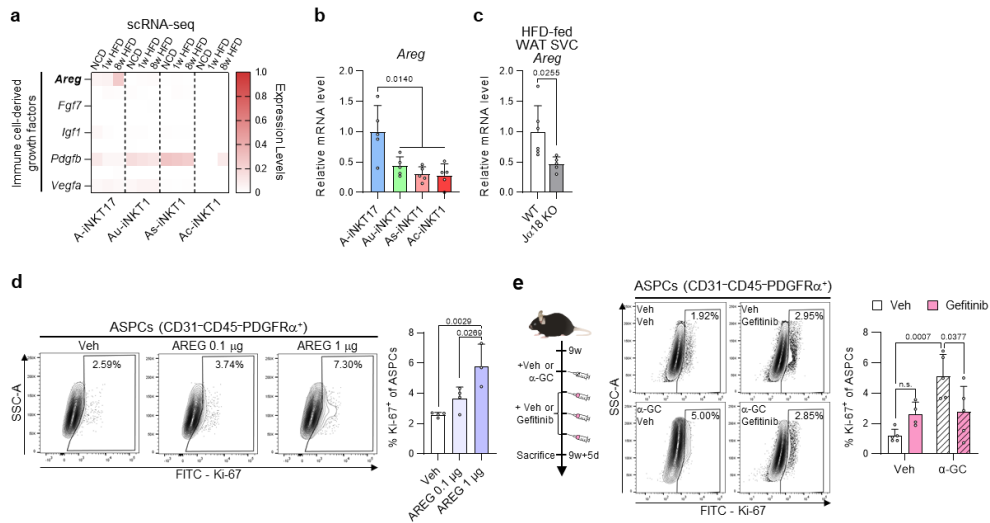


Figure 30. A-iNKT17 cells produce amphiregulin (AREG) which stimulates ASPC proliferation

a, Heatmap showing the expression levels of growth factors in adipose iNKT cell subpopulations. **b**, *Areg* mRNA level in *in vivo*-expanded iNKT cell subpopulations sorted from 10-week-old male mice (n = 5). **c**, *Areg* mRNA level in WAT SVFs from 8-week HFD-fed WT (n = 6) and Jα18 KO mice (n = 5). **d**, Representative FACS plots and proportion of Ki-67⁺ among ASPCs from WT WAT. Mice were injected with vehicle, AREG 0.1 μg (n = 4), or AREG 1 μg (n = 3). **e**, Experimental scheme, representative FACS plots, and the ratio of proliferating ASPCs (CD31⁻CD45⁺PDGFRα⁺) in α-GC and/or Gefitinib, EGFR inhibitor injection (Veh/Veh (n = 5), Veh/Gefitinib (n = 4), α-GC/Veh (n = 5), and α-GC/Gefitinib (n = 5)).

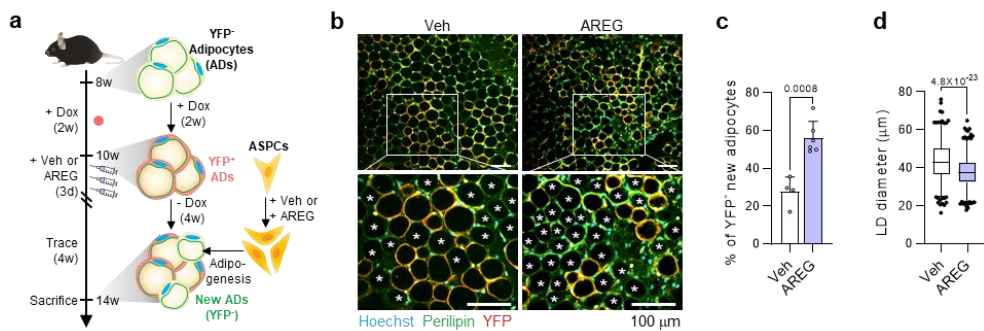


Figure 31. AREG-induced ASPC proliferation increases adipogenesis
a, Experimental scheme using C57BL/6J adipocyte lineage-tracing male mice.
b, Representative microscopic images of vehicle or AREG injected WAT 4 weeks after injection. Asterisks indicate perilipin⁺YFP⁻ new adipocytes. Scale bars, 100 μm. **c**, Proportion of YFP⁻ new adipocytes among total adipocytes from vehicle- (n=4) or AREG-injected mice (n=6). **d**, Quantification of lipid droplet (LD) size of vehicle (n=489) or AREG injected WAT (n=527) in (b).

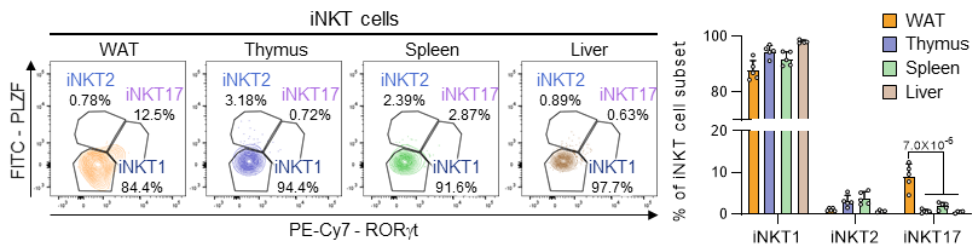


Figure 32. The proportion of iNKT cell subtypes in various organs
 Representative FACS plots and the proportion of iNKT1, iNKT2, and iNKT17 cells from 10-week-old male C57BL/6 mice (WAT (n = 5), Thymus (n = 5), Spleen (n = 5), Liver (n = 4)).

5. Discussion

In obesity, adipose iNKT cells exert protective functions by selectively removing dysfunctional adipocytes and promoting adipogenesis [51]. However, it has been unknown by which mechanisms adipose iNKT cells regulate diverse steps of adipocyte turnover process.

In this study, I uncovered the underlying mechanisms by which adipose iNKT cells control adipocyte turnover in obesity. In obese WAT, Ac-iNKT1 cells, which differentiated from As-iNKT1 cells, selectively removed dysfunctional adipocytes and recruited macrophages to clear dead adipocytes by secreting CCL5. In addition, I demonstrated that A-iNKT17 cells stimulated ASPC proliferation and adipogenesis through the secretion of AREG. Together, these findings suggest that diverse adipose iNKT cell subpopulations orchestrate adipocyte turnover through dynamic interactions with other cell types, including adipocytes, adipose immune cells, and ASCs.

Adipocyte death is frequently observed in obesity and is closely related to adipose tissue inflammation and whole-body energy metabolism. In obesity, adipocyte death occurs due to various stimuli, such as mechanical stress, hypoxia, hypertrophy, inflammatory cytokines, and adipose iNKT cells [19, 20, 25, 42, 51, 173, 174]. Components from dead adipocytes, such as lipids or cholesterol, should be sequestered and removed from the interstitium to minimize their harmful effects on neighboring cells [19, 28, 50]. Accordingly, it is important to temporally coordinate apoptosis induction and

elimination of apoptotic cells. Most studies have focused on macrophage recruitment after adipocyte death via cytokines and damage-associated molecular patterns (DAMPs) from dead adipocytes [163, 175-178]. Nevertheless, it remains unknown how apoptosis induction and efficient clearance of dead adipocytes are elaborately controlled in obese adipose tissue. Here, we suggest that Ac-iNKT1 cells would selectively get rid of hypertrophic and pro-inflammatory adipocytes and recruit phagocytic macrophages to clear them. Ac-iNKT1 cells exclusively expressed *Zeb2*, *Cx3cr1*, and *Gzma*, which are highly expressed in CD8⁺ effector T cells [162], implying that Ac-iNKT1 cells would be potent killer cells. Consistently, coculture experiments and adoptive transfer of iNKT cell subpopulations indicated that Ac-iNKT1 cells facilitated the death of unhealthy adipocytes. Given that the target specificity of iNKT cells depends on the type of V β and CDR3 β sequence [77, 179, 180], it appears that Ac-iNKT1 cells with highly invariable TCR chains might kill certain adipocytes bearing specific lipid antigens. Moreover, we found that Ac-iNKT1 cells highly expressed chemoattractant, *Ccl5*, whose expression in Ac-iNKT1 cells gradually increased upon HFD. CCL5 is known for macrophage recruitment and survival in obese adipose tissue [181]. Recent scRNA-seq analyses have shown that cytotoxic immune cells such as NK cells, CD8⁺ T cells, and NKT cells highly express *Ccl5* in adipose tissue [166, 182], implying that cytotoxic immune cells would contribute to effective clearance of dead cells via macrophage recruitment. Taken together, these data suggest that Ac-iNKT1

cells play crucial roles in the control of adipocyte turnover, particularly in obesity.

Immune cells are one of the key factors in determining the properties and fate of stem cells [183, 184]. For instance, in muscle and intestine, several immune cells such as macrophages, innate lymphoid cells (ILCs), T helper cells, and Regulatory T (Treg) cells mediate stem cell proliferation and differentiation through secreting epidermal growth factor (EGF) family [171, 185, 186]. EGFs activate cellular proliferation, differentiation, and survival by binding to their cognate receptors [187]. Despite these findings, the importance of crosstalk between immune cells and stem cells in adipose tissue remains largely unknown. In this study, we found that A-iNKT17 cells promoted the proliferation of ASCs via secretion of AREG, a member of the EGF family, which was followed by adipogenesis. Our previous reports and current studies [51, 70] have shown that activation of adipose iNKT cells would be accompanied by ASPC proliferation. In adipose tissue, it has been reported that Th2 CD4⁺ T cells, ILC2, and Treg cells express AREG [188, 189]. In this study, we have identified that A-iNKT17 could also secrete AREG. Although we assumed that AREG-EGFR signaling in WAT would be important for ASPC proliferation, it is not fully understood whether A-iNKT17 cells directly secrete AREG or indirectly stimulate other cell types (e.g. Treg cells or ILC2) to secrete AREG. Future studies are required to determine the complex interactions between immune cells and ASCs in adipose tissue. In addition, given that A-iNKT17 cells highly expressed IL-4,

it is likely that A-iNKT17 cells would be involved in the resolution of adipose tissue inflammation. Together, current data suggest that A-iNKT17 cells would contribute to healthy adipose tissue remodeling, potentially, by regulating ASPC proliferation, adipocyte differentiation, and inflammation.

In conclusion, we characterized adipose iNKT cells at a single-cell resolution and identified the mechanisms and physiological significance of iNKT cell-mediated adipocyte turnover. Our comprehensive analyses using scRNA-seq and experimental approaches provide substantial insights into the roles of adipose immune cells in the control of adipocyte quantity and quality. Collectively, our data suggest that dynamic cellular crosstalk between iNKT cells, macrophages, and (pre)adipocytes in adipose tissue is crucial for the maintenance of adipose tissue homeostasis.

CONCLUSION

Adipose tissue is composed of a diverse array of immune cells that regulate its pathophysiology. Deciphering their roles and characteristics is an important question for understanding adipose tissue biology. Among various immune cells residing in adipose tissue, iNKT cells have gained attention due to their ability to directly communicate with adipocytes via lipid antigens and their crucial roles in regulating adipose tissue homeostasis in obesity. Despite their importance, the characteristics of iNKT cells in adipose tissue and the mechanisms by which they regulate adipose tissue homeostasis are not completely understood.

In this dissertation, I propose that distinct subpopulations of adipose iNKT cells contribute to adipocyte turnover process in obesity. First, secretory factors from adipocytes induce the differentiation of KLRG1⁺ A_s-iNKT1 cells, which are specific to adipose tissue. Second, in obesity, A_s-iNKT1 cells further differentiate into cytotoxic A_c-iNKT1 cells, which eliminate dysfunctional adipocytes. Meanwhile, A_s-iNKT17 cells promote ASPC proliferation and subsequent adipogenesis through AREG secretion. Taken together, these findings suggest that adipose iNKT cells are modulated by adipose tissue microenvironment and metabolic stimuli to effectively target dysfunctional adipocytes, thereby orchestrating adipocyte turnover (Fig. 33).

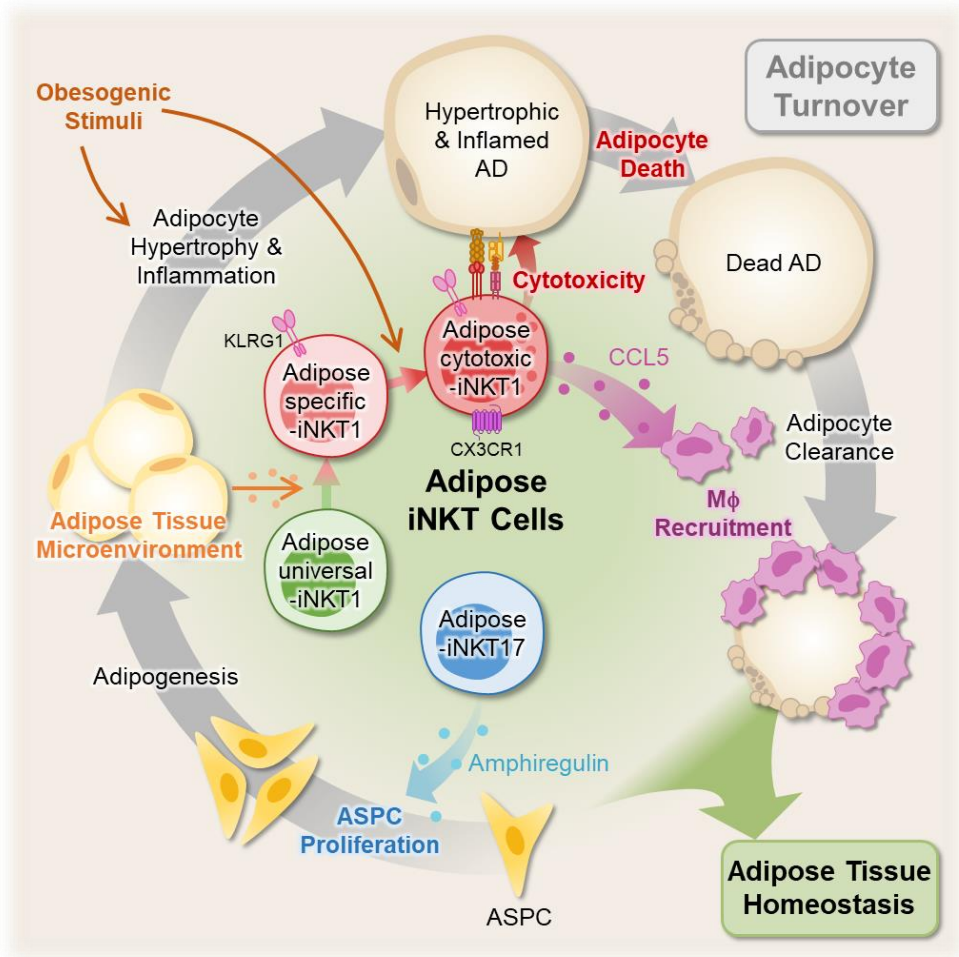


Figure 33. Graphical abstract of Chapters I and II

1. Adipose Tissue Microenvironment Mediates the Distinct Characteristics of Adipose iNKT Cells

For the past decade, studies on the characteristics of adipose iNKT cells have primarily focused on their IL-10-secreting properties and the upregulation of E4BP4 [99, 121, 122]. However, other genes upregulated in adipose iNKT cells have been poorly investigated, and it remains uncertain whether E4BP4 could fully explain these DEGs.

In this study, I identified a novel adipose tissue-specific iNKT cell subpopulation upregulating marker genes such as *Klrg1*, *Bhlhe40*, *Stk32c*, and *Tbx21*, while downregulating *Il7r*, *Satb1*, and *Klf2*, by comparing iNKT cells from multiple organs. These KLRG1-expressing iNKT cells were specifically enriched in adipose tissue, and the adoptive transfer experiments showed that these cells are induced by adipose tissue microenvironment. KLRG1⁺ As-iNKT1 cells were induced in a CD1d-independent manner, and some of As-iNKT1 signature genes could be induced by adipocyte-conditioned media, highlighting the importance of adipocyte-secreted factors in shaping the characteristics of adipose iNKT cells.

It remains uncertain which specific secretory factors induce the generation of As-iNKT1 cells. Adipose tissue microenvironment contains a high concentrations of lipid metabolites, adipokines, and lipokines [125], which shape the characteristics of adipose immune cells. For instance, in Treg cells, stromal cell-derived IL-33 and insulin play crucial roles in generating adipose-specific Treg populations [190-192]. Elucidating the precise

underlying mechanisms by which factors induce Th1-skewed As-iNKT1 cells, including transcriptional regulations and secretory factors involved, would be an interesting subject of study. As cancer therapies using iNKT cells, such as CAR-iNKT cells [193], are actively being investigated, this research could potentially enhance the anti-cancer activity of CAR-iNKT cells by upregulating their Th1 responses.

In addition, it would be an interesting topic to explore whether these phenotypic changes in iNKT cells within adipose tissue are also applicable to other immune cell types, such as NK cells or other T cells. NK cells and Th1 CD4⁺ cells have been proposed as similar cell populations to iNKT1 cells [194]. Similarly, CD8⁺ T cells might share characteristics with iNKT cells, as seen in the resemblance between Ac-iNKT1 cells and CD8⁺ terminally differentiated effector T cells (Fig. 26). Interestingly, similar genes were upregulated in both A-iNKT1 and A-iNKT17 cells compared to their thymic counterparts (Fig. 6). This suggests that adipose tissue microenvironment would upregulate genes involved in specific pathways in resident immune cells. This research could broaden our understanding of immune cell characteristics in adipose tissue and might offer additional insights into the early onset of adipose tissue inflammation in response to obesogenic stimuli.

In conclusion, this study identifies a novel subpopulation of adipose iNKT cells shaped by the adipose tissue microenvironment. These findings might have broader implications for other immune cells residing in adipose

tissue and enhance our understanding of tissue-specific immune cell subpopulations.

2. Various Adipose iNKT Cell Subpopulations Regulate Adipocyte Turnover in Obesity

Although adipocyte turnover has been suggested as an important process for maintaining adipose tissue homeostasis in obesity [72, 74, 119, 120], it has been unclear how this process is precisely orchestrated in obesity.

In this study, I demonstrated the changes in adipose iNKT cells in obese conditions and their interactions with other cell types involved in adipocyte turnover. I found that a subset of As-iNKT1 cells undergoes clonal expansion to become Ac-iNKT1 cells, which efficiently remove detrimental adipocytes. Additionally, in response to obesity, A-iNKT17 cells upregulated AREG, which could induce ASPC proliferation and subsequent adipogenesis.

Massive clonal expansion of Ac-iNKT1 cells in response to obesity is a remarkable finding. To my knowledge, this is the first time that specific peripheral iNKT clones have been identified that were clonally selected and expanded even without the administration of foreign lipid antigens. In the current study, I identified clonotypes of Ac-iNKT1 cells that were clonally selected using single-cell TCR sequencing. As obesity progressed, certain Ac-iNKT1 cell subsets with V β 8.3 (*Trbv13-1*) became enriched (Fig. 19). It has been suggested that peripheral iNKT cells could be modulated by local lipid antigens [77]. Thus, these results suggest that certain lipid antigens,

synthesized by adipocytes or microbes, might be presented on adipocytes in obesity, activating a specific subset of As-iNKT1 cells with high TCR affinity for these antigens, and leading to clonal expansion and the generation of Ac-iNKT1 cells.

Endogenous lipid antigens that modulate peripheral iNKT cell activity remain largely unknown. Since modulating the activity of adipose iNKT cells could induce the clearance of pathological adipocytes and their replacement with healthy ones [51], identifying the lipid antigen(s) driving these phenomena in adipose tissue could be a promising therapeutic target. Although it has been recently suggested that glucosylceramide generated by *Ugcg* might induce iNKT cell activation in lean mice [195], there is yet insufficient experimental evidence to confirm whether glucosylceramide is actually presented by adipocytes or how β -anomeric glycosyl lipids activate iNKT cells [90]. Therefore, future research should focus on identifying candidate endogenous lipid antigens based on criteria such as their presentation on the surface of adipocytes, their increase in obesity, and their ability to bind to Ac-iNKT1 TCRs.

In this study, I proposed that A-iNKT17 cell-derived AREG could modulate ASPC proliferation and adipogenesis. However, it remains unclear whether AREG directly influences the adipogenic program of ASPCs and whether A-iNKT17 cells are the major source of AREG. In addition, although we focused on AREG in this study, it would be interesting to investigate whether other secretory factors from A-iNKT17 cells could also modulate

ASPCs.

In conclusion, this study identifies the regulatory mechanisms of adipocyte turnover by iNKT cells. These findings suggest the presence of potent endogenous lipid antigens in obese adipose tissue and their potential therapeutic applications.

ACKNOWLEDGEMENTS

Parts of Chapters I and II in this thesis were published in *Nature Communications* (2024) Vol. 14 Issue 1 pp. 8512 and *Trends in Endocrinology & Metabolism* (2024) in an online version. In addition, parts of Chapters I and II were presented at the 2022 Korean Society for Molecular and Cellular Biology (KSMCB, International Conference Center Jeju, Jeju, Korea, September 28–30, 2022), 2023 KSMCB (International Conference Center Jeju, Jeju, Korea, November 6–8, 2023), KSMCB Winter Conference (Pyeong Chang Alpensia, Pyeong Chang, February 22–24, 2023), Experimental Biology 2022 (Pennsylvania Convention Center, Philadelphia, Pennsylvania, USA, April 2–5, 2022), and 5th International Conference on ImmunoMetabolism: Molecular and Cellular Immunology of Metabolism (Avra Imperial Hotel & Conference Center, Chania, Crete, Greece, May 21–26, 2023). This study was supported by the BK21 program and the National Research Foundation, funded by the Korean government (NRF-2018R1A5A1024340, NRF-2020R1A3B2078617, and RS-2023-00218616).

REFERENCES

1. Choe, S.S., et al., *Adipose Tissue Remodeling: Its Role in Energy Metabolism and Metabolic Disorders*. Front Endocrinol (Lausanne), 2016. **7**: p. 30.
2. Jaitin, D.A., et al., *Lipid-Associated Macrophages Control Metabolic Homeostasis in a Trem2-Dependent Manner*. Cell, 2019. **178**(3): p. 686-698 e614.
3. Grant, R.W.andDixit, V.D., *Adipose tissue as an immunological organ*. Obesity (Silver Spring), 2015. **23**(3): p. 512-518.
4. Gesta, S., et al., *Developmental origin of fat: tracking obesity to its source*. Cell, 2007. **131**(2): p. 242-256.
5. Sakers, A., et al., *Adipose-tissue plasticity in health and disease*. Cell, 2022. **185**(3): p. 419-446.
6. Friedman, J.M., et al., *Molecular mapping of the mouse ob mutation*. Genomics, 1991. **11**(4): p. 1054-1062.
7. Rondinone, C.M., *Adipocyte-derived hormones, cytokines, and mediators*. Endocrine, 2006. **29**(1): p. 81-90.
8. Richard, D.andPicard, F., *Brown fat biology and thermogenesis*. Front Biosci (Landmark Ed), 2011. **16**(4): p. 1233-1260.
9. Ikeda, K., et al., *The Common and Distinct Features of Brown and Beige Adipocytes*. Trends Endocrinol Metab, 2018. **29**(3): p. 191-200.
10. Fuster, J.J., et al., *Obesity-Induced Changes in Adipose Tissue Microenvironment and Their Impact on Cardiovascular Disease*. Circ Res, 2016. **118**(11): p. 1786-1807.
11. Lee, Y.S., et al., *Inflammation is necessary for long-term but not short-term high-fat diet-induced insulin resistance*. Diabetes, 2011. **60**(10): p. 2474-2483.
12. Zatterale, F., et al., *Chronic Adipose Tissue Inflammation Linking Obesity to Insulin Resistance and Type 2 Diabetes*. Front Physiol, 2019. **10**: p. 1607.
13. Makki, K., et al., *Adipose tissue in obesity-related inflammation and insulin resistance: cells, cytokines, and chemokines*. ISRN Inflamm, 2013. **2013**(1): p. 139239.
14. Vishvanath, L.andGupta, R.K., *Contribution of adipogenesis to healthy adipose tissue expansion in obesity*. J Clin Invest, 2019. **129**(10): p. 4022-4031.
15. Ghaben, A.L.andScherer, P.E., *Adipogenesis and metabolic health*. Nat Rev Mol Cell Biol, 2019. **20**(4): p. 242-258.
16. Reilly, S.M.andSaltiel, A.R., *Adapting to obesity with adipose tissue inflammation*. Nat Rev Endocrinol, 2017. **13**(11): p. 633-643.
17. Nishimura, S., et al., *CD8+ effector T cells contribute to macrophage recruitment and adipose tissue inflammation in obesity*. Nat Med, 2009. **15**(8): p. 914-920.

18. Gual, P., et al., *Positive and negative regulation of insulin signaling through IRS-1 phosphorylation*. *Biochimie*, 2005. **87**(1): p. 99-109.
19. Cinti, S., et al., *Adipocyte death defines macrophage localization and function in adipose tissue of obese mice and humans*. *J Lipid Res*, 2005. **46**(11): p. 2347-2355.
20. Xia, B., et al., *Adipose tissue deficiency of hormone-sensitive lipase causes fatty liver in mice*. *PLoS Genet*, 2017. **13**(12): p. e1007110.
21. Kim, J.I., et al., *Lipid-overloaded enlarged adipocytes provoke insulin resistance independent of inflammation*. *Mol Cell Biol*, 2015. **35**(10): p. 1686-1699.
22. Hosogai, N., et al., *Adipose tissue hypoxia in obesity and its impact on adipocytokine dysregulation*. *Diabetes*, 2007. **56**(4): p. 901-911.
23. Regazzetti, C., et al., *Hypoxia decreases insulin signaling pathways in adipocytes*. *Diabetes*, 2009. **58**(1): p. 95-103.
24. Halberg, N., et al., *Hypoxia-inducible factor 1alpha induces fibrosis and insulin resistance in white adipose tissue*. *Mol Cell Biol*, 2009. **29**(16): p. 4467-4483.
25. Sung, H.K., et al., *Adipose vascular endothelial growth factor regulates metabolic homeostasis through angiogenesis*. *Cell Metab*, 2013. **17**(1): p. 61-72.
26. Sun, K., et al., *Extracellular Matrix (ECM) and Fibrosis in Adipose Tissue: Overview and Perspectives*. *Compr Physiol*, 2023. **13**(1): p. 4387-4407.
27. Sarvari, A.K., et al., *Plasticity of Epididymal Adipose Tissue in Response to Diet-Induced Obesity at Single-Nucleus Resolution*. *Cell Metab*, 2021. **33**(2): p. 437-453 e435.
28. Choi, C., et al., *TM4SF19-mediated control of lysosomal activity in macrophages contributes to obesity-induced inflammation and metabolic dysfunction*. *Nat Commun*, 2024. **15**(1): p. 2779.
29. Lee, G., et al., *SREBP1c-PARP1 axis tunes anti-senescence activity of adipocytes and ameliorates metabolic imbalance in obesity*. *Cell Metab*, 2022. **34**(5): p. 702-718 e705.
30. Pellettieri, J. and Sanchez Alvarado, A., *Cell turnover and adult tissue homeostasis: from humans to planarians*. *Annu Rev Genet*, 2007. **41**(1): p. 83-105.
31. Spalding, K.L., et al., *Dynamics of fat cell turnover in humans*. *Nature*, 2008. **453**(7196): p. 783-787.
32. Johnson, P.R. and Hirsch, J., *Cellularity of adipose depots in six strains of genetically obese mice*. *J Lipid Res*, 1972. **13**(1): p. 2-11.
33. Bourgeois, F., et al., *Dietary-induced obesity: effect of dietary fats on adipose tissue cellularity in mice*. *Br J Nutr*, 1983. **49**(1): p. 17-26.
34. Lee, Y.H., et al., *Identification of an adipogenic niche for adipose tissue remodeling and restoration*. *Cell Metab*, 2013. **18**(3): p. 355-367.
35. Lee, Y.H., et al., *Adipogenic role of alternatively activated*

- macrophages in beta-adrenergic remodeling of white adipose tissue.* Am J Physiol Regul Integr Comp Physiol, 2016. **310**(1): p. R55-65.
36. Han, S.M., et al., *How obesity affects adipocyte turnover.* Trends Endocrinol Metab, 2024.
 37. Sender, R. and Milo, R., *The distribution of cellular turnover in the human body.* Nat Med, 2021. **27**(1): p. 45-48.
 38. Lindhorst, A., et al., *Adipocyte death triggers a pro-inflammatory response and induces metabolic activation of resident macrophages.* Cell Death Dis, 2021. **12**(6): p. 579.
 39. Roszer, T., *Adipose Tissue Immunometabolism and Apoptotic Cell Clearance.* Cells, 2021. **10**(9): p. 2288.
 40. Kuroda, M. and Sakaue, H., *Adipocyte Death and Chronic Inflammation in Obesity.* J Med Invest, 2017. **64**(3.4): p. 193-196.
 41. Murano, I., et al., *Time course of histomorphological changes in adipose tissue upon acute lipotrophy.* Nutr Metab Cardiovasc Dis, 2013. **23**(8): p. 723-731.
 42. Monji, A., et al., *A Cycle of Inflammatory Adipocyte Death and Regeneration in Murine Adipose Tissue.* Diabetes, 2022. **71**(3): p. 412-423.
 43. Wang, Q.A., et al., *Tracking adipogenesis during white adipose tissue development, expansion and regeneration.* Nat Med, 2013. **19**(10): p. 1338-1344.
 44. White, U. and Ravussin, E., *Dynamics of adipose tissue turnover in human metabolic health and disease.* Diabetologia, 2019. **62**(1): p. 17-23.
 45. Neese, R.A., et al., *Measurement in vivo of proliferation rates of slow turnover cells by 2H2O labeling of the deoxyribose moiety of DNA.* Proc Natl Acad Sci U S A, 2002. **99**(24): p. 15345-15350.
 46. Rigamonti, A., et al., *Rapid cellular turnover in adipose tissue.* PLoS One, 2011. **6**(3): p. e17637.
 47. Jeffery, E., et al., *Rapid depot-specific activation of adipocyte precursor cells at the onset of obesity.* Nat Cell Biol, 2015. **17**(4): p. 376-385.
 48. Lee, Y.H., et al., *In vivo identification of bipotential adipocyte progenitors recruited by beta3-adrenoceptor activation and high-fat feeding.* Cell Metab, 2012. **15**(4): p. 480-491.
 49. Shao, M., et al., *De novo adipocyte differentiation from Pdgfrbeta(+) preadipocytes protects against pathologic visceral adipose expansion in obesity.* Nat Commun, 2018. **9**(1): p. 890.
 50. Coats, B.R., et al., *Metabolically Activated Adipose Tissue Macrophages Perform Detrimental and Beneficial Functions during Diet-Induced Obesity.* Cell Rep, 2017. **20**(13): p. 3149-3161.
 51. Park, J., et al., *Activation of invariant natural killer T cells stimulates adipose tissue remodeling via adipocyte death and birth in obesity.* Genes Dev, 2019. **33**(23-24): p. 1657-1672.

52. Arner, E., et al., *Adipocyte turnover: relevance to human adipose tissue morphology*. *Diabetes*, 2010. **59**(1): p. 105-109.
53. Gustafson, B., et al., *Reduced subcutaneous adipogenesis in human hypertrophic obesity is linked to senescent precursor cells*. *Nat Commun*, 2019. **10**(1): p. 2757.
54. Arner, P., et al., *Genetic predisposition for Type 2 diabetes, but not for overweight/obesity, is associated with a restricted adipogenesis*. *PLoS One*, 2011. **6**(4): p. e18284.
55. McLaughlin, T.M., et al., *Pioglitazone increases the proportion of small cells in human abdominal subcutaneous adipose tissue*. *Obesity (Silver Spring)*, 2010. **18**(5): p. 926-931.
56. McLaughlin, T., et al., *Adipose Cell Size and Regional Fat Deposition as Predictors of Metabolic Response to Overfeeding in Insulin-Resistant and Insulin-Sensitive Humans*. *Diabetes*, 2016. **65**(5): p. 1245-1254.
57. White, U., et al., *A higher proportion of small adipocytes is associated with increased visceral and ectopic lipid accumulation during weight gain in response to overfeeding in men*. *Int J Obes (Lond)*, 2022. **46**(8): p. 1560-1563.
58. Johannsen, D.L., et al., *Effect of 8 weeks of overfeeding on ectopic fat deposition and insulin sensitivity: testing the "adipose tissue expandability" hypothesis*. *Diabetes Care*, 2014. **37**(10): p. 2789-2797.
59. White, U.A., et al., *Association of In Vivo Adipose Tissue Cellular Kinetics With Markers of Metabolic Health in Humans*. *J Clin Endocrinol Metab*, 2017. **102**(7): p. 2171-2178.
60. Pajvani, U.B., et al., *Fat apoptosis through targeted activation of caspase 8: a new mouse model of inducible and reversible lipodatrophy*. *Nat Med*, 2005. **11**(7): p. 797-803.
61. Kim, S.J., et al., *Adipocyte Death Preferentially Induces Liver Injury and Inflammation Through the Activation of Chemokine (C-C Motif) Receptor 2-Positive Macrophages and Lipolysis*. *Hepatology*, 2019. **69**(5): p. 1965-1982.
62. Sakaguchi, M., et al., *Adipocyte Dynamics and Reversible Metabolic Syndrome in Mice with an Inducible Adipocyte-Specific Deletion of the Insulin Receptor*. *Cell Metab*, 2017. **25**(2): p. 448-462.
63. Stienstra, R., et al., *Mannose-binding lectin is required for the effective clearance of apoptotic cells by adipose tissue macrophages during obesity*. *Diabetes*, 2014. **63**(12): p. 4143-4153.
64. Petrus, P., et al., *Transforming Growth Factor-beta3 Regulates Adipocyte Number in Subcutaneous White Adipose Tissue*. *Cell Rep*, 2018. **25**(3): p. 551-560 e555.
65. Wang, S., et al., *Adipocyte Piezo1 mediates obesogenic adipogenesis through the FGF1/FGFR1 signaling pathway in mice*. *Nat Commun*, 2020. **11**(1): p. 2303.

66. Wernstedt Asterholm, I., et al., *Adipocyte inflammation is essential for healthy adipose tissue expansion and remodeling*. Cell Metab, 2014. **20**(1): p. 103-118.
67. Zhu, Q., et al., *Suppressing adipocyte inflammation promotes insulin resistance in mice*. Mol Metab, 2020. **39**: p. 101010.
68. Huh, J.Y., et al., *Crosstalk between adipocytes and immune cells in adipose tissue inflammation and metabolic dysregulation in obesity*. Mol Cells, 2014. **37**(5): p. 365-371.
69. Trim, W.V.andLynch, L., *Immune and non-immune functions of adipose tissue leukocytes*. Nat Rev Immunol, 2022. **22**(6): p. 371-386.
70. Park, J., et al., *Adipocytes Are the Control Tower That Manages Adipose Tissue Immunity by Regulating Lipid Metabolism*. Front Immunol, 2020. **11**(3631): p. 598566.
71. van Eijkeren, R.J., et al., *Endogenous lipid antigens for invariant natural killer T cells hold the reins in adipose tissue homeostasis*. Immunology, 2018. **153**(2): p. 179-189.
72. Lynch, L., et al., *Adipose tissue invariant NKT cells protect against diet-induced obesity and metabolic disorder through regulatory cytokine production*. Immunity, 2012. **37**(3): p. 574-587.
73. Schipper, H.S., et al., *Natural killer T cells in adipose tissue prevent insulin resistance*. J Clin Invest, 2012. **122**(9): p. 3343-3354.
74. Huh, J.Y., et al., *Deletion of CD1d in Adipocytes Aggravates Adipose Tissue Inflammation and Insulin Resistance in Obesity*. Diabetes, 2017. **66**(4): p. 835-847.
75. Liao, C.M., et al., *The functions of type I and type II natural killer T cells in inflammatory bowel diseases*. Inflamm Bowel Dis, 2013. **19**(6): p. 1330-1338.
76. Brennan, P.J., et al., *Invariant natural killer T cells: an innate activation scheme linked to diverse effector functions*. Nat Rev Immunol, 2013. **13**(2): p. 101-117.
77. Jimeno, R., et al., *Tissue-specific shaping of the TCR repertoire and antigen specificity of iNKT cells*. Elife, 2019. **8**.
78. Crosby, C.M.andKronenberg, M., *Tissue-specific functions of invariant natural killer T cells*. Nat Rev Immunol, 2018. **18**(9): p. 559-574.
79. Lee, Y.J., et al., *Steady-state production of IL-4 modulates immunity in mouse strains and is determined by lineage diversity of iNKT cells*. Nat Immunol, 2013. **14**(11): p. 1146-1154.
80. Lee, W.Y., et al., *An intravascular immune response to *Borrelia burgdorferi* involves Kupffer cells and iNKT cells*. Nat Immunol, 2010. **11**(4): p. 295-302.
81. Miyaki, E., et al., *Interferon alpha treatment stimulates interferon gamma expression in type I NKT cells and enhances their antiviral effect against hepatitis C virus*. PLoS One, 2017. **12**(3): p. e0172412.
82. Kinjo, Y., et al., *Invariant natural killer T cells recognize glycolipids*

- from pathogenic Gram-positive bacteria*. Nat Immunol, 2011. **12**(10): p. 966-974.
83. Nakamatsu, M., et al., *Role of interferon-gamma in Valpha14+ natural killer T cell-mediated host defense against Streptococcus pneumoniae infection in murine lungs*. Microbes Infect, 2007. **9**(3): p. 364-374.
84. De Santo, C., et al., *Invariant NKT cells reduce the immunosuppressive activity of influenza A virus-induced myeloid-derived suppressor cells in mice and humans*. J Clin Invest, 2008. **118**(12): p. 4036-4048.
85. Syn, W.K., et al., *Accumulation of natural killer T cells in progressive nonalcoholic fatty liver disease*. Hepatology, 2010. **51**(6): p. 1998-2007.
86. Lappas, C.M., et al., *Adenosine A2A receptor activation reduces hepatic ischemia reperfusion injury by inhibiting CD1d-dependent NKT cell activation*. J Exp Med, 2006. **203**(12): p. 2639-2648.
87. Facciotti, F., et al., *Peroxisome-derived lipids are self antigens that stimulate invariant natural killer T cells in the thymus*. Nat Immunol, 2012. **13**(5): p. 474-480.
88. Huang, S., et al., *CD1 lipidomes reveal lipid-binding motifs and size-based antigen-display mechanisms*. Cell, 2023. **186**(21): p. 4583-4596 e4513.
89. Zhou, D., et al., *Lysosomal glycosphingolipid recognition by NKT cells*. Science, 2004. **306**(5702): p. 1786-1789.
90. Brennan, P.J., et al., *Structural determination of lipid antigens captured at the CD1d-T-cell receptor interface*. Proc Natl Acad Sci U S A, 2017. **114**(31): p. 8348-8353.
91. Kain, L., et al., *The identification of the endogenous ligands of natural killer T cells reveals the presence of mammalian alpha-linked glycosylceramides*. Immunity, 2014. **41**(4): p. 543-554.
92. Porubsky, S., et al., *Normal development and function of invariant natural killer T cells in mice with isoglobotrihexosylceramide (iGb3) deficiency*. Proc Natl Acad Sci U S A, 2007. **104**(14): p. 5977-5982.
93. Speak, A.O., et al., *Implications for invariant natural killer T cell ligands due to the restricted presence of isoglobotrihexosylceramide in mammals*. Proc Natl Acad Sci U S A, 2007. **104**(14): p. 5971-5976.
94. Brigl, M., et al., *Mechanism of CD1d-restricted natural killer T cell activation during microbial infection*. Nat Immunol, 2003. **4**(12): p. 1230-1237.
95. Nagarajan, N.A. and Kronenberg, M., *Invariant NKT cells amplify the innate immune response to lipopolysaccharide*. J Immunol, 2007. **178**(5): p. 2706-2713.
96. Rachitskaya, A.V., et al., *Cutting edge: NKT cells constitutively express IL-23 receptor and RORgamma and rapidly produce IL-17 upon receptor ligation in an IL-6-independent fashion*. J Immunol,

2008. **180**(8): p. 5167-5171.
97. Terashima, A., et al., *A novel subset of mouse NKT cells bearing the IL-17 receptor B responds to IL-25 and contributes to airway hyperreactivity*. J Exp Med, 2008. **205**(12): p. 2727-2733.
 98. Stock, P., et al., *Induction of airway hyperreactivity by IL-25 is dependent on a subset of invariant NKT cells expressing IL-17RB*. J Immunol, 2009. **182**(8): p. 5116-5122.
 99. Lynch, L., et al., *Regulatory iNKT cells lack expression of the transcription factor PLZF and control the homeostasis of T(reg) cells and macrophages in adipose tissue*. Nat Immunol, 2015. **16**(1): p. 85-95.
 100. Krovi, S.H. and Gapin, L., *Invariant Natural Killer T Cell Subsets-More Than Just Developmental Intermediates*. Front Immunol, 2018. **9**: p. 1393.
 101. Bendelac, A., *Positive selection of mouse NK1+ T cells by CD1-expressing cortical thymocytes*. J Exp Med, 1995. **182**(6): p. 2091-2096.
 102. Chun, T., et al., *CD1d-expressing dendritic cells but not thymic epithelial cells can mediate negative selection of NKT cells*. J Exp Med, 2003. **197**(7): p. 907-918.
 103. Pellicci, D.G., et al., *Intrathymic NKT cell development is blocked by the presence of alpha-galactosylceramide*. Eur J Immunol, 2003. **33**(7): p. 1816-1823.
 104. Bedel, R., et al., *Effective functional maturation of invariant natural killer T cells is constrained by negative selection and T-cell antigen receptor affinity*. Proc Natl Acad Sci U S A, 2014. **111**(1): p. E119-128.
 105. Griewank, K., et al., *Homotypic interactions mediated by Slamf1 and Slamf6 receptors control NKT cell lineage development*. Immunity, 2007. **27**(5): p. 751-762.
 106. Seiler, M.P., et al., *Elevated and sustained expression of the transcription factors Egr1 and Egr2 controls NKT lineage differentiation in response to TCR signaling*. Nat Immunol, 2012. **13**(3): p. 264-271.
 107. Mao, A.P., et al., *A shared Runx1-bound Zbtb16 enhancer directs innate and innate-like lymphoid lineage development*. Nat Commun, 2017. **8**(1): p. 863.
 108. Mao, A.P., et al., *Multiple layers of transcriptional regulation by PLZF in NKT-cell development*. Proc Natl Acad Sci U S A, 2016. **113**(27): p. 7602-7607.
 109. Pellicci, D.G., et al., *Thymic development of unconventional T cells: how NKT cells, MAIT cells and gammadelta T cells emerge*. Nat Rev Immunol, 2020. **20**(12): p. 756-770.
 110. Benlagha, K., et al., *A thymic precursor to the NK T cell lineage*. Science, 2002. **296**(5567): p. 553-555.

111. Pellicci, D.G., et al., *A natural killer T (NKT) cell developmental pathway involving a thymus-dependent NK1.1(-)CD4(+) CD1d-dependent precursor stage*. J Exp Med, 2002. **195**(7): p. 835-844.
112. Wang, H.andHogquist, K.A., *CCR7 defines a precursor for murine iNKT cells in thymus and periphery*. Elife, 2018. **7**.
113. Wang, H.andHogquist, K.A., *How Lipid-Specific T Cells Become Effectors: The Differentiation of iNKT Subsets*. Front Immunol, 2018. **9**: p. 1450.
114. Bennisstein, S.B., *Unraveling Natural Killer T-Cells Development*. Front Immunol, 2017. **8**: p. 1950.
115. Harsha Krovi, S., et al., *Thymic iNKT single cell analyses unmask the common developmental program of mouse innate T cells*. Nat Commun, 2020. **11**(1): p. 6238.
116. Wang, J., et al., *Integrative scATAC-seq and scRNA-seq analyses map thymic iNKT cell development and identify Cfbeta for its commitment*. Cell Discov, 2023. **9**(1): p. 61.
117. Baranek, T., et al., *High Dimensional Single-Cell Analysis Reveals iNKT Cell Developmental Trajectories and Effector Fate Decision*. Cell Rep, 2020. **32**(10): p. 108116.
118. Bortoluzzi, S., et al., *Brief homogeneous TCR signals instruct common iNKT progenitors whose effector diversification is characterized by subsequent cytokine signaling*. Immunity, 2021. **54**(11): p. 2497-2513 e2499.
119. Huh, J.Y., et al., *A novel function of adipocytes in lipid antigen presentation to iNKT cells*. Mol Cell Biol, 2013. **33**(2): p. 328-339.
120. Ji, Y., et al., *Activation of natural killer T cells promotes M2 Macrophage polarization in adipose tissue and improves systemic glucose tolerance via interleukin-4 (IL-4)/STAT6 protein signaling axis in obesity*. J Biol Chem, 2012. **287**(17): p. 13561-13571.
121. LaMarche, N.M., et al., *Distinct iNKT Cell Populations Use IFNgamma or ER Stress-Induced IL-10 to Control Adipose Tissue Homeostasis*. Cell Metab, 2020. **32**(2): p. 243-258 e246.
122. Sag, D., et al., *IL-10-producing NKT10 cells are a distinct regulatory invariant NKT cell subset*. J Clin Invest, 2014. **124**(9): p. 3725-3740.
123. Vieth, J.A., et al., *TCRalpha-TCRbeta pairing controls recognition of CD1d and directs the development of adipose NKT cells*. Nat Immunol, 2017. **18**(1): p. 36-44.
124. Hogquist, K.andGeorgiev, H., *Recent advances in iNKT cell development*. F1000Res, 2020. **9**.
125. Caputa, G., et al., *Metabolic adaptations of tissue-resident immune cells*. Nat Immunol, 2019. **20**(7): p. 793-801.
126. van Eijkeren, R.J., et al., *Cytokine Output of Adipocyte-iNKT Cell Interplay Is Skewed by a Lipid-Rich Microenvironment*. Front Endocrinol (Lausanne), 2020. **11**: p. 479.
127. Kim, J.H., et al., *Donor bone marrow type II (non-Valpha14Jalpha18*

- CD1d-restricted) NKT cells suppress graft-versus-host disease by producing IFN-gamma and IL-4.* J Immunol, 2007. **179**(10): p. 6579-6587.
128. Cui, J., et al., *Requirement for Valpha14 NKT cells in IL-12-mediated rejection of tumors.* Science, 1997. **278**(5343): p. 1623-1626.
 129. Lun, A.T.L., et al., *EmptyDrops: distinguishing cells from empty droplets in droplet-based single-cell RNA sequencing data.* Genome Biol, 2019. **20**(1): p. 63.
 130. McCarthy, D.J., et al., *Scater: pre-processing, quality control, normalization and visualization of single-cell RNA-seq data in R.* Bioinformatics, 2017. **33**(8): p. 1179-1186.
 131. Lun, A.T., et al., *A step-by-step workflow for low-level analysis of single-cell RNA-seq data with Bioconductor.* F1000Res, 2016. **5**: p. 2122.
 132. Butler, A., et al., *Integrating single-cell transcriptomic data across different conditions, technologies, and species.* Nat Biotechnol, 2018. **36**(5): p. 411-420.
 133. Sherman, B.T., et al., *DAVID: a web server for functional enrichment analysis and functional annotation of gene lists (2021 update).* Nucleic Acids Res, 2022. **50**(W1): p. W216-W221.
 134. Huang da, W., et al., *Systematic and integrative analysis of large gene lists using DAVID bioinformatics resources.* Nat Protoc, 2009. **4**(1): p. 44-57.
 135. Mouselimis, L., *KernelKnn: Kernel k Nearest Neighbors.* 2021. <https://CRAN.R-project.org/package=KernelKnn>
 136. Nahmgoong, H., et al., *Distinct properties of adipose stem cell subpopulations determine fat depot-specific characteristics.* Cell Metab, 2022. **34**(3): p. 458-472 e456.
 137. Zhang, J., et al., *Isolation of lymphocytes and their innate immune characterizations from liver, intestine, lung and uterus.* Cell Mol Immunol, 2005. **2**(4): p. 271-280.
 138. Ko, J.S., et al., *Palmitate inhibits arthritis by inducing t-bet and gata-3 mRNA degradation in iNKT cells via IRE1alpha-dependent decay.* Sci Rep, 2017. **7**(1): p. 14940.
 139. Kim, Y.Y., et al., *Hepatic GSK3beta-Dependent CRY1 Degradation Contributes to Diabetic Hyperglycemia.* Diabetes, 2022. **71**(7): p. 1373-1387.
 140. Engel, I., et al., *Innate-like functions of natural killer T cell subsets result from highly divergent gene programs.* Nat Immunol, 2016. **17**(6): p. 728-739.
 141. Wang, J., et al., *Single-cell analysis reveals differences among iNKT cells colonizing peripheral organs and identifies Klf2 as a key gene for iNKT emigration.* Cell Discov, 2022. **8**(1): p. 75.
 142. Vieth, J.A. and Sant'Angelo, D.B., *Are fat NKT cells born that way?* Cell Mol Immunol, 2017. **14**(8): p. 658-661.

143. Gaud, G., et al., *Regulatory mechanisms in T cell receptor signalling*. Nat Rev Immunol, 2018. **18**(8): p. 485-497.
144. Boucher, J., et al., *Insulin receptor signaling in normal and insulin-resistant states*. Cold Spring Harb Perspect Biol, 2014. **6**(1)
145. Bai, Y., et al., *Single-Cell Transcriptome Analysis Reveals RGS1 as a New Marker and Promoting Factor for T-Cell Exhaustion in Multiple Cancers*. Front Immunol, 2021. **12**: p. 767070.
146. Wang, L., et al., *KLRG1-expressing CD8+ T cells are exhausted and polyfunctional in patients with chronic hepatitis B*. PLoS One, 2024. **19**(5): p. e0303945.
147. Kanda, M., et al., *Transcriptional regulator Bhlhe40 works as a cofactor of T-bet in the regulation of IFN-gamma production in iNKT cells*. Proc Natl Acad Sci U S A, 2016. **113**(24): p. E3394-3402.
148. Huang, Z., et al., *CD226: An Emerging Role in Immunologic Diseases*. Front Cell Dev Biol, 2020. **8**: p. 564.
149. Jennings, E., et al., *Nr4a1 and Nr4a3 Reporter Mice Are Differentially Sensitive to T Cell Receptor Signal Strength and Duration*. Cell Rep, 2020. **33**(5): p. 108328.
150. Shimizu, K., et al., *KLRG+ invariant natural killer T cells are long-lived effectors*. Proc Natl Acad Sci U S A, 2014. **111**(34): p. 12474-12479.
151. Kane, H., et al., *Longitudinal analysis of invariant natural killer T cell activation reveals a cMAF-associated transcriptional state of NKT10 cells*. Elife, 2022. **11**: p. e76586.
152. Iyoda, T., et al., *Zeb2 regulates differentiation of long-lived effector of invariant natural killer T cells*. Commun Biol, 2023. **6**(1): p. 1070.
153. Vasanthakumar, A., et al., *Sex-specific adipose tissue imprinting of regulatory T cells*. Nature, 2020. **579**(7800): p. 581-585.
154. Sun, K., et al., *Adipose tissue remodeling and obesity*. J Clin Invest, 2011. **121**(6): p. 2094-2101.
155. Rosen, E.D. and Spiegelman, B.M., *What we talk about when we talk about fat*. Cell, 2014. **156**(1-2): p. 20-44.
156. Forbes, S.J. and Rosenthal, N., *Preparing the ground for tissue regeneration: from mechanism to therapy*. Nat Med, 2014. **20**(8): p. 857-869.
157. Street, K., et al., *Slingshot: cell lineage and pseudotime inference for single-cell transcriptomics*. BMC Genomics, 2018. **19**(1): p. 477.
158. Lee, M., et al., *Single-cell RNA sequencing identifies shared differentiation paths of mouse thymic innate T cells*. Nat Commun, 2020. **11**(1): p. 4367.
159. Zikherman, J., et al., *Endogenous antigen tunes the responsiveness of naive B cells but not T cells*. Nature, 2012. **489**(7414): p. 160-164.
160. Bostik, P., et al., *Dysregulation of the polo-like kinase pathway in CD4+ T cells is characteristic of pathogenic simian immunodeficiency virus infection*. J Virol, 2004. **78**(3): p. 1464-1472.

161. Fang, P., et al., *Immune cell subset differentiation and tissue inflammation*. J Hematol Oncol, 2018. **11**(1): p. 97.
162. Huang, H., et al., *In vivo CRISPR screening reveals nutrient signaling processes underpinning CD8(+) T cell fate decisions*. Cell, 2021. **184**(5): p. 1245-1261 e1221.
163. Xu, H., et al., *Chronic inflammation in fat plays a crucial role in the development of obesity-related insulin resistance*. J Clin Invest, 2003. **112**(12): p. 1821-1830.
164. Bai, Y. and Sun, Q., *Macrophage recruitment in obese adipose tissue*. Obes Rev, 2015. **16**(2): p. 127-136.
165. Kitade, H., et al., *CCR5 plays a critical role in obesity-induced adipose tissue inflammation and insulin resistance by regulating both macrophage recruitment and M1/M2 status*. Diabetes, 2012. **61**(7): p. 1680-1690.
166. Cottam, M.A., et al., *Multiomics reveals persistence of obesity-associated immune cell phenotypes in adipose tissue during weight loss and weight regain in mice*. Nat Commun, 2022. **13**(1): p. 2950.
167. Li, J., et al., *Regulatory T-Cells: Potential Regulator of Tissue Repair and Regeneration*. Front Immunol, 2018. **9**: p. 585.
168. Julier, Z., et al., *Promoting tissue regeneration by modulating the immune system*. Acta Biomater, 2017. **53**: p. 13-28.
169. Gause, W.C., et al., *Type 2 immunity and wound healing: evolutionary refinement of adaptive immunity by helminths*. Nat Rev Immunol, 2013. **13**(8): p. 607-614.
170. Munoz-Rojas, A.R. and Mathis, D., *Tissue regulatory T cells: regulatory chameleons*. Nat Rev Immunol, 2021. **21**(9): p. 597-611.
171. Burzyn, D., et al., *A special population of regulatory T cells potentiates muscle repair*. Cell, 2013. **155**(6): p. 1282-1295.
172. Johnson, J.A., et al., *Prolonged decrease of adipocyte size after rosiglitazone treatment in high- and low-fat-fed rats*. Obesity (Silver Spring), 2007. **15**(11): p. 2653-2663.
173. Khan, T., et al., *Metabolic dysregulation and adipose tissue fibrosis: role of collagen VI*. Mol Cell Biol, 2009. **29**(6): p. 1575-1591.
174. Prins, J.B., et al., *Tumor necrosis factor-alpha induces apoptosis of human adipose cells*. Diabetes, 1997. **46**(12): p. 1939-1944.
175. Eguchi, A., et al., *Microparticles release by adipocytes act as "find-me" signals to promote macrophage migration*. PLoS One, 2015. **10**(4): p. e0123110.
176. Feng, D., et al., *High-fat diet-induced adipocyte cell death occurs through a cyclophilin D intrinsic signaling pathway independent of adipose tissue inflammation*. Diabetes, 2011. **60**(8): p. 2134-2143.
177. Sekimoto, R., et al., *Visualized macrophage dynamics and significance of S100A8 in obese fat*. Proc Natl Acad Sci U S A, 2015. **112**(16): p. E2058-2066.
178. Kamei, N., et al., *Overexpression of monocyte chemoattractant*

- protein-1 in adipose tissues causes macrophage recruitment and insulin resistance.* J Biol Chem, 2006. **281**(36): p. 26602-26614.
179. Mallevaey, T., et al., *T cell receptor CDR2 beta and CDR3 beta loops collaborate functionally to shape the iNKT cell repertoire.* Immunity, 2009. **31**(1): p. 60-71.
180. Cameron, G., et al., *Antigen Specificity of Type I NKT Cells Is Governed by TCR beta-Chain Diversity.* J Immunol, 2015. **195**(10): p. 4604-4614.
181. Keophipath, M., et al., *CCL5 promotes macrophage recruitment and survival in human adipose tissue.* Arterioscler Thromb Vasc Biol, 2010. **30**(1): p. 39-45.
182. Emont, M.P., et al., *A single-cell atlas of human and mouse white adipose tissue.* Nature, 2022. **603**(7903): p. 926-933.
183. Biton, M., et al., *T Helper Cell Cytokines Modulate Intestinal Stem Cell Renewal and Differentiation.* Cell, 2018. **175**(5): p. 1307-1320 e1322.
184. Harrell, C.R., et al., *The Cross-Talk between Mesenchymal Stem Cells and Immune Cells in Tissue Repair and Regeneration.* Int J Mol Sci, 2021. **22**(5): p. 2472.
185. Jarde, T., et al., *Mesenchymal Niche-Derived Neuregulin-1 Drives Intestinal Stem Cell Proliferation and Regeneration of Damaged Epithelium.* Cell Stem Cell, 2020. **27**(4): p. 646-662 e647.
186. Zaiss, D.M.W., et al., *Emerging functions of amphiregulin in orchestrating immunity, inflammation, and tissue repair.* Immunity, 2015. **42**(2): p. 216-226.
187. Oda, K., et al., *A comprehensive pathway map of epidermal growth factor receptor signaling.* Mol Syst Biol, 2005. **1**(1): p. 2005 0010.
188. Kabat, A.M., et al., *Resident T(H)2 cells orchestrate adipose tissue remodeling at a site adjacent to infection.* Science immunology, 2022. **7**(76): p. eadd3263.
189. Kim, J., et al., *Innate Lymphoid Cells in Tissue Homeostasis and Disease Pathogenesis.* Mol Cells, 2021. **44**(5): p. 301-309.
190. Li, Y., et al., *Insulin signaling establishes a developmental trajectory of adipose regulatory T cells.* Nat Immunol, 2021. **22**(9): p. 1175-1185.
191. Vasanthakumar, A., et al., *The transcriptional regulators IRF4, BATF and IL-33 orchestrate development and maintenance of adipose tissue-resident regulatory T cells.* Nat Immunol, 2015. **16**(3): p. 276-285.
192. Spallanzani, R.G., et al., *Distinct immunocyte-promoting and adipocyte-generating stromal components coordinate adipose tissue immune and metabolic tenors.* Science immunology, 2019. **4**(35): p. eaaw3658.
193. Liu, Y., et al., *iNKT: A new avenue for CAR-based cancer immunotherapy.* Transl Oncol, 2022. **17**: p. 101342.

194. Lee, Y.J., et al., *Lineage-Specific Effector Signatures of Invariant NKT Cells Are Shared amongst gammadelta T, Innate Lymphoid, and Th Cells*. *J Immunol*, 2016. **197**(4): p. 1460-1470.
195. Rakhshandehroo, M., et al., *Adipocytes harbor a glucosylceramide biosynthesis pathway involved in iNKT cell activation*. *Biochim Biophys Acta Mol Cell Biol Lipids*, 2019. **1864**(8): p. 1157-1167.

극문 초록

지방조직은 핵심 에너지 대사기관으로써 에너지를 저장 및 공급하고, 다양한 호르몬을 분비하며, 비만상황에서 면역 반응을 조절함으로써 전신적 대사 항상성을 조절한다. 지방조직은 비만상황에서 지방세포의 비대, 염증반응 증가, 지방세포 교체율 증가, 인슐린 저항성 등의 상당한 재구성 과정을 겪는다. 지방조직에는 염증 조절을 포함한 병리·생리학적 기능에서 중요한 역할을 하는 풍부한 면역 세포들이 존재한다. 이러한 면역 세포들 중 불변성 자연살해 T (Invariant natural killer T, iNKT) 세포는 다른 면역 세포들과 차별화된 독특한 특성을 지니고 있으며, 비만상황에서 지방조직의 항상성을 유지하는 데 중요한 역할을 한다. iNKT 세포는 지방세포 표면에서 CD1d 분자에 의해 제시되는 지질 항원을 인식함으로써 직접적으로 지방세포와 상호작용한다. 이러한 상호작용은 지방조직 iNKT 세포의 항염증 기능뿐만 아니라 지방세포 교체를 촉진하여 비만 지방조직의 병리적 재구성을 완화하는 데 필수적이다. 그러나 지방조직 iNKT 세포가 이러한 다양한 기능을 어떻게 매개하는지는 아직 완전히 밝혀지지 않았다.

지방조직 iNKT 세포의 또 다른 흥미로운 특징은 다른 기관의 iNKT 세포와는 차별화된 조직-특이적 특성을 나타낸다는 점이다. 지방조직 iNKT 세포와 같은 말초 면역세포는 1차 림프기관에서 성숙이 시작되고 말초조직으로 이동하여 그곳에서 자리잡고 기능을 수행하기 때문에, 말초조직의 극소적인 미세환경에 적응하는 것이 매우 중요하다. 그럼에도 불구하고, 지방조직 iNKT 세포의 이러한 독특한 조직-특이성이 어떻

게 형성되는지에 대한 종합적인 이해는 부족하다.

1장에서는 지방조직 iNKT 세포를 다른 기관의 iNKT 세포와 비교하여 지방조직 iNKT 세포의 독특한 특성을 조사하였다. 지방조직 iNKT 세포에서 KLRG1을 발현하는 하위 집단을 발견했으며, 이는 지방조직-특이적으로 나타났다. 이 하위 집단은 지방세포에서 분비된 인자로 인해 유도된 것으로 관찰되었으며, 지방조직-특이적(adipose-specific, As)-iNKT1 세포로 명명되었다.

2장에서는 비만에서 지방조직 iNKT 세포가 지방조직 항상성을 유지하는 조절 기전을 지방세포 교체 과정에 초점을 맞춰 연구하였다. 비만에 반응하여, As-iNKT1 세포는 Fas ligand와 granzyme B를 상향 조절하는 세포독성 하위 집단으로 분화하였으며, 이 하위 집단을 지방조직 세포독성(adipose cytotoxic, Ac)-iNKT1 세포로 명명하였다. Ac-iNKT1 세포는 *in vitro* 및 *in vivo* 조건 모두에서 지방세포 사멸을 유도할 수 있었다. 또한, Ac-iNKT1 세포는 대식세포의 침윤을 유발하는 사이토카인인 CCL5를 높은 수준으로 발현하였다. 한편, 비만 상태에서 지방조직 iNKT17 세포는 상피세포 성장인자 수용체(EGFR)에 결합하는 amphiregulin(AREG)의 발현을 증가시켰다. AREG은 지방 줄기 및 전구 세포(adipose stem and progenitor cell, ASPC)의 증식을 자극하여 지방세포분화(adipogenesis)를 촉진하였다. 이러한 발견들은 다양한 지방조직 iNKT 세포 하위 집단이 지방세포 교체 과정을 조절함을 시사한다.

결론적으로, 본 학위논문은 지방조직 iNKT 세포의 조절 기전과 지방조직 항상성 유지에서 그들의 역할을 설명한다. 지방조직 iNKT 세

포는 지방조직 내에서 조직-특이적 특성을 획득하고, 이러한 특성은 비만상황에서 지방세포 교체를 촉진하는 기능을 갖는다. 본 학위논문의 연구결과는 지방조직의 생리학적 조절 측면에서 말초 면역 세포에 대한 이해를 확장시킨다.

주요어: 지방조직, 백색지방조직, 불변성 자연살해 T 세포, 지방세포 교체, 지방조직 재구성, 비만

학번: 2019-28710